Ontario

Ontario Geological Survey
Open File Report 6171

Paleomagnetism, Geochronology and Geochemistry of Several Proterozoic Mafic Dike Swarms in Northwestern Ontario

2005

ERRATUM

Open File Report 6171

Paleomagnetism, Geochronology and Geochemistry of Several Proterozoic Mafic Dike Swarms in Northwestern Ontario

Please note the following correction to the Abstract, page xi, 5th paragraph, 1st line. "N polarity" should be "R polarity". The first line should read:

"A new age of 2459 ± 5 Ma for a Matachewan dike of **R** polarity in English River Subprovince, north of the"

106-01028/

Ontario

ONTARIO GEOLOGICAL SURVEY

Open File Report 6171

Paleomagnetism, Geochronology and Geochemistry of Several Proterozoic Mafic Dike Swarms in Northwestern Ontario

by

H.C. Halls, G.M. Stott and D.W. Davis

2005

Parts of this publication may be quoted if credit is given. It is recommended that reference to this publication be made in the following form:

Halls, H.C., Stott, G.M. and Davis, D.W. 2005. Paleomagnetism, geochronology and geochemistry of several Proterozoic mafic dike swarms in northwestern Ontario; Ontario Geological Survey, Open File Report 6171, 59p.

© Queen's Printer for Ontario, 2005

© Queen's Printer for Ontario, 2005.

Open File Reports of the Ontario Geological Survey are available for viewing at the Mines Library in Sudbury, at the Mines and Minerals Information Centre in Toronto, and at the regional Mines and Minerals office whose district includes the area covered by the report (see below).

Copies can be purchased at Publication Sales and the office whose district includes the area covered by the report. Although a particular report may not be in stock at locations other than the Publication Sales office in Sudbury, they can generally be obtained within 3 working days. All telephone, fax, mail and e-mail orders should be directed to the Publication Sales office in Sudbury. Use of VISA or MasterCard ensures the fastest possible service. Cheques or money orders should be made payable to the *Minister of Finance.*

Mines and Minerals Information Centre (MMIC) Macdonald Block, Room M2-17 900 Bay St. Toronto, Ontario M7A 1C3	Tel:	(416) 314-3800
Mines Library 933 Ramsey Lake Road, Level A3 Sudbury, Ontario P3E 6B5	Tel:	(705) 670-5615
Publication Sales 933 Ramsey Lake Rd., Level A3 Sudbury, Ontario P3E 6B5	Tel: Fax: E-mail:	(705) 670-5691(local) 1-888-415-9845(toll-free) (705) 670-5770 pubsales@ndm.gov.on.ca

Regional Mines and Minerals Offices:

Kenora - Suite 104, 810 Robertson St., Kenora P9N 4J2

Kirkland Lake - 10 Government Rd. E., Kirkland Lake P2N 1A8

Red Lake - Box 324, Ontario Government Building, Red Lake P0V 2M0

Sault Ste. Marie - 70 Foster Dr., Ste. 200, Sault Ste. Marie P6A 6V8

Southern Ontario - P.O. Bag Service 43, 126 Old Troy Rd., Tweed K0K 3J0

Sudbury - Level B3, 933 Ramsey Lake Rd., Sudbury P3E 6B5

Thunder Bay - Suite B002, 435 James St. S., Thunder Bay P7E 6S7

Timmins - Ontario Government Complex, P.O. Bag 3060, Hwy. 101 East, South Porcupine P0N 1H0

Toronto - MMIC, Macdonald Block, Room M2-17, 900 Bay St., Toronto M7A 1C3

This report has not received a technical edit. Discrepancies may occur for which the Ontario Ministry of Northern Development and Mines does not assume any liability. Source references are included in the report and users are urged to verify critical information. Recommendations and statements of opinions expressed are those of the author or authors and are not to be construed as statements of government policy.

If you wish to reproduce any of the text, tables or illustrations in this report, please write for permission to the Team Leader, Publication Services, Ministry of Northern Development and Mines, 933 Ramsey Lake Road, Level B4, Sudbury, Ontario P3E 6B5.

Cette publication est disponible en anglais seulement.

Parts of this report may be quoted if credit is given. It is recommended that reference be made in the following form:

Halls, H.C., Stott, G.M. and Davis, D.W. 2005. Paleomagnetism, geochronology and geochemistry of several Proterozoic mafic dike swarms in northwestern Ontario; Ontario Geological Survey, Open File Report 6171, 59p.

Contents

Abstract xi

Introduction 1

Acknowledgements 7

Previous Work 7

Geochronology 7
- Methods 8
- Sampling and Results 9
- Discussion 17

Paleomagnetism 18
- Sampling Procedures 18
- Results 19
  - Matachewan Dikes 19
  - Biscotasing Dikes 20
  - Marathon Dikes 22
  - Kapuskasing Dikes 23
  - Keweenawan Dikes 25
  - Dikes of Other Affinities 25
- Discussion 25

Geochemistry 26
- Methodology 26
- Results 26
  - Matachewan Dikes 28
  - Biscotasing Dikes 28
  - Marathon Dikes 28
  - Kapuskasing Dikes 32
  - Keweenawan Dikes 32
  - Abitibi Dikes 32
- Microprobe Mineral Analyses 32
- Discussion 33

Conclusions 33

References 35

Appendix 41

Metric Conversion Table 59

FIGURES

1. Geological map of the Lake Nipigon region showing the locations of sampled mafic dikes, with location symbols coded according to the age of the dike, as determined from radiometric age and/or paleomagnetic data 2
2. Geological map of the area east of the Kapuskasing Zone (KZ), showing the locations of sampling sites in north- to northeast-trending dikes 3
3. A map highlighting the distribution of mafic dike swarms under the Phanerozoic cover rocks of the James Bay Lowlands and the spatial correlation with kimberlite pipes 5
4. Detail of an aeromagnetic map in the vicinity of Marten Falls, east of Fort Hope and within the margin of the James Bay Lowlands. This shows 2 mafic dikes, a north-striking "Marathon" dike and a northeast-striking "Biscotasing" dike 6
5. Geological map east of Lake Nipigon showing locations in bold of mafic dikes for which U/Pb dating is presented here 10
6. Concordia diagrams showing U/Pb analyses for baddeleyite from samples of mafic dikes: a) crossing the Deeds pluton; b) at kilometre 24 on Kinghorn Rd; and c) 5 km west of Hillsport 11
7. Images of baddeleyite from each of the 3 mafic dikes as listed in Table 1 in the Appendix with analytical results illustrated in Figure 6 12
8. Concordia diagrams showing U/Pb analyses for baddeleyite from a) a mafic sill at site LL16, southeast of Beardmore; b) a mafic dike northeast of O'Sullivan Lake; and c) a dike northeast of Abamasagi Lake 14
9. Images of baddeleyite from site LL16, the analytical results from which are shown in Figure 8 and listed in Table 2 in the Appendix 15
10. Concordia diagram showing U/Pb analyses for baddeleyite and apatite from 2 sites: DP6 (03GRS-001) and DP8 (03GRS-003) 16
11. Images of apatite analyzed from a) site DP6 and b) site DP8 on which U/Pb age determinations were completed 16
12. Map showing the distribution of Matachewan dike sites east of Lake Nipigon and south of Wawa, in the Gamitagama and Ranger Lake areas. The inset equal-area projections show mean site directions for the Nipigon area and for the Gamitagama and Ranger Lake areas combined 21
13. Major element analyses illustrating dominant tholeiitic character of the mafic dikes swarms 24
14. Selected plots of trace elements for the dike swarms, illustrating some limited discrimination among some of the dike swarms 27
15. Extended trace element plots normalized to primitive mantle illustrating the overlapping spread amongst the dike swarms. a) Marathon; b) Kapuskasing; c) Biscotasing and Matachewan; d) Keweenawan and Abitibi 29
16. Selected trace element plots illustrating limited discrimination amongst dike swarms. Analytical spread is greatest for Marathon and Kapuskasing dikes 30
17. Selected trace element plots for mafic dike swarms with some discrimination as noted in the text 31

PHOTOS

1. H.C. Halls orienting a drill core sample to be used for paleomagnetic analysis; from a Matachewan mafic dike on the Kinghorn Road in the Onaman–Tashota greenstone belt 19

TABLES

1. U/Pb isotopic data on baddeleyite from mafic dikes at Sites DP1, DP2 and DP4 42
2. U/Pb isotopic data on baddeleyite for sample site LL16 43
3. Paleomagnetic results for all Matachewan dike sites 44
4. Paleomagnetic results for all N-ENE-trending dikes 44
5. Paleomagnetic results for Keweenawan mafic intrusions 46
6. Summary of paleomagnetic results from the Lake Gamitagama and Ranger Lake areas 46
7. Summary of mean paleomagnetic directions and pole positions for different dike swarms and combinations of data 47
8. All paleomagnetic sites in N- to ENE-striking dikes that did not attain the acceptance criteria of $N \geq 4$ and/or $\alpha_{95} \leq 15°$ 47
9. Geochemistry of selected Proterozoic mafic dikes east of Lake Nipigon and in the region of the Kapuskasing Zone 48
10a. Microprobe analyses of pyroxenes from Marathon and Matachewan dikes 57
10b. Microprobe analyses of amphiboles from Marathon dikes 58
10c. Microprobe analyses of plagioclase feldspar from Marathon and Matachewan dikes 58
10d. Microprobe analyses of ilmenite and magnetite from Marathon dikes 58

Abstract

Proterozoic dike swarms mark major episodes of crustal extension and voluminous mafic magmatism that affected large areas of the Superior Province craton but about which we know relatively little. This report presents paleomagnetic data and ages based on baddeleyite and apatite that allow us to characterize several dike swarms in the region east of Lake Nipigon and the Kapuskasing Zone.

A large, west-dipping sill southeast of Beardmore has R-magnetic polarity and is dated at 1103.7 ± 2.3 Ma. This is the youngest and easternmost known representative of mafic Keweenawan magmatism associated with the Nipigon Embayment. Only 1 northward-trending dike, at Beardmore, was identified as Keweenawan in age. New U/Pb baddeleyite ages of Marathon dikes include 2109.1 ± 1.6 Ma from a dike on the Kinghorn Road; 2112 ± 9 Ma from a north-northeast-striking dike intruding the Deeds pluton in northern Onaman–Tashota greenstone belt; 2106 ± 5 Ma from an N-polarity Marathon dike parallel to and southwest of the Deeds pluton dike; and 2125.7 ± 1.2 Ma from a northeast-striking, N-polarity dike in the English River Subprovince, northwest of O'Sullivan Lake. A northeast-striking dike near Hillsport, southeast of Longlac, is dated at 2170.7 ± 1.1 Ma and is therefore shown to belong to the Biscotasing swarm. One example of the Matachewan dikes in English River Subprovince, northeast of O'Sullivan Lake, gives a U/Pb baddeleyite age of 2459 ± 5 Ma, which compares with Matachewan dikes previously dated by Heaman (1997) and confirms a *circa* 25 m.y. span of mafic magmatism for this swarm.

Most north- to northeast-striking dikes east of Lake Nipigon appear to be of Marathon age and the paleomagnetic signatures in each case show N magnetic polarity for the older 2121 to 2125 Ma Marathon suite and R polarity for the younger suite, *circa* <2110 Ma. One dike near Lake Nipigon gives a Marathon baddeleyite age but a paleomagnetic direction similar to Keweenawan sills, suggesting that this dike might have been heated from above by a younger sill, since removed by erosion. A major discovery is that 6 dikes in the vicinity of the Kapuskasing Zone (KZ) have paleomagnetic signatures similar to N and R Marathon dikes, demonstrating that the Marathon swarm is more widespread than previously thought, radiating from a focal area south of eastern Lake Superior. These dikes near the KZ show mean declinations that are rotated about 10 to 15° clockwise from dikes farther west.

Biscotasing dikes occur farther west than previously recognized based on the new age for the Hillsport dike in this study, which is the first documented R-polarity dike of this swarm and demonstrates that the Biscotasing episode spanned at least 1 reversal of the Earth's field within a period of *circa* 5 million years. Pole positions indicate that the western Biscotasing dikes, like the Marathon dikes, have been rotated counterclockwise by about 15° with respect to the eastern ones on the opposite side of the KZ.

A new age of 2459 ± 5 Ma for a Matachewan dike of N polarity in English River Subprovince, north of the Onaman–Tashota greenstone belt, confirms that only a single reversal from R to N polarity characterised the Matachewan magmatic episode and shows that the R polarity epoch for the western half of the Matachewan swarm lasted at least 10 m.y. Correlations with previous work by Bates and Halls (1991) show that an originally more linear Matachewan swarm was also differentially rotated about vertical axes across the KZ. On a larger scale, the previous results indicated that the western half of the Superior Province has rotated counterclockwise at least 10 to 15° with respect to the eastern half that lies on the opposite side of the KZ. New results from this study east of Lake Nipigon show that the mean paleomagnetic direction is significantly different from the combined mean of paleomagnetic data from the Lake Gamitagama and Ranger Lake areas south of Wawa, so that a counterclockwise rotation of 23 ± 8° for the Lake Nipigon area can be calculated relative to south of Wawa.

The geochemistry of these dike swarms, based on 61 samples, mainly from chilled margins of dikes east of Lake Nipigon and in the vicinity of the KZ, provides limited evidence that the swarms can be effectively distinguished by geochemistry alone. Some evidence of differences in the relative size of clustering of trace element ratios and differences in the ratios on some geochemical plots might provide a complementary indication of dike affinity to the N- or R-polarity suites in a given swarm but provide unreliable discrimination between parallel dikes of different swarms.

Paleomagnetism, Geochronology and Geochemistry of Several Proterozoic Mafic Dike Swarms in Northwestern Ontario

H.C. Halls[1], G.M. Stott[2] and D.W. Davis[1]

Ontario Geological Survey
Open File Report 6171
2005

---

[1] Department of Geology, University of Toronto, Toronto, Ontario M5S 3B1
[2] Precambrian Geoscience Section, Ontario Geological Survey, Sudbury, Ontario P3E 6B5

Introduction

This project is an ongoing collaborative partnership, initiated in 2002, between the Ontario Geological Survey and the University of Toronto to investigate the age, geochemistry and paleomagnetism of Proterozoic mafic dike swarms.

The study of diabase dike swarms provides useful insight into a range of tectonic issues, such as crustal plate reconstruction through worldwide correlation of dike swarms, paleomagnetic evidence of continental drift, evidence of within-plate deformation, and locations of ancient mantle plume centres as well as their timing and role in continental break-up. Diabase dike swarms across Ontario have received intermittent attention over the years. Osmani (1991) summarized the state of knowledge over 10 years ago. Buchan and Ernst (2004) published a more recent Canada-wide map compilation. Proterozoic diabase dike swarms of at least 10 different ages intrude the Superior Province of northern Ontario (Osmani 1991; Fahrig 1987; Buchan and Halls 1990; Halls and Davis 2004). Samples from all of these dike swarms have been precisely dated by the U/Pb method on zircon and/or baddeleyite. They represent relatively short (5-30 Ma) bursts of igneous activity. They can be grouped into 3 main time periods: Early Paleoproterozoic (~2.47-2.45 Ga Matachewan dikes), Late Paleoproterozoic (2.2-2.0 Ga Senneterre, Biscotasing, Marathon, Cauchon, Fort Frances, and Kapuskasing dikes; 1.88 Ga Molson dikes), and Mesoproterozoic (1.3-1.1 Ga, Sudbury, Abitibi–Kipling, and Keweenawan dikes). Paleoproterozoic dikes, apart from those of the Molson swarm, are generally quartz tholeiites composed of plagioclase and pyroxene, typically with visible quartz and myrmekite. Mesoproterozoic dikes are more alkalic and characteristically possess fresh olivine (*see* Table 17.1 of Osmani 1991).

Over the last 15 years a major paleomagnetic and U/Pb geochronology program of Ontario dike swarms has been underway. The purpose is to distinguish the various dike swarms and examine their usefulness as structural elements to detect crustal uplift, tilting and rotation (Bates and Halls 1991; Halls and Zhang 1998; Buchan, Mortensen and Card 1993; Buchan, Halls and Mortensen 1996; Halls and Davis 2004). However, there remain significant gaps in our knowledge of the ages and origin of many of the dike swarms in Ontario. The current study focuses on Proterozoic mafic dikes east of Lake Nipigon (Figure 1) and from the vicinity of the Kapuskasing Zone farther east (Figure 2). It was initiated during a compilation of the bedrock geology east of Lake Nipigon (Stott et al. 2002) where information is limited about the various dike swarms.

Proterozoic mafic magma systems have attracted exploration interest for their platinum group element (PGE) potential, especially the *circa* 1100 Ma Keweenawan sills in the vicinity of Lake Nipigon. The Keweenawan Nipigon sills and associated ring dike systems have attracted strong exploration interest as possible host rocks for magmatic Ni-Cu-PGE mineralization. The lateral dimensions of this magmatic province are presently defined by the distribution of the Nipigon sills and associated ring dikes. However, it is possible that many of the dikes represent feeder systems beyond the current size of the Nipigon Embayment.

It has been suggested that the association of the north-striking Black Sturgeon fault along the west side of Lake Nipigon with the Keweenawan intrusions bears some similarity to the structural and magmatic setting of the Noril'sk Ni-Cu-PGE camp in Russia (Naldrett and Lightfoot 1993). The possible association of Keweenawan magmatism with potentially important mineralisation requires that the full areal extent of the Keweenawan igneous province be known and especially the location of the dike systems that fed the sills. Keweenawan dikes east of Lake Nipigon have not been reported although their presence is suspected (cf. Osmani 1991).

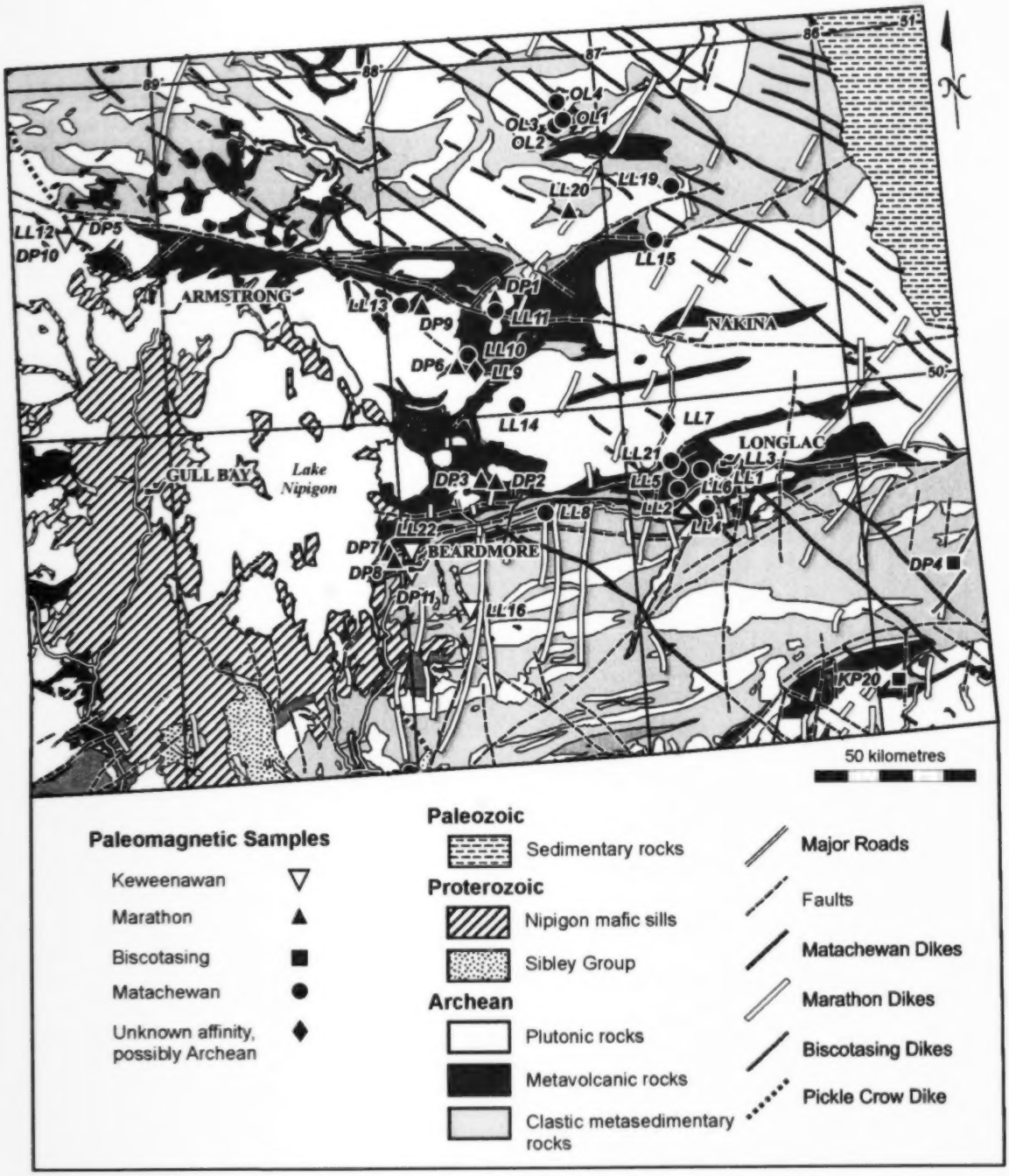

Figure 1. Geological map of the Lake Nipigon region showing the locations of sampled mafic dikes, with location symbols coded according to the age of the dike, as determined from radiometric age and/or paleomagnetic data. Sites DP5 and LL16 are from Keweenawan sills. Chilled margin samples provided both paleomagnetic and geochemical data.

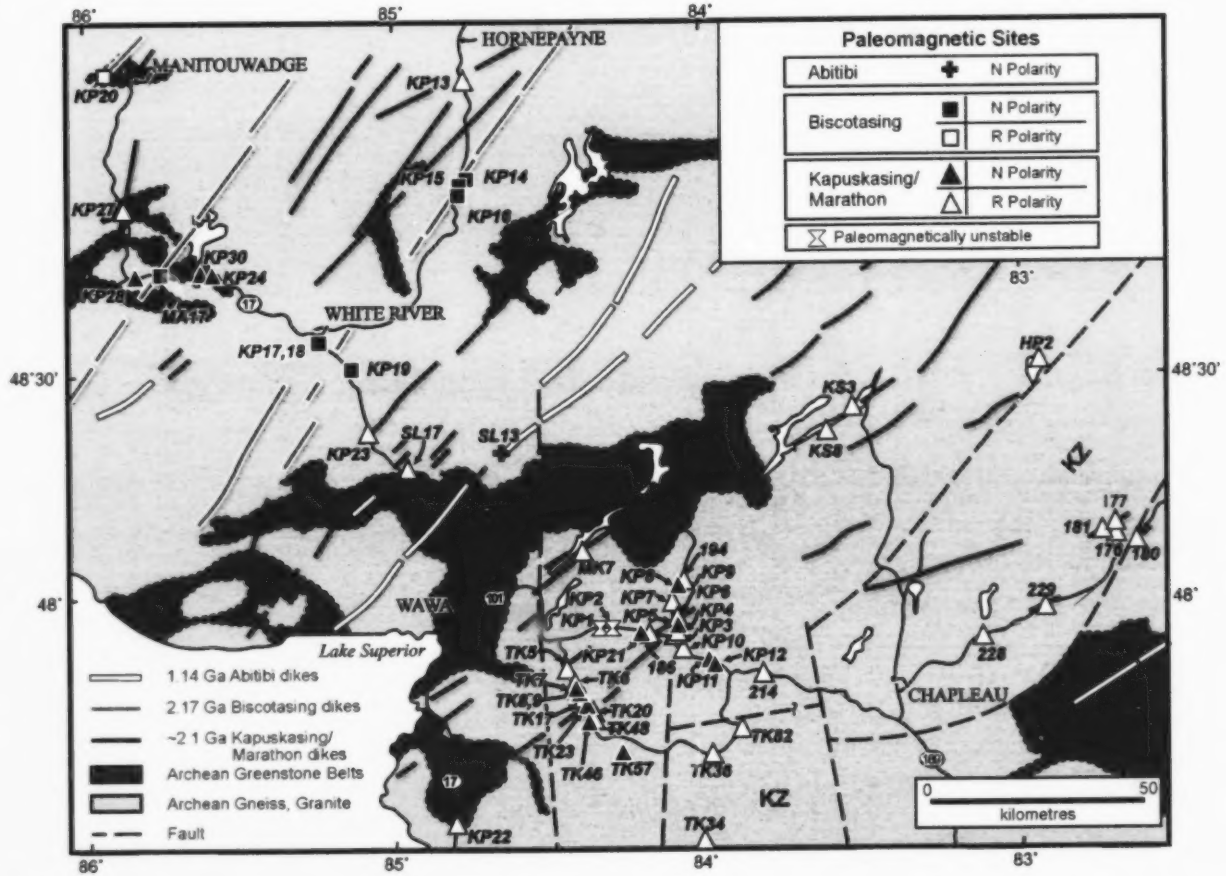

Figure 2. Geological map of the area east of the Kapuskasing Zone (KZ), showing the locations of sampling sites in north- to northeast-trending dikes. Open or closed symbols correspond to R or N paleomagnetic polarity at the location. Triangles are sites in Marathon or Kapuskasing dikes, squares are from Biscotasing dikes and crosses are from Abitibi dikes. Hourglass symbols give the locations of paleomagnetically unstable dikes of unknown polarity. The dikes at sites MK7 and TK 48 have U/Pb ages. Positive paleomagnetic baked contact tests, signifying that the remanent magnetization is primary, have been obtained at sites KP22, TK36, 214 and SL13. Halls and Palmer (1990) have reported the paleomagnetic results for all numbered sites. Within granulite gneisses of the KZ, east of Chapleau, paleomagnetic directions in the dikes are secondary and related to KZ crustal uplift (*see* Halls et al. 1994 for summary). Chilled margin samples provided both paleomagnetic and geochemical data.

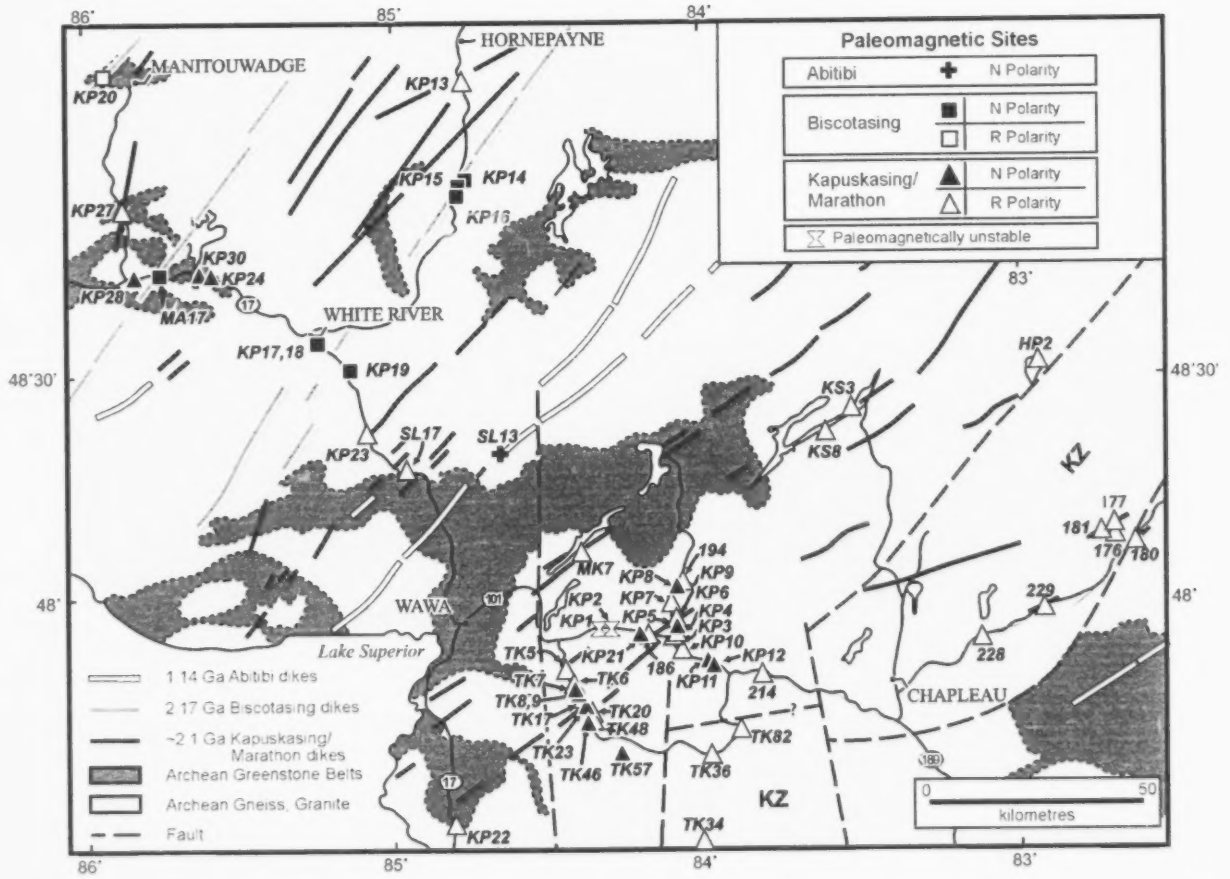

Figure 2. Geological map of the area east of the Kapuskasing Zone (KZ), showing the locations of sampling sites in north- to northeast-trending dikes. Open or closed symbols correspond to R or N paleomagnetic polarity at the location. Triangles are sites in Marathon or Kapuskasing dikes, squares are from Biscotasing dikes and crosses are from Abitibi dikes. Hourglass symbols give the locations of paleomagnetically unstable dikes of unknown polarity. The dikes at sites MK7 and TK 48 have U/Pb ages. Positive paleomagnetic baked contact tests, signifying that the remanent magnetization is primary, have been obtained at sites KP22, TK36, 214 and SL13. Halls and Palmer (1990) have reported the paleomagnetic results for all numbered sites. Within granulite gneisses of the KZ, east of Chapleau, paleomagnetic directions in the dikes are secondary and related to KZ crustal uplift (see Halls et al. 1994 for summary). Chilled margin samples provided both paleomagnetic and geochemical data.

A further justification for studying diabase dike systems in the eastern Wabigoon Subprovince arises from the recognition that north-striking dikes extend into the James Bay Lowlands (Ontario Geological Survey 1992; Stott and Halls 2002; Stott 2003) where diamond-bearing kimberlite pipes have been discovered (Sage 1997, 2000), and that north and northwest-striking dikes and postulated deep fractures might have focussed the emplacement of kimberlite pipes in the lowlands. Active exploration for diamond-bearing kimberlite pipes has stimulated an interest in understanding the structural controls for the emplacement of these pipes. Paleoproterozoic diabase dikes were injected along major fracture systems arising from the emplacement of mantle plumes (e.g., Ernst and Buchan 2001). A possible correlation is recognized between the presence of kimberlite pipes and major crustal faults. However, little attention has been placed on the potential significance of the diabase dikes as aeromagnetic markers of deep fracture systems that could have controlled kimberlite pipe emplacement (Stott 2003; Wilkinson et al. 2001). For example, the early Jurassic kimberlite pipes in the vicinity of the Victor pipe near Attawapiskat River are distributed close to the Winisk fault (Figure 3). They also form a significant linear trend along strike with a group of closely spaced northwest-striking Matachewan dikes (*see* Figure 3) (also cf. Figure Area A, Zalnieriunas and Sage 1995; and the diabase dike traces in the James Bay Lowlands, Ontario Geological Survey 1992). Similarly, the Proterozoic kimberlite pipes farther west of the Victor pipe, known as the Kyle pipes (Sage 1997, 2000), occur close to a north-striking set of Marathon dikes (*see* Figure 3). These observations suggest that the kimberlite pipes of different ages (Mesoproterozoic and Early Jurassic) intruded along plume-generated fractures that accommodated diabase dikes of different Paleoproterozoic ages (2121 Ma Marathon and 2446 Ma Matachewan dikes). Thus, the diabase dikes may provide a prominent indication of regional fracture trends and their concentrations, which can be identified on aeromagnetic maps. This points to the possibility of focussing kimberlite exploration near mafic dikes using aeromagnetic evidence (e.g., Figure 4). It is noteworthy that an overlap of both Matachewan and Marathon dike sets occurs east of the Victor deposit near longitude 83° and the Winisk fault. This area might provide a test for correlation between mafic dikes and kimberlite pipes. We also need to explore why there is an apparent correlation between different groups of deep crustal fractures and younger kimberlite pipes. Are the Matachewan and Marathon fracture systems near the Winisk fault second-order (re-opened?) fracture "splays" associated with the Archean fault? Did these fractures also provide a preferred emplacement pathway for kimberlite pipe intrusions? A more concerted effort is clearly needed to understand the relation between these dike/fracture systems and the clusters and trains of kimberlite pipes, including those still hidden in and under the lowland cover rocks.

Another consideration in our study of these dike swarms is the recognition by Manson and Halls (1997) of broad crustal segments characterized by relative differences in thermal stability reflected in differences in K/Ar biotite and amphibole ages across the southern Superior Province. These segments are bounded by major northeast-striking faults. One broad northeast-striking segment, between the Kapuskasing Structural Zone and the Gravel River fault near Longlac, corresponds to a regional gap in known kimberlite pipes between Wawa and the Attawapiskat–Missisa intrusions in the northern James Bay Lowlands (*see* Zalnieriunas and Sage 1995). Whether these northeast-striking segments contrasting crustal stability control the spatial distribution of fracture systems that in turn control the distribution of kimberlite pipes remains unclear. In summary, there is economically relevant justification for re-examining the Proterozoic history of mafic magmatism, fracture-generation and thermal perturbations across the Superior Province.

The complex and variable mix of dike orientations east of Lake Nipigon (Figure 1; *see also* Stott et al. 2002) and the uncertainty about assigning north- and northeast-striking dikes to specific swarms has demonstrated a need to distinguish these dikes from each other. Therefore, the main objectives of this study are 1) to identify the different ages, paleomagnetic and geochemical characteristics of dikes east of

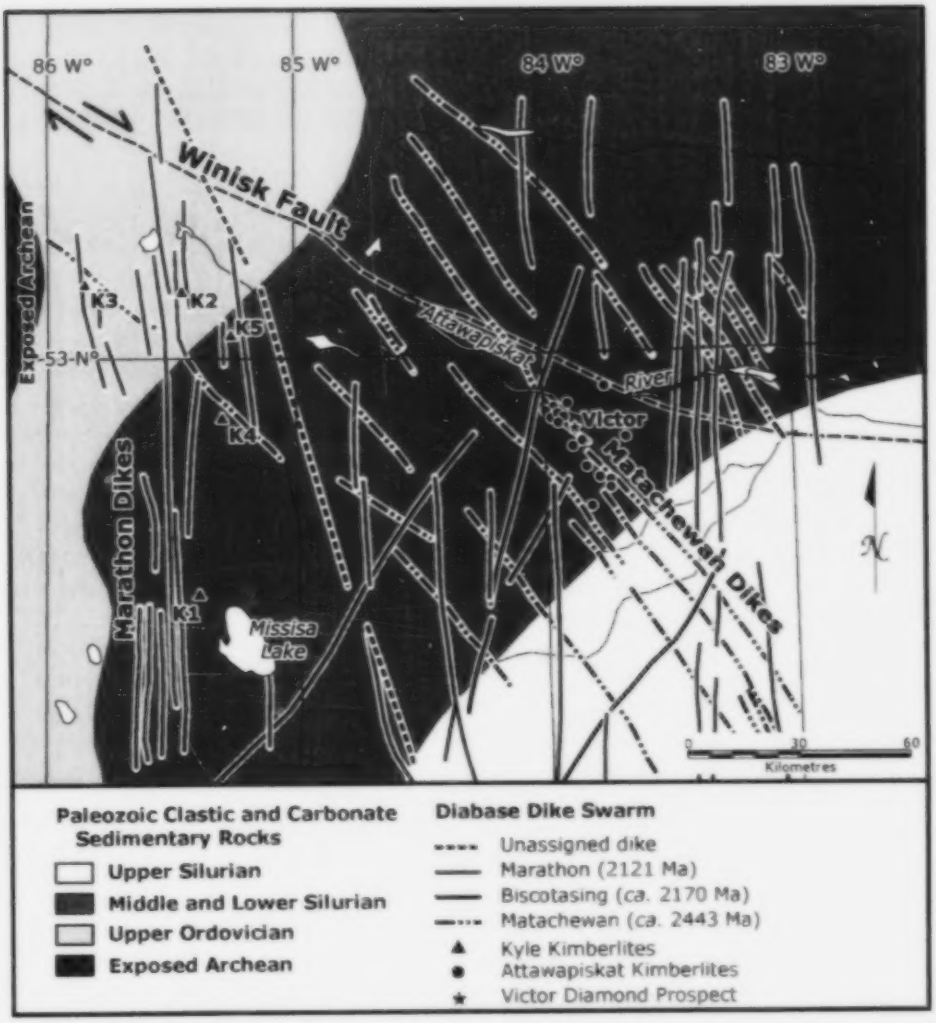

Figure 3. A map highlighting the distribution of mafic dike swarms under the Phanerozoic cover rocks of the James Bay Lowlands and the spatial correlation with kimberlite pipes. Early Jurassic kimberlite pipes, near Attawapiskat River, including the Victor diamond deposit, concentrate in a train parallel to 1 dike in a group of northwest-striking Matachewan (ca. 2446 Ma) mafic dikes and inferred associated fractures. The north-trending cluster of Mesoproterozoic (1100 Ma) "Kyle" kimberlite pipes (K1 to K5) intruded close to individual mafic dikes interpreted here as part of the north-striking Marathon (ca. 2121 Ma) swarm. Figure is from Stott (2003).

Lake Nipigon; 2) to correlate these dikes with known swarms outside the Lake Nipigon region, notably in the Kapuskasing Zone where the senior author has conducted a long term study to assess vertical-axis crustal rotation across the Kapuskasing Zone; and 3) to identify dikes that are associated with Keweenawan intrusive episodes known to be associated with magmatic Ni-Cu-PGE mineralization. This project also contributes to identifying dike swarms that contributed to post-Archean crustal uplifts across Ontario (Halls and Zhang 2003) and to the location of Proterozoic mantle plumes, which commonly occur where radiating dike swarms converge (e.g., Buchan et al. 2003; Ernst and Buchan 1997).

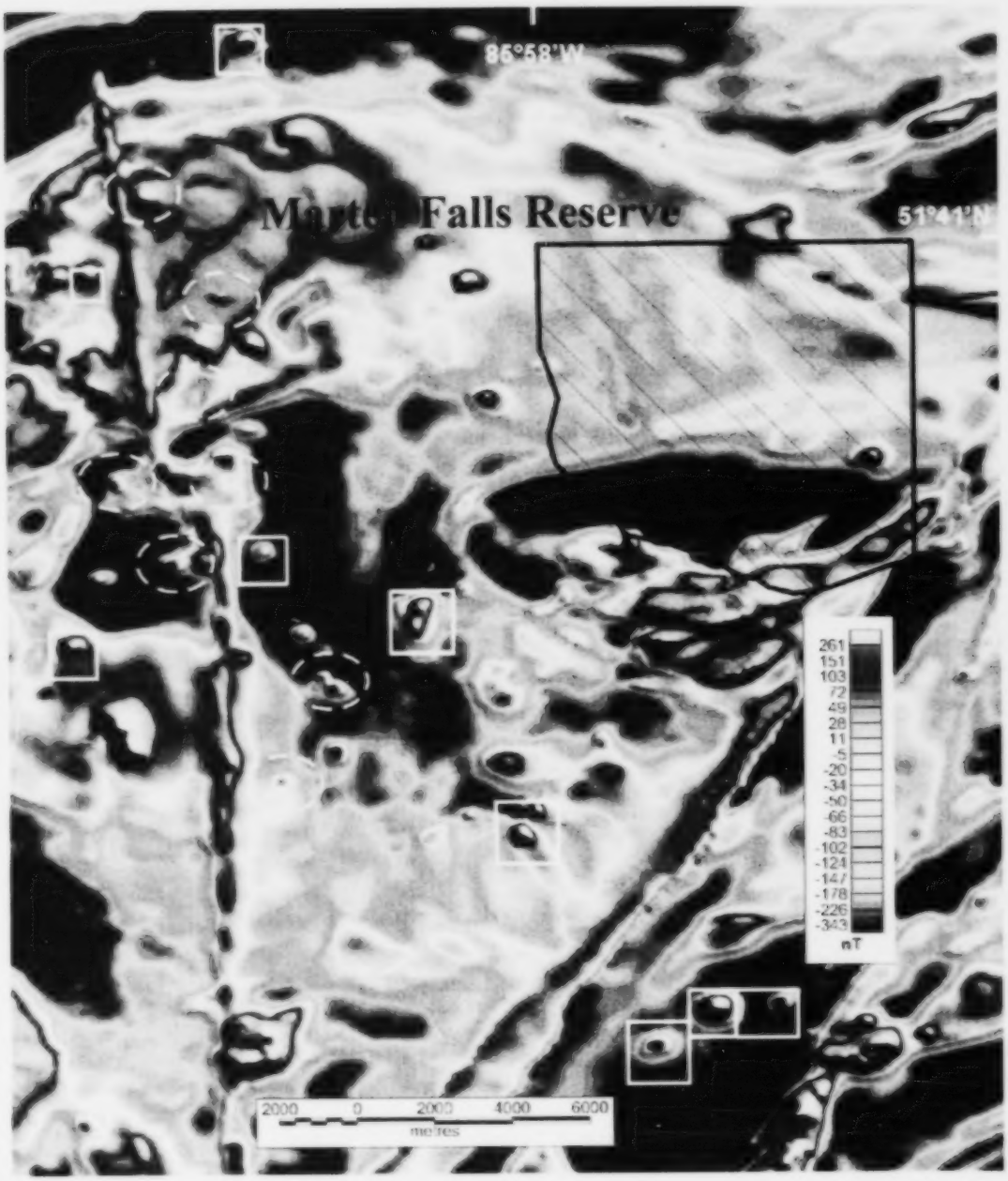

Figure 4. Detail of an aeromagnetic map in the vicinity of Marten Falls, east of Fort Hope and within the margin of the James Bay Lowlands. This shows 2 mafic dikes, a north-striking "Marathon" dike and a northeast-striking "Biscotasing" dike. Note the presence of small aeromagnetic anomalies, some of which are outlined or shown as staked for exploration, occurring close to the north-striking dike. This is a pattern of spatial correlation between anomalies and dikes similar to the "Kyle" kimberlite pipes farther north as shown in Figure 3.

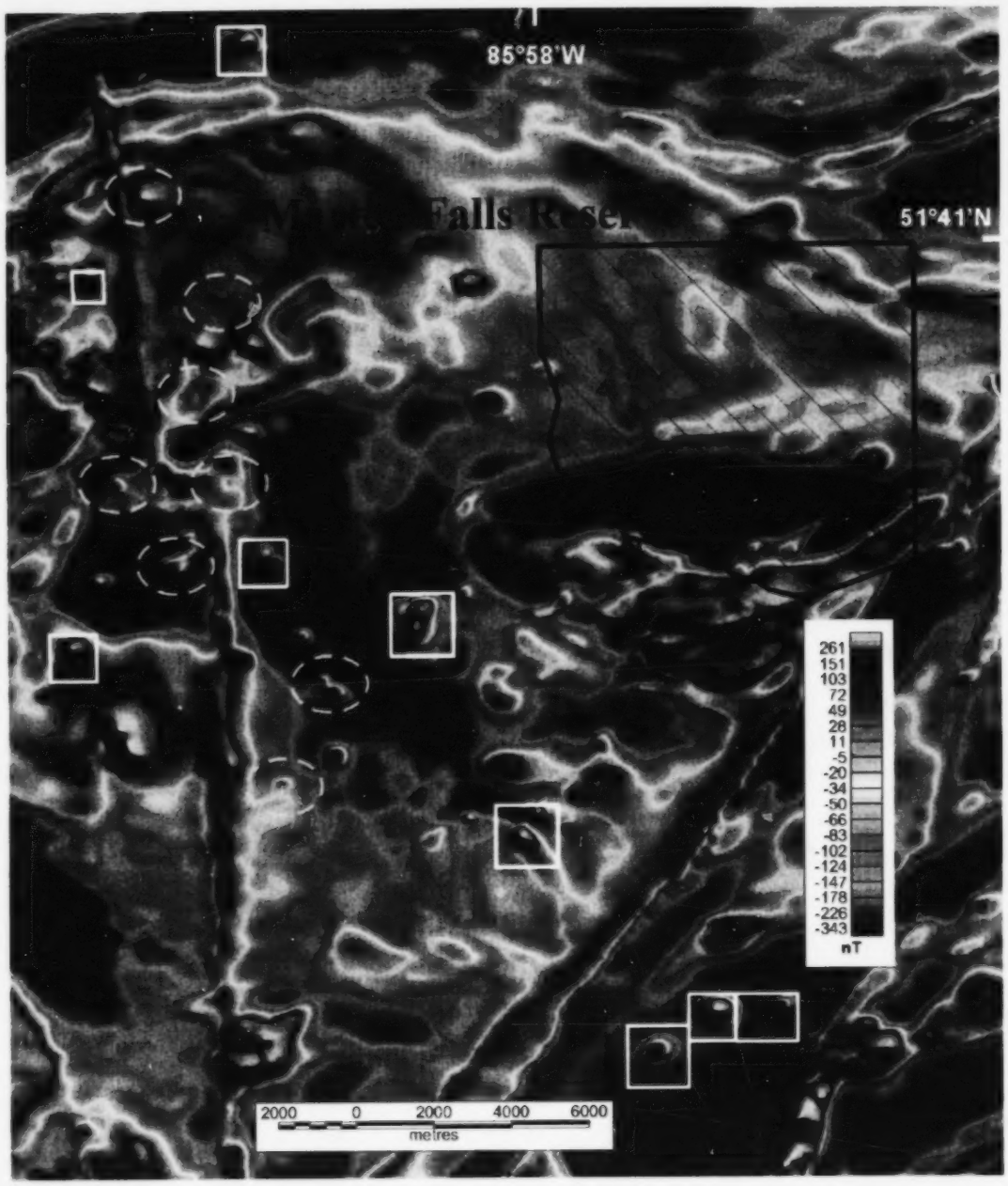

Some currently staked anomalies

Figure 4. Detail of an aeromagnetic map in the vicinity of Marten Falls, east of Fort Hope and within the margin of the James Bay Lowlands. This shows 2 mafic dikes, a north-striking "Marathon" dike and a northeast-striking "Biscotasing" dike. Note the presence of small aeromagnetic anomalies, some of which are outlined or shown as staked for exploration, occurring close to the north-striking dike. This is a pattern of spatial correlation between anomalies and dikes similar to the "Kyle" kimberlite pipes farther north as shown in Figure 3.

Acknowledgements

HCH thanks the following: Field and laboratory assistants Jaime Estrada, Stefan Tylak, Adrian van Rythoven, John Henderson and Alan Lovette for help in collecting and measuring the paleomagnetic samples. The paleomagnetic research was supported by Discovery Grant Number A7824 awarded to HCH from the Natural Science and Engineering Research Council of Canada.

Previous Work

Paleoproterozoic dikes of northern Ontario belong to at least 10 separate swarms defined by their U/Pb geochonological age and by their characteristic paleomagnetic pole position. Most of the paleomagnetic and U/Pb work relevant to this report has been carried out in the last 20 years after pioneering studies by Fahrig et al. (1965). Dikes from the Matachewan swarm were dated at 2446 and 2473 Ma by Heaman (1997). They were studies paleomagnetically by Ernst and Halls (1984); Bates and Halls (1991), Halls and Shaw (1988); Halls (1991); Halls and Zhang (1995, 2003), and Vandall and Symons (1990) and geochemically by Phinney and Halls (2001). Paleomagnetism and geochronology of the 2170 Ma Biscotasing swarm was reported by Buchan et al. (1993) and by Halls and Davis (2004). The 2101 to 2121 Ma Marathon swarm was dated by Hamilton et al. (2002) and also by Buchan et al. (1996), who measured paleomagnetism and geochemistry as well. The 2076 Ma Fort Frances swarm was dated by Buchan et al. (1996), with paleomagnetism and geochemistry determined by Halls (1986). The *circa* 2040 Ma Kapuskasing dikes were dated using Ar/Ar by Hanes et al. (1988). Paleomagnetism was studied by Halls and Palmer (1990), Symons et al. (1994) and Halls et al. (1994). Finally the 1140 Ma Abitibi dikes were documented by Ernst and Buchan (1993). Noteworthy in these investigations has been the recognition of at least 1 magnetic field reversal in all these swarms with the exception of the Fort Frances. In addition, companion studies have used the dikes as indicators of block faulting, uplift and rotation of the Archean crust. The principal work in this regard has been that done by Halls and Zhang (2003) on the Matachewan swarm in connection with the structural definition of the Kapuskasing Zone and broad scale crustal tilting. The Matachewan, Biscotasing and Fort Frances swarms have also been used to show that the western half of the Superior Province has rotated ~20° counter-clockwise relative to the eastern half across the Kapuskasing Zone (Bates and Halls 1991; Halls and Davis 2004; Buchan et al. 2004).

Work in the vicinity of Lake Nipigon (Davis and Sutcliffe 1985; reinterpreted by Davis and Green 1997) determined the age of Keweenawan mafic sills at 1108 ± 1 Ma. Halls and Pesonen (1982) carried out early paleomagnetic studies on Keweenawan rocks and Van Schmus et al. (1982) summarized early geochronological work on these rocks. Work has recently been conducted by L. Heaman on the geochronology of Sibley Group sediments and the sills and mafic flows of Keweenawan age around Lake Nipigon for the Lake Nipigon Regional Geoscience Initiative (unpublished report for LNRGI, 2004; Heaman and Easton 2005), administered by the Ontario Prospectors Association. R.E. Ernst has commenced paleomagnetic studies for LNRGI in 2004 on mafic dikes in the vicinity of and particularly west of Lake Nipigon.

Geochronology

Age determinations of the various mafic dike swarms provide critical discriminations to complement the paleomagnetic study. Samples obtained from both the areas east of Lake Nipigon and from the vicinity of the Kapuskasing Zone were dated by the U/Pb method on baddeleyite and apatite at the Jack Satterly Geochonology Laboratory, University of Toronto. The results of the Lake Nipigon data, which form part

of this OGS collaborative project, are fully reported here, whereas the Kapuskasing data are only reported as unpublished data by Davis and Halls (2004). For the Lake Nipigon data, Davis and Stott (2003) reported initial results for 3 dikes, 2 north- and north-northeast-striking dikes and 1 northeast-striking dike near Hillsport, north of Manitouwadge. The following is taken from Davis and Stott (2003) with new results for 5 other samples. Sample locations are shown in bold on Figure 5.

METHODS

The samples weighed about 10 to 15 kg and were crushed using a jaw crusher followed by a disk mill. Initial separation of heavy minerals was carried out with a Wilfley table. This was followed by paramagnetic separations with a Frantz isodynamic separator, and density separations using bromoform and methylene iodide. In some cases, this method failed to yield baddeleyite or zircon. Where no baddeleyite could be found, an alternate approach was tried in which small amounts of rock powder (ca. 100 g) were passed over the Wilfley table following the method of Söderlund and Johansson (2002). After careful examination of the heavy mineral fraction, a few grains of baddeleyite could in some cases be recovered. Where there was little or no baddeleyite, apatite crystals were picked from the mineral fraction that sank in bromoform and floated in methylene iodide. Feldspar was picked from the fraction that floated in bromoform in order to determine an initial value for common Pb in the apatite.

Baddeleyite occurs as tiny (1 μg or less), flat, brown, fragments that can easily be lost during conventional mineral separation, possibly by sticking to larger grains. Fortunately baddeleyite is not susceptible to significant Pb loss, like zircon, so laboratory abrasion (Krogh 1982), which would not have been possible with such tiny grains, is not required. The freshest-looking baddeleyite crystals, based on high lustre, were chosen for analysis. Other crystals have a dull appearance either because of alteration or because they may be partially replaced by zircon. Weights of single-grain mineral fractions were estimated from digital photomicrographs (Matthews and Davis 1999). Estimated weights should be accurate to about ±20 %. This affects only U and Pb concentrations, not age information, which depends only on isotope ratio measurements (Table 1, *see* Appendix).

Apatite occurs generally as small hexagonal rods that are fresh and free of inclusions. The concentration of apatite varied widely in the dikes from quite abundant to very little. It was necessary to pick at least 50 μg of apatite because of its low U concentration and because uncertainty in the total amount of blank in an analysis increases the error in Pb isotopic measurements in proportion to the ratio of blank to sample Pb.

Feldspar occurs as cloudy to colourless fragments. The clearest inclusion-free fragments were chosen for analysis and leached in warm nitric acid (HNO_3) overnight. At least several hundred micrograms were analyzed because the Pb concentration is normally only a few ppm.

Baddeleyite and feldspar grains were washed in HNO_3 prior to dissolution. Apatite was only washed in water because it will dissolve in weak acid. ^{205}Pb-^{235}U spike was added to the dissolution capsules during sample loading. Single baddeleyite grains were dissolved using concentrated HF in teflon bombs at 200°C (Krogh 1973). Feldspar was dissolved in HF in Savillex capsules. Apaptite was dissolved in Savillex capsules using 6N HCl. Samples were dried and redissolved in 3N HCl to ensure equilibration with the spike. No further chemistry needed to be carried out on baddeleyite. Pb and U were separated from apatite and feldspar using 50 ml anion exchange columns washed with HBr, HCl and HNO_3. Total solutions were loaded directly onto rhenium filaments with silica gel. Pb and U were analyzed on a VG354 mass spectrometer using a Daly collector in pulse counting mode. The mass discrimination correction for the Daly detector is constant at 0.07%/AMU. Thermal mass discrimination corrections are

0.10% /AMU. Dead time of the measuring system was 22.9 nsec as determined using the NBS SRM 982 Pb standard.

SAMPLING AND RESULTS

Locations of samples that were successfully dated are shown in Figure 5 and results of U/Pb isotopic analyses are given in Table 1 (errors at 2 σ). Data are plotted on concordia diagrams in Figure 6 with 2 σ error ellipses. Analyses are numbered on the diagrams according to Table 1. Average age errors are given at 95% confidence levels and are based on averaging $^{207}Pb/^{206}Pb$ ages using the program of Davis (1982). This procedure has generally been found to give correct ages when applied to near-concordant data from baddeleyite or abraded zircon. Probabilities of fit are expected to be 50% on average for random data with correctly chosen analytical errors. Pb/Pb isochron were calculated using IsoPlot/Ex 3 (Ludwig 2003). All age errors are quoted at the 2 σ level.

02GRS-01A – site DP1 (Figure 6a)

This 60 m wide dike strikes 025° and dips 80°W across a hornblende monzonite phase of the Deeds pluton in the northern part of the Onaman–Tashota greenstone belt. It is well exposed in a clear-cut area, close to a logging road. The sample is taken from the medium-grained and varitextured hornblende porphyritic centre of the dike.

Only 2 tiny baddeleyite grains could be found in this sample (Figure 7a). Total radiogenic Pb contents in these grains were about 3 and 8 pg. Fortunately, blanks were at the sub-picogram level so they could be dated with reasonable precision. The analyses gave concordant and near-concordant data with overlapping $^{207}Pb/^{206}Pb$ ages that average to 2112 ± 9 Ma (51% probability of fit). This is likely to represent the age of dike emplacement.

02GRS-02A – site DP2 (Figure 6b)

A north-striking mafic dike was sampled beside the Kinghorn Road at kilometre 24, north of Jellicoe. This dike is about 29 m wide and strikes 005° and dips 80°W. The sample is from the coarsest inner part of the dike with mineral grains that are 2 to 3 mm in diameter.

A few tiny baddeleyite grains were recovered from this sample. They are mostly flat brownish fragments. Three single grains that appeared fresh, as shown by shiny surfaces (Figure 7b), were analyzed. Isotopic ratios from analysis 3 (DWD4346) changed during the course of the mass spectrometer analysis. This is likely caused by a source of common Pb on the filament that is only partially mixed with the sample, such as a grain of dust. Because all Pb ratios are measured together within a single data block, reduced concordia data can be averaged between the blocks and a correct standard deviation calculated, despite the dispersion of the measured ratios. All 3 analyses gave concordant to near-concordant data with overlapping $^{207}Pb/^{206}Pb$ ages that average to 2109.1 ± 1.6 Ma (73% probability of fit). This probably represents the age of emplacement of the dike.

02GRS-03A – site DP4 (Figure 6c)

A northeast-striking mafic dike, previously mapped by Milne (1964), is located 5 km west of the small village of Hillsport, north of Manitouwadge and well to the east of the previous samples. It is 100 to 133 m wide and strikes 040°. This dike is one of a set of widely spaced northeast-striking dikes in east-central Ontario that can be traced aeromagnetically for many tens of kilometres and that also extends under the James Bay Lowlands (Ontario Geological Survey 1992). The Hillsport dike is currently being

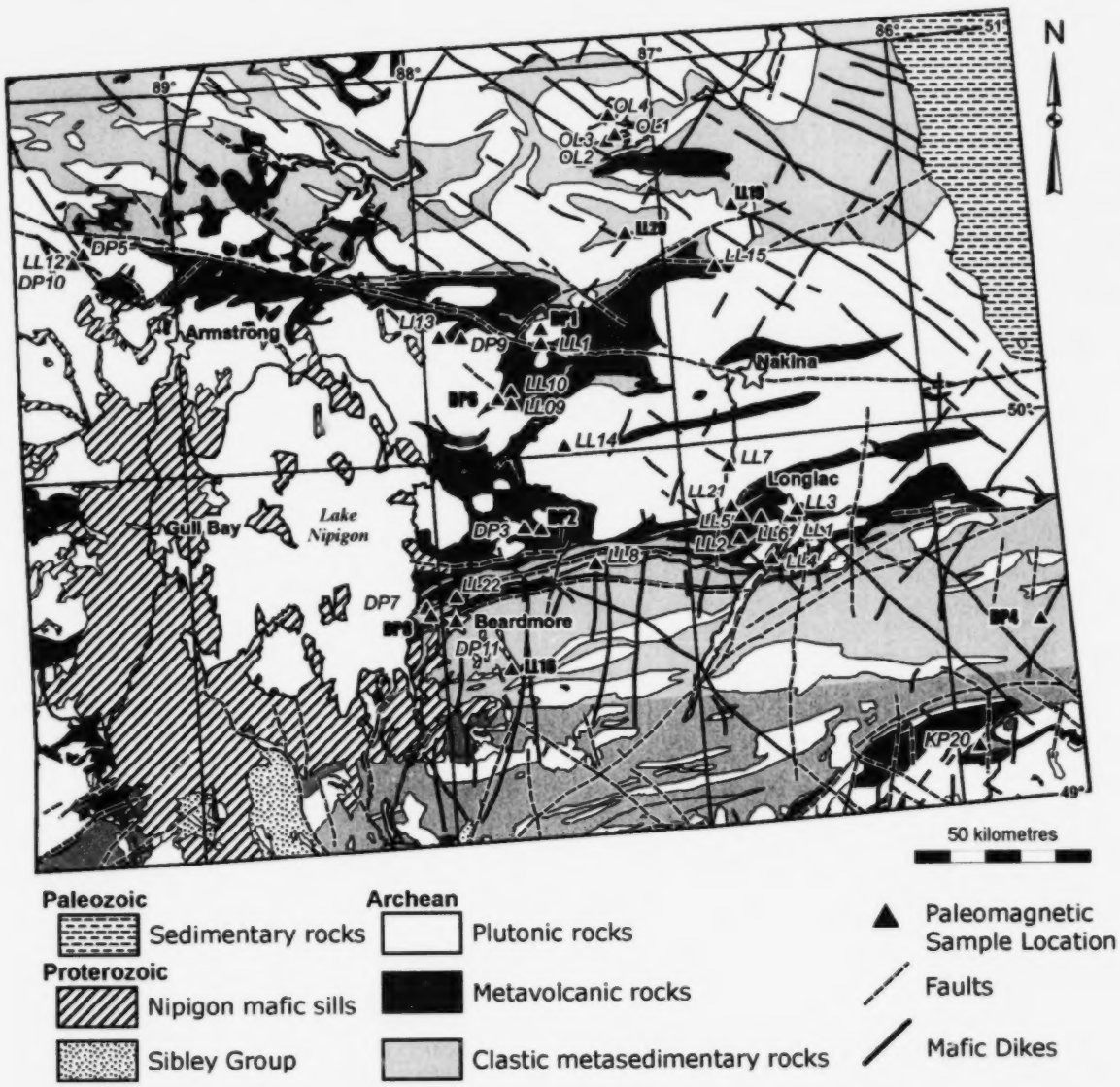

Figure 5. Geological map east of Lake Nipigon showing locations in **bold** of mafic dikes for which U/Pb dating is presented here.

quarried as a source of railroad ballast. Sample 02GRS-3A was taken from the coarsest, gabbro to leucogabbro portion of the dike, with grains 2 to 4 mm in diameter and feldspar laths up to 1 cm long.

A few baddeleyite flakes were recovered from this sample as well as a few tiny grains of zircon, which are probably inherited from wall rocks. All the baddeleyite grains have dull surfaces and do not appear as fresh as in the previous samples. However, baddeleyite is typically much less susceptible to Pb loss from alteration than zircon, even without abrasion, so the 3 freshest-looking baddeleyite grains (Figure 7c) were analyzed. These gave slightly discordant data but the $^{207}Pb/^{206}Pb$ ages agree within error. Their average age of 2170.7 ± 1.1 Ma (52% probability of fit) is probably the age of emplacement of this dike.

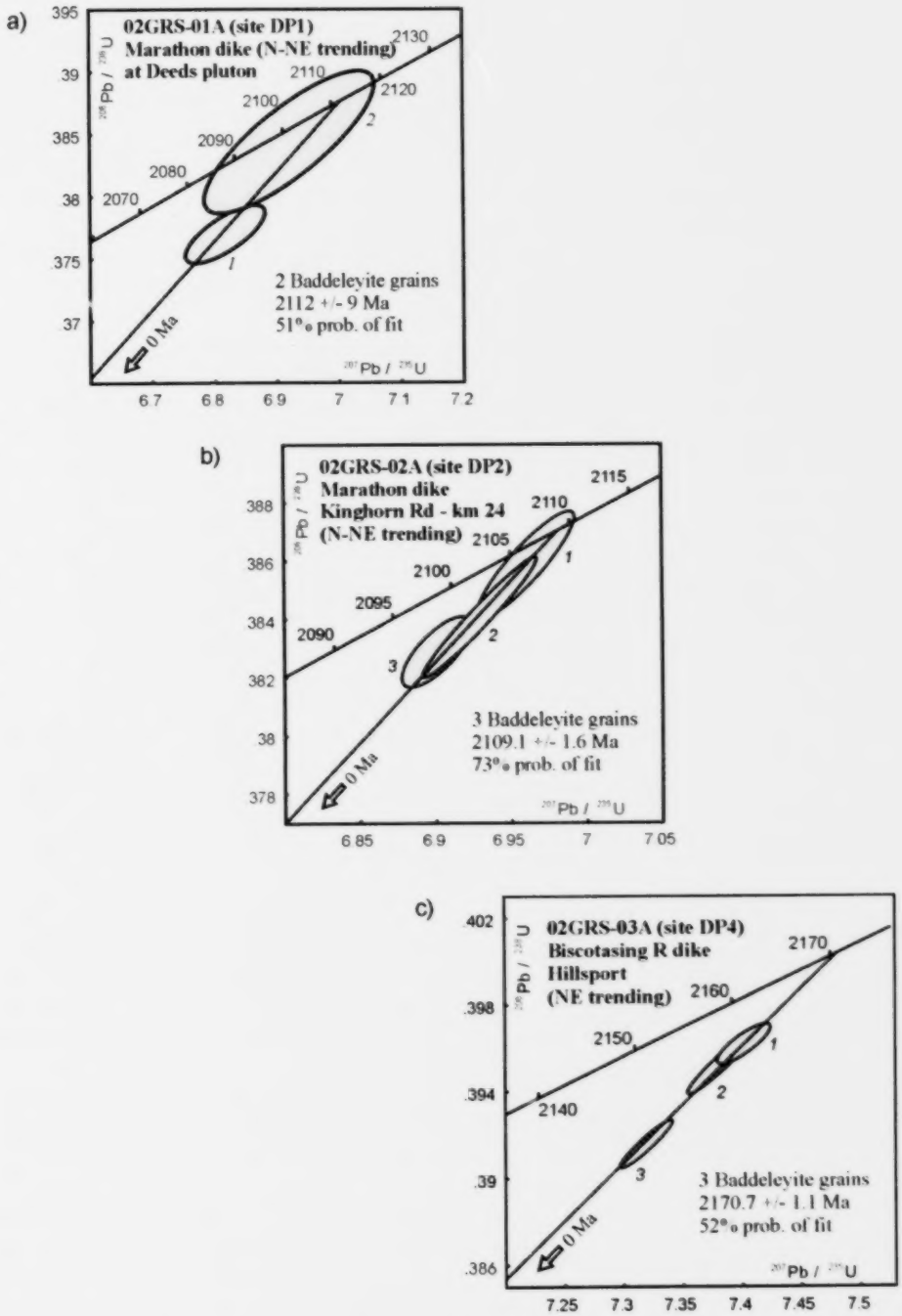

Figure 6. Concordia diagrams showing U/Pb analyses for baddeleyite from samples of mafic dikes: a) crossing the Deeds pluton; b) at kilometre 24 on Kinghorn Rd; and c) 5 km west of Hillsport.

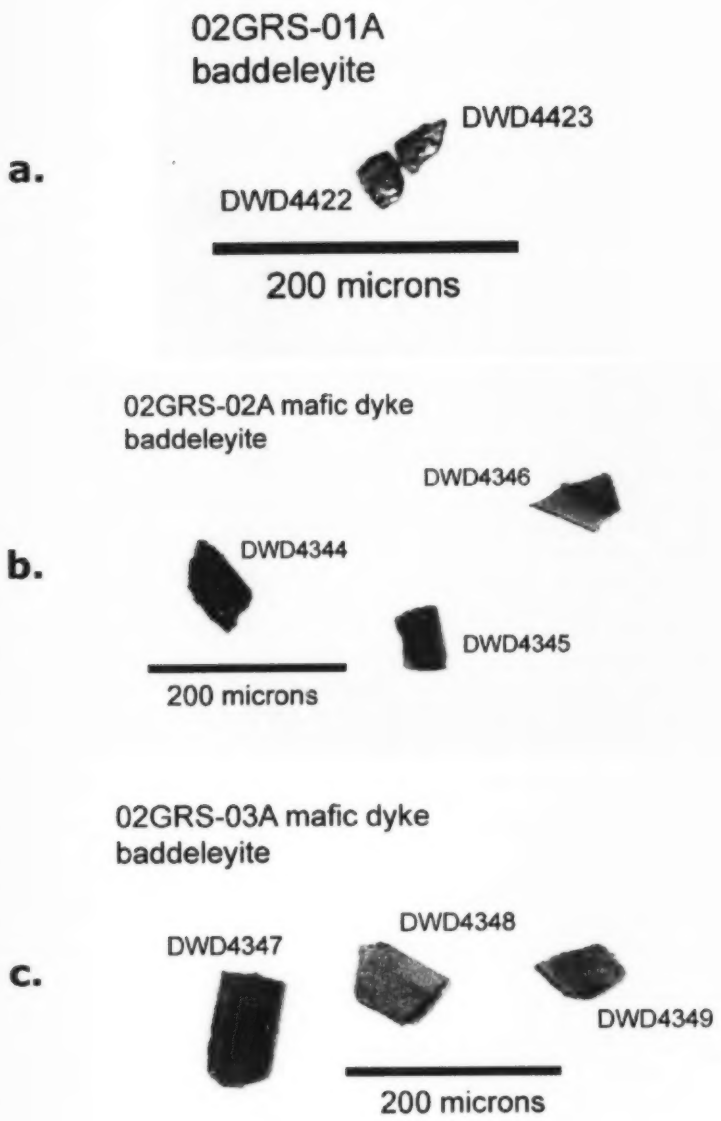

Figure 7. Images of baddeleyite from each of the 3 mafic dikes as listed in Table 1 in the Appendix with analytical results illustrated in Figure 6.

03GRS-29 – site LL16 (Figure 8a)

A locally feldspar porphyritic mafic sill, up to 2 km across in map view, was sampled approximately 25 km southeast of Beardmore. The strike of minerals weakly aligned in this unit and the alignment of local, plagioclase feldspar-rich bands are 160°, with dip 75°W. The western contact of the sill against granitoid rocks appears to be dipping shallowly westward.

Five long, thin, tabular baddeleyite grains, comprising mostly fragments, were picked from this sample. The 4 freshest grains (Figure 9) are concordant and give an age of 1103.7 ± 2.3 Ma.

04GRS-03A – site LL19 (Figure 8b)

This sample was from a northwest-striking mafic dike in the eastern English River Subprovince, northeast of O'Sullivan Lake. Three baddeleyite grains produced a discordant age of 2459 ± 5 Ma, confirming that this dike is part of the Matachewan dike swarm. Only 2 other baddeleyite ages for the Matachewan swarm have been previously reported, farther east (Heaman 1997), as 2473 +16/-9 Ma, east of the Kapuskasing Zone, and 2445.8 +2.9/-2.6 Ma, west of the Kapuskasing Zone.

04GRS-07A - site LL20 (Figure 8c)

This sample was taken from a northeast-striking dike within the English River Subprovince, north of the Onaman–Tashota greenstone belt and northeast of Abamasagi Lake. Preliminary results from 3 baddeleyite grains give an age of 2125.7 ± 1.2 Ma. This is the oldest dike of Marathon age found thus far and its northeast strike diverges significantly from the more predominant north and north-northeast trends of other Marathon dikes to the south. Dikes of this trend in the eastern English River Subprovince appear to provide a link to the aggregate of north-striking dikes of the western margin of James Bay Lowlands, close to where the Kyle kimberlite pipes are located (*see* Figure 3). This could imply the existence of a major northeast-trending kink band of dike-filled fractures joining the 2 north-striking segments of Marathon dikes trending through the Onaman–Tashota greenstone belt and western James Bay Lowlands.

03GRS-001D - site DP6 (Figure 10)

This sample was from a north- to northeast-striking dike south of McDonough Lake stock and west of Metcalfe Lake. The sample yielded only a few tiny baddeleyite grains of generally poor quality. One baddeleyite gave a somewhat discordant datum with a $^{207}Pb/^{206}U$ age of 2106 ± 5 Ma. Analysis of a multi-grain fraction of apatite gives a $^{206}Pb/^{238}U$ age of 2113 ± 32 Ma (Figure 10). The high common Pb content results in low precision, which was corrected using Stacey and Kramers (1975) crustal Pb average. Precision is sufficient to identify this dike as a member of the Marathon swarm. This dike also appears to be parallel to a dike intruding the Deeds pluton at site DP1. The Marathon age results for site DP6 also correspond with a discordant $^{207}Pb/^{206}Pb$ age of 2106 ± 5 Ma (Figure 10) from a tiny baddeleyite grain. This grain was the best of several tiny grains of not very good quality recovered off the Wilfley table using a method proposed by Söderlund and Johansson (2002). A fraction of apatite (Figure 11a) corrected for initial common Pb, based on the measured $^{238}U/^{204}Pb$ ratio, gives a $^{206}Pb/^{238}U$ age of 2149 ± 22 Ma and a $^{207}Pb/^{206}Pb$ age of 2175 ± 36 Ma. If the measured isotopic composition of the feldspar Pb is used, the $^{207}Pb/^{206}Pb$ age is the same but the $^{206}Pb/^{238}U$ age drops to 2076 ± 14 Ma. A Stacey and Kramers (1975) growth curve correction (with 2 σ error of 0.4%) produces the most concordant datum with a $^{206}Pb/^{238}U$ age of 2125 ± 32 Ma. The latter age agrees best with the baddeleyite analysis, suggesting that the Stacey and Kramers model provides a good approximation for initial common Pb in the apatite and that the measured $^{238}U/^{204}Pb$ ratio in the feldspars is slightly too high, perhaps because of the presence of unsupported U that was not removed during the leaching process.

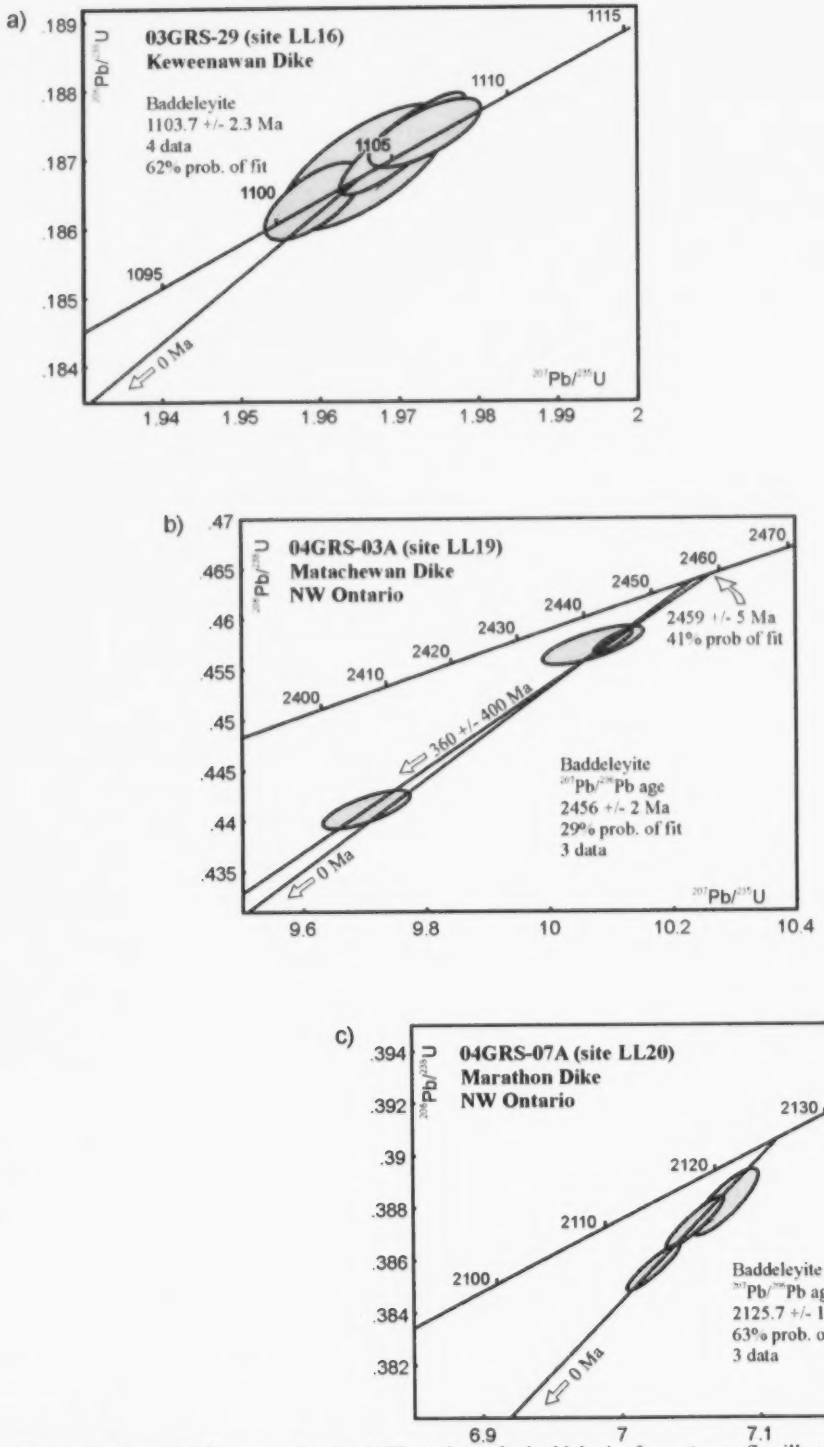

Figure 8. Concordia diagrams showing U/Pb analyses for baddeleyite from a) a mafic sill at site LL16, southeast of Beardmore. (This is the easternmost sill relatable to the ca. 1109 Ma Nipigon embayment and gives the youngest age associated with this magmatic event; b) a mafic dike northeast of O'Sullivan Lake; and c) a dike northeast of Abamasagi Lake, which gives the oldest age associated with the Marathon swarm. This dike strikes northeastward, unlike most Marathon dikes east and southeast of Lake Nipigon.

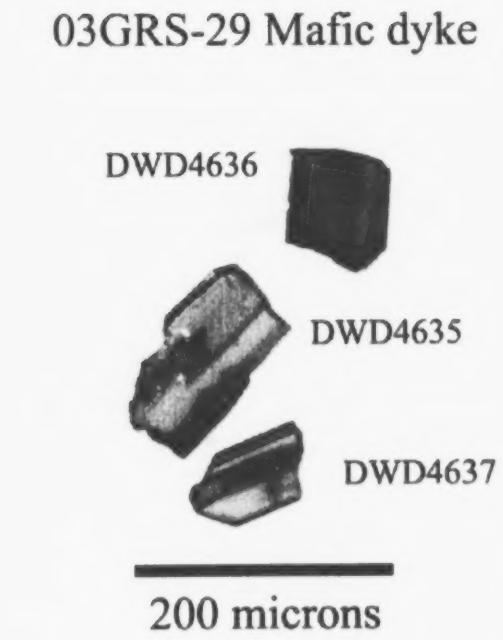

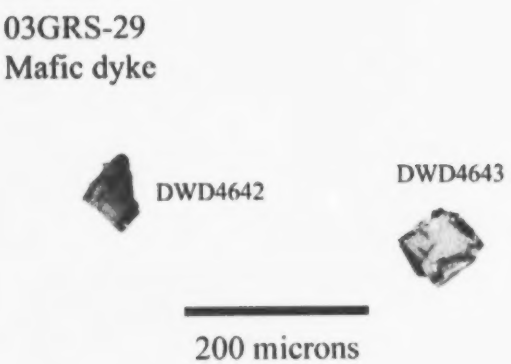

Figure 9. Images of baddeleyite from site LL16, the analytical results from which are shown in Figure 8 and listed in Table 2 in the Appendix.

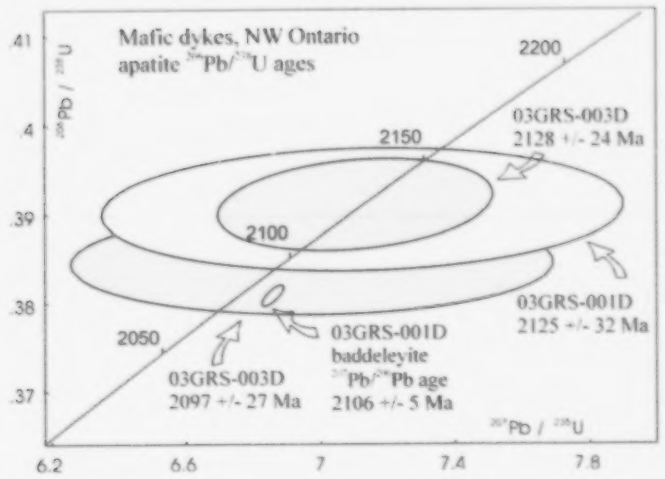

Figure 10. Concordia diagram showing U/Pb analyses for baddeleyite and apatite from 2 sites: DP6 (03GRS-001) and DP8 (03GRS-003). See Figure 5 for geographic locations.

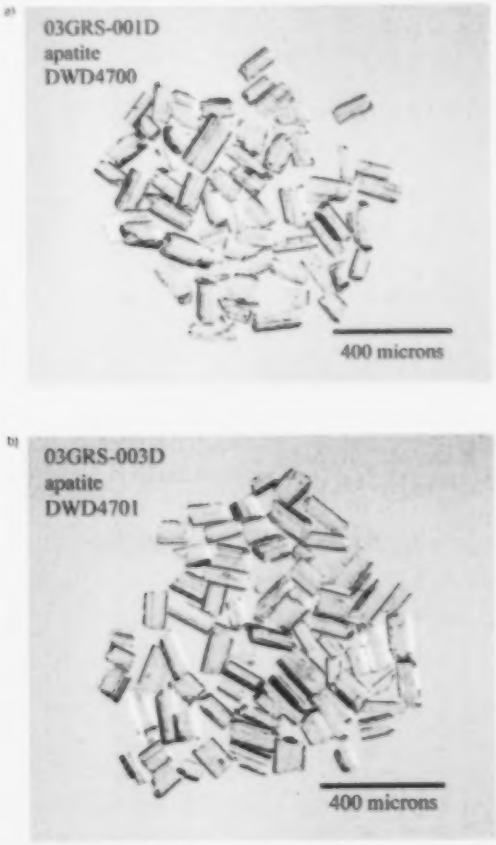

Figure 11. Images of apatite analyzed from a) site DP6 and b) site DP8 on which U/Pb age determinations were completed.

03GRS-003D – site DP8 (Figure 10)

This north-striking dike, is south of Undersill Lake, close to the Keweenawan sills on Lake Nipigon. No baddeleyite was recovered but 2 apatite (Figure 11b) and 2 feldspar fractions were analyzed. Both feldspar fractions gave Pb isotopic compositions with a large radiogenic Pb component ($^{206}Pb/^{204}Pb$ of 30-40). Measured $^{238}U/^{204}Pb$ ratios are also high but corrected Pb isotopic ratios are unrealistically low, indicating again the presence of unsupported U. A Pb/Pb isochron based on the 4 data gives a slope age of 2132 ± 120 Ma. The data do not fit the isochron within error (mean square weighted deviate = 13, probability of fit = 0), which is the reason for the large error. Initial Pb compositions based on the Stacey and Kramers model again give the most concordant U/Pb data with $^{206}Pb/^{238}U$ ages of 2128 ± 24 Ma and 2097 ± 27 Ma for the 2 apatite fractions. Therefore, like most north- and north-northeast-striking dikes crossing the Onaman–Tashota greenstone belt, this is part of the Marathon swarm.

DISCUSSION

Dating of extremely small baddeleyite crystals containing a few picograms of radiogenic Pb is feasible if analytical blanks can be kept at the sub-picogram level. The precision of such ages is sufficient to distinguish between dike swarms. The major problem with dating mafic dikes is recovery of baddeleyite because of the typical small size and tabular habit of the crystals. It is recommended that rock sample sizes be restricted to no more than a few kilograms and mineral separation be carried out using special methods that do not involve working with dry sample. A few hundred grams of powder may be the largest amount that it is practical to work with using such methods, but baddeleyite should be recoverable from such small amounts in many cases, especially if it is visible in thin section.

Where baddeleyite cannot be recovered, apatite may give ages that are sufficiently precise and accurate to distinguish between swarms. The U/Pb system in apatite can be reset at temperatures of 400 to >500°C (Cherniak et al. 1991) depending on cooling rate and grain size. Most mafic dike swarms in the Superior Province have intruded into a stable continental platform that has suffered little erosion and remained well below this temperature, at least near the surface, since Archean time. Apatite ages could be made more precise if reliable initial Pb isotopic compositions could be measured using plagioclase. In the present study, plagioclase in the dikes was found to have low concentrations of Pb (generally much less than 1 ppm). This makes measured Pb compositions susceptible to bias from labile Pb and U components. The approach taken in the present study was to carefully hand pick the highest quality plagioclase crystals, a time-consuming process that only allows a small amount of sample to be selected, and subject the crystals to a mild leach. Another approach (Chamberlain and Bowring 2000) is to isolate a larger amount and subject it to a much stronger leach, dissolving over 90% of the material, to arrive at the primary Pb isotopic composition. This may be more effective in future studies.

The 2 north-northeast-striking mafic dikes from east of Lake Nipigon agree in age at 2109 Ma, which indicates that they likely belong to the **Marathon swarm**. Previous work on geochronology and paleomagnetism of the Marathon swarm has shown that R- and N-polarity Marathon dikes give different ages (2101 ± 2 Ma for R and 2121 +14/-7 Ma for N; Hamilton et al. 2002, Buchan et al. 1996) and different pole positions (Buchan et al. 1996). The 2109 Ma age of the Marathon dikes, east of Lake Nipigon, falls between these ages.

The Hillsport dike gives a distinctly older age of 2170.7 ± 1.1 Ma, which indicates that it is part of the **Biscotasing swarm**. Previous ages from this swarm are 2167.8 ± 2.2 Ma and 2171.6 ± 1.2 Ma on baddeleyite from 2 dikes (Halls and Davis 2004) and 2166.7 ±1.4 Ma on baddeleyite and zircon from another dike (Buchan et al. 1993).

A mafic sill, dipping shallowly westward, southeast of Beardmore, with an age of 1103.7 ± 2.3 Ma, is the youngest representative known of the voluminous, *circa* 1109 Ma **Keweenawan** mafic intrusive activity centred on Lake Nipigon.

Paleomagnetism

SAMPLING PROCEDURES

Samples, oriented using both a magnetic and sun compass (Photo 1), were collected from north to east-northeast- and northwest-striking dikes which are the most common Paleoproterozoic dike trends in the area bordering the northern and eastern shores of Lake Superior (*see* Figures 1 and 2). Typically 5 to 10 samples were collected from each site with emphasis on chilled margins where, due to the small size of magnetite carriers, primary remanence is most likely to survive. The majority of samples were collected by field drilling, but a few, from more finely jointed chilled margins, were collected as blocks which were then subsequently cored in the laboratory. After the cores were cut into cylindrical specimens 2.45 cm in length and in diameter, at least 1 specimen per sample was subject to stepwise alternating field (AF) demagnetization, using a Schonstedt TD-1 instrument, to a maximum field of 100mT. After each incremental increase in alternating field demagnetization to remove secondary magnetization components, the natural remanent magnetization (NRM) was measured on a modified DIGICO magnetometer with reproducibility down to 10^{-3} Am^{-1}. The data were then analysed using Principal Component Analysis (Kirschvink 1980) in combination with stereoplots and vector diagrams, following normal paleomagnetic procedures.

The paleomagnetic results, which are given in Tables 3 to 8 in the Appendix, represent sample collections from 2 sources. More than 30 of the sites, those with designations LL and DP, have been collected as part of this OGS project over the last 3 years from locations mostly east of Lake Nipigon but west of Manitouwadge, where northwest-trending, *circa* 2.45 Ga Matachewan dikes and younger north to northeast trending, *circa* 2.11 Ga Marathon, *circa* 2.17 Ga Biscotasing and *circa* 1.10 Ga Keweenawan dikes outcrop. Approximately 50 more sites, mainly in northeast- to east-northeast-trending dikes, have been collected prior to 2002 from the area between Manitouwadge, in the west, to Wawa and the general region of the Kapuskasing Zone (KZ) in the east (Figure 2). Site designations for these dikes are KP, KS, HP, MK, TK and numbers without letters, all signifying that the dikes were collected during different field seasons between 1987 and 2002 and were primarily aimed at sampling Matachewan dikes. This report therefore includes a compilation of paleomagnetic results from all north- to east-northeast-trending dikes, represented in the west by the Marathon swarm and in the east by east-northeast-trending ~2.04 Ga Kapuskasing dikes (Halls et al. 1994). Most of the northeast-trending dikes between these 2 extremes were once referred to informally as the "White River" swarm (Ernst and Halls 1984). Some of the dikes, particularly the thicker ones, are now known to belong to the Biscotasing dike swarm (Halls and Davis 2004), but it is now clear from the new U/Pb data that Marathon equivalents are also present.

Photo 1. H.C. Halls orienting a drill core sample to be used for paleomagnetic analysis; from a Matachewan mafic dike on the Kinghorn Road in the Onaman–Tashota greenstone belt.

RESULTS

Matachewan Dikes

Previous studies have shown that Matachewan dikes possess a unique paleomagnetic direction in Canada, in having shallow negative inclinations toward the south-southwest, designated as R polarity, and a virtually antipodal remanence designated as N polarity. Paleomagnetic field tests show conclusively that these remanences are primary and that only a single reversal of the earth's magnetic field, from R to N, characterised the Matachewan igneous episode (Halls 1991), which spans about 30 million years, from 2446 to 2473 Ma (Heaman 1997). Further observations are that whereas both polarities are represented close to the focal area of the swarm in the Lake Huron area, N-polarity dikes gradually die out northwards (Bates and Halls 1991). One baddeleyite U/Pb age has been obtained from the dike at site LL19 and gives an age of 2459 ± 5 Ma. The reversal is closely dated because 2 dikes of opposite polarity have virtually the same age of 2446 Ma (Heaman 1997). The new age is in harmony with the earlier conclusion that only a single reversal from R to N polarity characterised the Matachewan magmatic episode, and shows that the R-polarity epoch for the western half of the Matachewan swarm lasted at least 10 million years. The ability of the U/Pb method to resolve small time intervals implies that further measurements could show how the swarm evolved spatially.

Previous paleomagnetic studies have shown a positive correlation between regional dike trend and magnetization declination suggesting that the western half of the swarm, when followed northwards, has been differentially rotated about vertical axes on passing across the KZ (Bates and Halls 1991). The net result is that an originally more linear swarm has been distorted into an open Z-shaped pattern, with the stem of the Z corresponding to that segment of the swarm which transects the KZ. The age of this deformation is uncertain but probably accompanied major uplift and dextral fault motion along the KZ at about 2 Ga (Halls and Davis 2004). On a larger scale the results indicated that the western half of the Superior Province has rotated counterclockwise at least 10 to 15° with respect to the eastern half that lies on the opposite side of the KZ. The rotation was thought to increase to approximately 20° farther west in the Lake Ogoki area, but the amount of data (from the OL sites in Figure 1) was too small to allow a firm conclusion. However our new results (Table 3) from the region immediately east of Lake Nipigon, at the extreme western end of the swarm (Figure 12), show, using the method of McFadden and Lowes (1981), that the mean direction is significantly different ($p = 0.05$) from the combined mean of paleomagnetic data from the Lake Gamitagama (Symons et al. 1994) and Ranger Lake (Halls and Shaw 1988) areas south of Wawa (Table 6) where dikes occur along strike of, and thus may correlate with, those east of Lake Nipigon. A counterclockwise rotation of 23 ± 8° of the Lake Nipigon area, relative to that south of Wawa, can be calculated using the method of Beck (1983). An important observation is that the Gamitagama data lie to the *north* of the KZ, and therefore that other hitherto unrecognized faults, associated with the KZ and involved in the rotation, should be expected in the Wawa area. For example a noticeable change in Matachewan dike trend occurs along the northern margin of the Michipicoten greenstone belt and may signify an intervening fault zone. Here also Matachewan dikes exhibit anomalously high feldspar clouding intensity, which may indicate that they have been uplifted (Halls and Palmer 1990; Halls and Zhang 2003), possibly as a result of this faulting. The new data in Table 3 show that the Matachewan dikes near Lake Nipigon are exclusively of R polarity, in keeping with earlier observations that the N-polarity dikes are more common towards the focus of the radiating swarm and were emplaced during its final waning stages, when igneous activity had shrunk to more proximal areas of the plume.

Biscotasing Dikes

The Biscotasing dikes were originally defined by Buchan et al. (1993) on the eastern side of the KZ, where they formed a series of wide northeast-trending dikes that curved northwards to more east-northeast trends and showed repeated sinistral offsets across north-trending Onaping faults (Buchan and Ernst 1994). One of the dikes gave a U/Pb age of 2166 ± 1.4 Ma. More recent U/Pb dating has shown that Biscotasing dikes also occur to the west of the KZ, where they yield baddeleyite ages of 2171.6 ± 1.2 and 2167 ± 2.2 Ma (Halls and Davis 2004). A paleomagnetic comparison across the entire Biscotasing swarm suggests that the western dikes have been rotated counterclockwise by about 15° with respect to the eastern ones on the opposite side of the KZ (Halls and Davis 2004), and therefore support the rotations given by the Matachewan dikes. However the Biscotasing results are less secure, because the number of dikes (6 for both the western and eastern populations) is relatively small and their remanence direction, being relatively steep, is less sensitive to vertical-axis rotation.

New U/Pb baddeleyite data from the 100 m wide Hillsport dike (site DP4) gives an age of 2170.7 ± 1.1 Ma (Figure 6c). This dike is therefore a member of the Biscotasing swarm but differs in that it is the first to have R polarity. It has a paleomagnetic direction (D = 104°, I = - 57°, Table 4) that is only about 10E away from being antipodal to N-polarity Biscotasing dikes. This dike was originally thought to be part of the 1141 Ma Abitibi dike swarm (Ernst and Buchan 1993, their site A1). The dike is presently being quarried as road ballast for railway track beds. Another northeast-trending dike (KP20) lies at the western end of Swill Lake, west of Manitouwadge, and is lithologically similar to the Hillsport dike and is

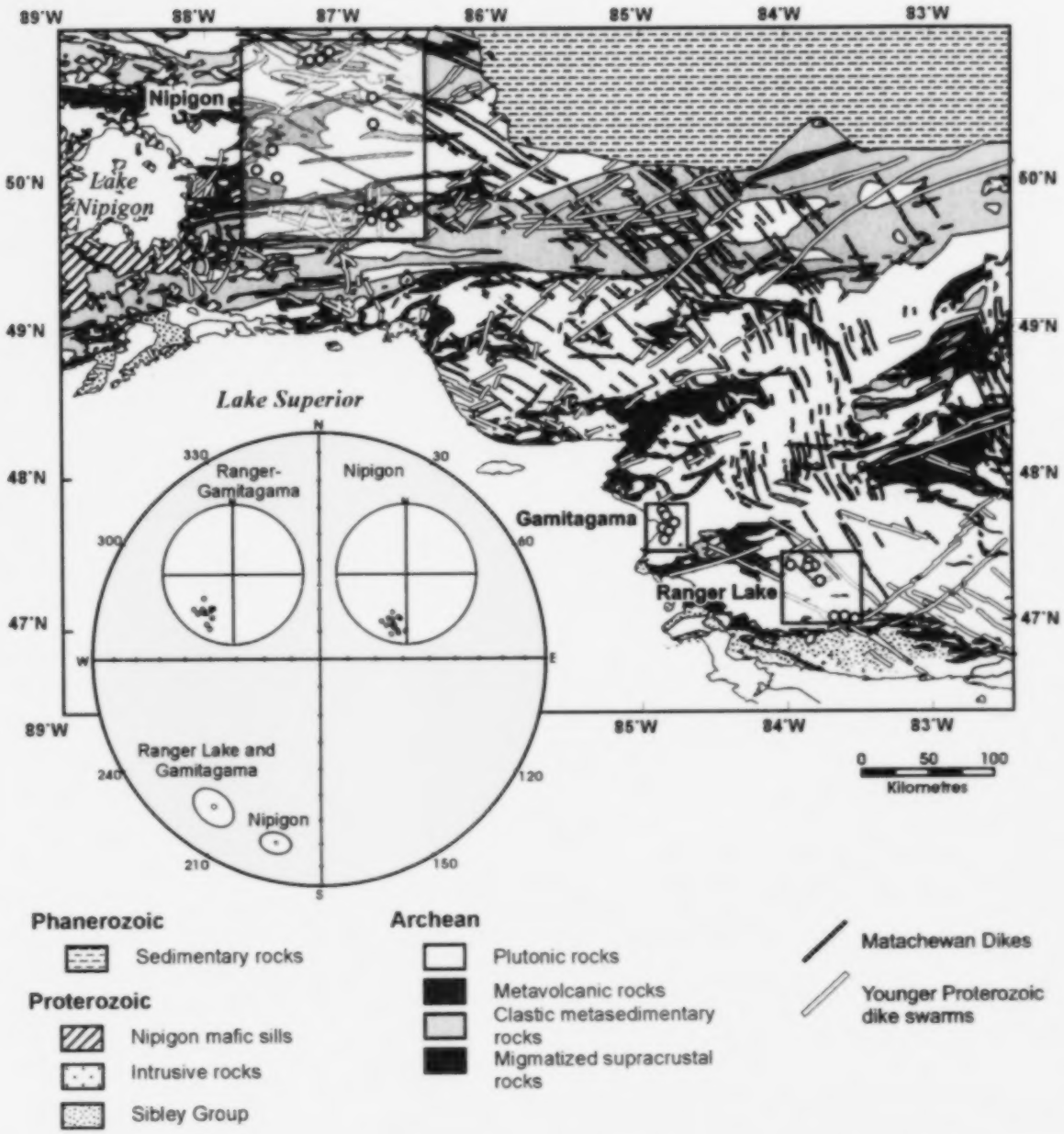

Figure 12. Map showing the distribution of Matachewan dike sites east of Lake Nipigon and south of Wawa, in the Gamitagama and Ranger Lake areas. The inset equal-area projections show mean site directions for the Nipigon area and for the Gamitagama and Ranger Lake areas combined. All directions are recomputed to a common site at 48°N, 79°W, and only site data have been accepted where N ≥4 (N is the number of samples yielding stable end points), and $\alpha_{95} \leq 15°$ (α_{95} is the radius of the 95% confidence circle about the mean direction). The mean directions of Nipigon and combined Gamitagama–Ranger Lake are significantly different at the 95% confidence level, a result of a 23° difference in declination but only 3° in inclination. Assuming that horizontal rotation is the cause and using the statistical method of Beck (1980), the Nipigon area has rotated 23° ±8° relative to the Wawa area. Paleomagnetic data sources: Gamitagama, Vandall and Symons (1990); Ranger Lake, Halls and Shaw (1988); and Lake Nipigon, Halls and Stott (2003, 2004).

about 60 m wide. It gives a remanence direction that is virtually identical to the Hillsport dike (Table 4). This suggests that both sites DP4 and KP20 are from the same dike, a correlation not readily apparent from aeromagnetic data due to highly magnetic host rocks in the vicinity of Manitouwadge. The Manitouwadge site is readily accessible by road and represents a potential quarry site for further railroad ballast extraction.

Our new results from Biscotasing dikes have not contributed further to the crustal rotation story but they have demonstrated for the first time that the Biscotasing igneous episode spanned at least 1 reversal of the Earth's field. The age of the R-polarity dike is not significantly different from ages previously reported for the N-polarity dikes; the only conclusion is that dike emplacement lasted about 5 million years and included at least 1 field reversal of unknown sense. One feature in common with all of the dike swarms having ages of about 2.1 Ga is that R and N directions are not exactly antipodal; in each case the R declination is displaced in a clockwise direction from that which is antipodal to N by about 5 to 20° (Table 7). The Biscotasing data look similar: the R direction is again displaced clockwise from the antipodal N direction. The similarity in asymmetry between different ages of dikes is curious but the size of the declination asymmetry emphasizes the need in rotation studies to only compare dikes having the same remanence polarity.

Marathon Dikes

Marathon dikes yield 2 magnetic polarities (Buchan et al. 1996): a younger R one (D = 133.5°, I = -50.7°, α_{95} = 6.8°, N = 12), dated by U/Pb on baddeleyite at 2101 ± 1.6 Ma (Hamilton et al. 2002), and an older N-polarity suite (D = 294.8°, I = 57.0°, α_{95} = 6.3°, N = 16), dated by U/Pb also on baddeleyite at 2121+14/-7 Ma (Buchan et al. 1996).

New age data reported here not only help to further constrain the time of the polarity reversal but also show that the Marathon swarm is more extensive than previously thought. Three R-polarity dikes give the following U/Pb baddeleyite ages: (DP6: 2106 ± 5 (this report), MK7 and TK48: 2106.3 ± 3.5 and 2104.6 ± 1.8 Ma, respectively (Davis and Halls, unpublished data, 2004). These ages show that the younger R-polarity interval lasted at least from 2101 to about 2107 Ma. However 2 baddeleyite ages from N-polarity dikes, 2121+14/-7 Ma (Buchan et al. 1996), and a more precise one of 2125.7 ± 2 Ma (this report) show that the field had changed polarity no more than 15 to 20 million years later. Two dikes (sites DP1 and DP2) respectively gave U/Pb baddeleyite ages of 2112 ± 9 Ma and 2109.1 ± 1.6 Ma (this report), which identifies them as members of the Marathon swarm, but both were paleomagnetically unstable. The dike at DP1 lies about 20 km northeast of DP6, which has a well-defined R polarity (Table 4). At both locations the dikes have similar widths (approximately 60 m) and northeast trends and, on the basis of aeromagnetic data, may represent the same dike. The erratic paleomagnetic behaviour of sites DP1 and DP2 is a puzzle. One possibility is that their slightly older ages, although not significantly different from R-polarity dikes, may be real, in which case both dikes may have acquired their magnetizations during the transition from R to N polarity when the Earth's magnetic field had an anomalous direction and low intensity. The poor paleomagnetic results at site DP1 were a surprise; the dike had fresh, unjointed chilled margins against granite and did not appear to be lightning-struck.

Site DP8 yielded a paleomagnetic direction similar to that given by nearby Keweenawan Logan diabase sills, raising suspicion that the remanence is the result of Keweenawan re-heating of a Marathon dike heated from above by a sill since removed by erosion. $^{206}Pb/^{238}U$ ages of 2128 ± 24 Ma and 2097 ± 27 Ma for 2 apatite fractions from this dike confirm that this dike is part of the Marathon swarm.

A major discovery is that 6 dikes with northeast to east-northeast trends that occur in the vicinity of the KZ have paleomagnetic signatures similar to N and R Marathon dikes. Two of these dikes (MK7 and

TK48) have baddeleyite ages confirming that they are part of the Marathon swarm. These results, together with the new Marathon dikes discovered east of Lake Nipigon, demonstrate that the Marathon swarm is more widespread than hitherto known and has a radiating pattern, with a focal area south of eastern Lake Superior. Although only a few Marathon dikes near the Kapuskasing structure have been identified with confidence, their paleomagnetic results, for both N *and* R dikes, show mean declinations that are rotated about 10 to 15° clockwise from equivalent results farther west (Table 7 and Figure 12).

Kapuskasing Dikes

A large number of mainly east-northeast-trending dikes occurs in the vicinity of the KZ, and are known informally as Kapuskasing dikes (Halls et al. 1994; Symons et al. 1994). The only age data available are from a baked zone of a dike within the KZ, from which a hornblende Ar/Ar age of 2043 ±14 Ma was obtained by Hanes et al. (1988). The dikes are known to pre-date uplift within the KZ; here they exhibit feldspar clouding and 3 give a negative baked contact test (see review by Halls et al. 1994). So far no dikes have been identified that would be suitable for U/Pb dating. Paleomagnetically, the dikes yield steep magnetization directions of either N or R polarity, whether or not they are inside or outside of the KZ, but only those sites are given in Table 4 for dikes that are vertical and unrotated within the KZ. At 5 sites (SL13, TK36, KP22, 186 and 214) detailed baked contact tests have been carried out where a Kapuskasing dike is observed to crosscut a Matachewan dike. All 5 tests are positive because the baked host rocks give the same direction as that in the younger dike, and typical Matachewan directions appear beyond the baked zone. These results indicate that outside the KZ the steep N and R remanences are primary and formed at the time of original dike cooling and not at some later date. The swarm affinity of SL13 is conjectural because it has anomalous geochemistry with respect to all other dikes in this part of the Superior Province and may represent apophyses from an Abitibi dike that outcrops nearby.

Some Kapuskasing dikes may belong to the Marathon swarm, because known Marathon dikes of comparable trend occur in their midst. However if Kapuskasing dikes outside of the KZ are identified based on their steep (>60°) paleomagnetic inclination, the mean directions for R and N Kapuskasing dikes are significantly different at the 95% confidence level from R and N Marathon dikes, respectively (Table 7 and Figure 13). If some of these Kapuskasing dikes are Marathon in age, they are unlikely to change the mean declination of either the Marathon East N and R populations, so that the observation that the eastern Marathon dikes are rotated clockwise with respect to the western ones is likely to be strengthened. Most of the Kapuskasing dikes are of R polarity and the inclusion of some of them into the Marathon East R group would increase the mean remanence inclination towards that given by the western population, a requirement for vertical axis rotation. Since the eastern data are derived from dikes that are close to, but also on the western side of, the KZ, it means that the western half of the Superior Province has not behaved as a rigid unit, a conclusion also reached from the Matachewan data of Bates and Halls (1991). If *all* the dikes in the vicinity of the KZ are Marathon dikes, the mean N and R populations retain the same declination as the separate (Marathon, Kapuskasing) populations, but the mean inclination is significantly steeper than the western population. There is no evidence from the dip of the dikes that regional northward tilting of the crust of about 10° has occurred, so it is suspected that most of the Kapuskasing dikes are not the same age as their western counterparts. This would indicate that the reversal is not the same one as that recorded for the Marathon dikes. However, an R magnetization, with a steep upward inclination, occurs within the Chapleau block of the KZ and is known to be secondary and related to crustal uplift. The dikes within the Chapleau block have acquired a later magnetization in the same way as the Matachewan dikes, which show younger N polarity within versus dominantly R outside the KZ (Halls and Zhang 2003). For Kapuskasing dikes, R magnetization is therefore younger than N. This is the same age relationship between polarities found for Marathon dikes, inviting speculation that the Kapuskasing dikes *are* equivalent to the Marathon. Only U/Pb dating of the Kapuskasing dikes will resolve the issue.

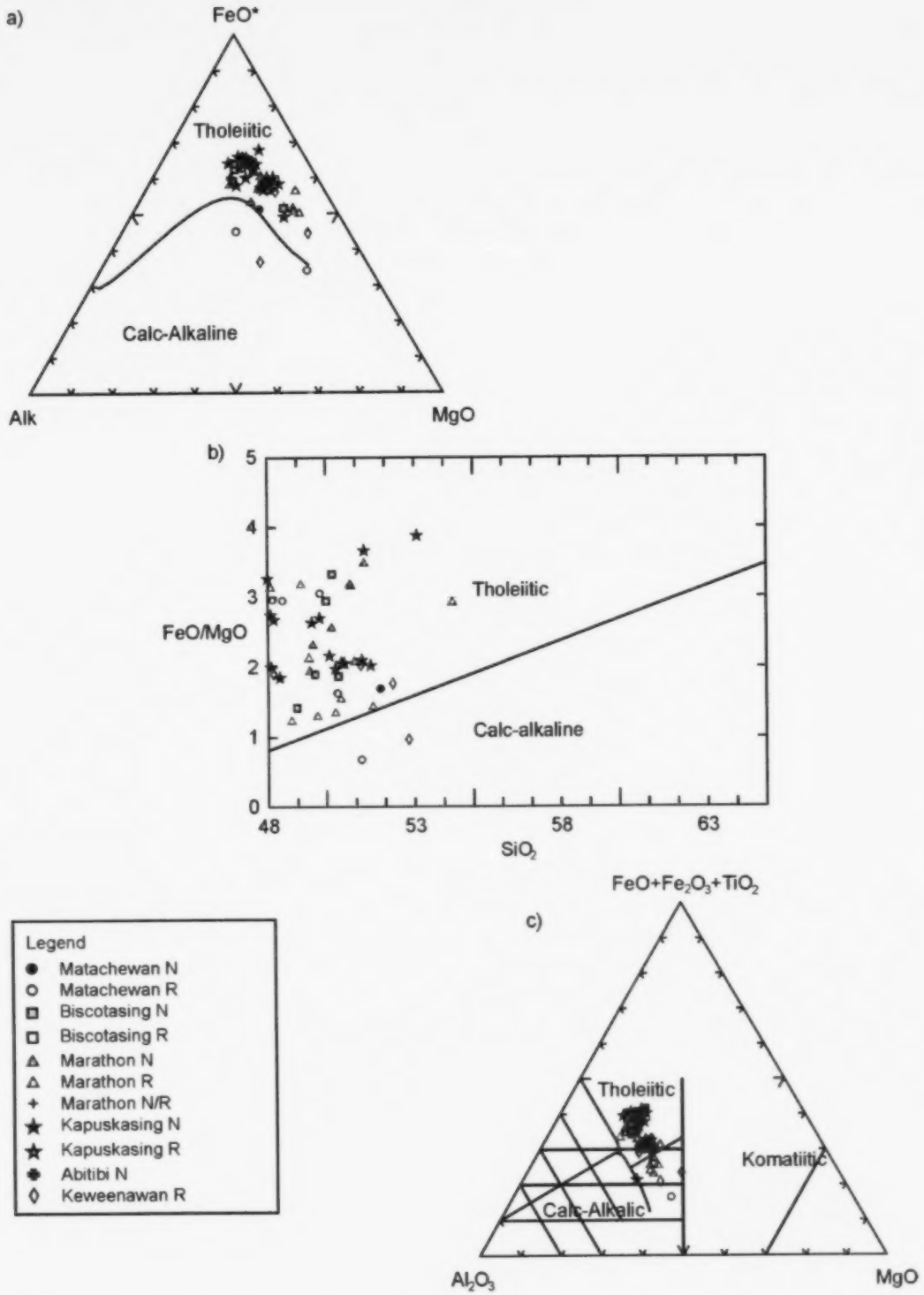

Figure 13. Major element analyses illustrating dominant tholeiitic character of the mafic dikes swarms.

Keweenawan Dikes

One of the aims of this project was to test the eastern extent of the Keweenawan Lake Nipigon igneous province, and to find suspected feeders for the sills. The Keweenawan data are given in Table 5. Three observations may be made: 1) only 1 dike, more or less north trending, is considered to be a Keweenawan dike; 2) at 2 sites (LL22 and DP11), which are more or less on strike, a dike with similar thickness and lithology (abundant feldspar phenocrysts arranged in dike-parallel layers) gave virtually the same steep, upward, easterly-directed paleomagnetic direction that characterises the Logan intrusions; 3) at site DP10, northwest of Lake Nipigon, a diabase body gave directions similar to 2 nearby sites (DP5 and LL12) in northwest-trending dikes. It is possible that these dikes are either feeders for the diabase or are older, with a magnetization that has been reset by the diabase. At site LL16, on the eastern side of Lake Nipigon a large west-dipping diabase sill occurs. This is the easternmost of several thick, slightly arcuate, west-dipping sills in the Beardmore region, northeast of Barbara Lake in the Quetico Subprovince. The typical Keweenawan R paleomagnetic signature and U/Pb age of 1103 ±3 Ma have been obtained from a sill at site LL16, rendering it the youngest intrusion yet discovered for Keweenawan R igneous rocks.

Dikes of Other Affinities

Site SL13 shows a younger set of east-northeast-trending dikes cutting a Matachewan dike. A positive baked contact test shows that the remanence of the younger dikes is primary, but their geochemistry is anomalous suggesting they may be apophyses of a large Abitibi dike that passes the site to the immediate south. At site LL7, a series of dikes, each a few centimetres wide, cut granite. The dikes trend northwest and yet give a direction similar to that of the north- to northeast-trending Marathon dikes (Table 4). A poorly exposed, but much wider (20-40 m) northwest-trending dike occurs about 200 m to the north and may be the main feeder dike. Dikes having the same age but which are orthogonal to one another are known from Greenland and northern Canada and could indicate that crustal deviatoric stress was low at the time of intrusion, so that intrusion of one dike set rotates the minimum stress direction to favour subsequent orthogonal intrusion. Another possibility is that the dikes at LL7 are the same age as the west-northwest-trending Wabigoon dike as it also gives a northwest-directed and steep down magnetization (Dunlop 1983).

DISCUSSION

U/Pb geochronology and paleomagnetism show that the 2101 to 2107 Ma R-polarity Marathon swarm is more extensive than previously known and forms a large radiating dike swarm extending from the Wawa–Chapleau region in the east to Lake Nipigon in the west. The age of the R to N polarity reversal is now constrained to lie between about 2107 and 2121 Ma, with the possibility that the erratic paleomagnetic results from dikes dated at 2109 and 2112 Ma were formed during the time of the polarity transition.

The paleomagnetic data from Matachewan dikes in the Lake Nipigon region, at the extreme western end of the swarm, show that the Superior Province to the west of the KZ has rotated counterclockwise by as much as 20° with respect to the eastern side of the KZ. The amount and sense of rotation is comparable to that recently reported by Buchan et al. (2004) using the 2076 Ma Fort Frances and 2069 Ma Lac Esprit swarms that lie respectively to the west and east of the KZ. These results, together with the new data from the Marathon swarm, reinforce the idea that Matachewan and Marathon dikes within about 50 to 100 km northwest of the KZ (Bates and Halls 1991) have been rotated relatively clockwise with respect to their

counterparts farther west in the Lake Nipigon and Hornepayne areas. This observation suggests that the KZ, in keeping with earlier observations from radiometric dating of Archean rocks (Manson and Halls 1997), is much broader than presently recognized and that significant northeast-trending faults associated with this structure extend for several hundred kilometres to the northwest of the main fault-bounded zone of uplift but may be particularly significant at a distance of about 100 km, along the northwestern margin of the Michipicoten Greenstone belt.

Geochemistry

METHODOLOGY

Whole rock major and trace element geochemical analyses are presented in Table 9 (in the Appendix) for 61 samples of dikes, mostly taken from within 30 cm of chilled margins. These samples, of drill core and fresh rock, were obtained from each of the different dike swarms on which paleomagnetic analyses were done. The intent of this study was to provide additional discrimination amongst the mafic dike swarms. The analyses were conducted in the Geoscience Laboratories of the Ontario Geological Survey. Major elements were determined by X-ray fluorescence spectrometry (XRF). Trace elements, including rare earth elements (REEs), were analyzed by inductively coupled plasma mass spectrometry (ICP-MS). Selected metals, including Co, Cu, Ni, V, were analyzed by inductively coupled plasma atomic emission spectroscopy (ICP-AES). A separate ICP-AES analysis was conducted for Pt, Pd and Au in some samples.

RESULTS

Samples plotted in Figures 13 to 17 include for consistency only those from chilled margins of dikes. Alteration in variable amounts is visible in thin sections of most dikes sampled. Consequently, the elements that are mobile in hydrothermal fluids, especially in the coarser portions of the dikes, were at least partially remobilized and of limited value for petrogenetic interpretation. Loss on Ignition (LOI) varied from less than 0.01 to 7.07%, mostly less than 2%, and reflects internal alteration affecting each of these dike swarms. Major element geochemistry of the dike swarms is illustrated in Figure 13. The dike swarms are mostly tholeiitic as is evident from major element diagrams (Figures 13a and 13b). They are dominantly high-iron tholeiitic with high-magnesium tholeiitic compositions among some other dikes, the Marathon and Keweenawan R sites in particular (Figure 13c). Considerable variations in both major and trace element compositions are evident amongst the dike swarms, especially of Marathon and Kapuskasing dikes, so that geochemical discrimination amongst the dike swarms is limited.

The relatively low values of Ni (less than 138 ppm), Cr (less than 315 ppm) and Co (less than 72 ppm) indicate the parent magmas were not derived from a peridotitic mantle source but are consistent with crustal contamination of the source in each case. No clear temporal evolution in the major and trace element composition of the dike swarms is apparent regionally.

Previous workers (e.g., Condie 2003, 1997; Schmitz et al. 1995) have shown that binary plots of ratios of trace elements that are incompatible in the mantle, such as Th/Ta – La/Yb, provide a useful discrimination of magma sources. They have been used by Condie (2003) to illustrate broad temporal evolution from the Archean to Phanerozoic but also provide limited discrimination with considerable overlap amongst some of the dike swarms. Such plots are shown in Figure 14 and some relevant features and apparent grouping patterns from them are described below, keeping in mind the limited sample set for

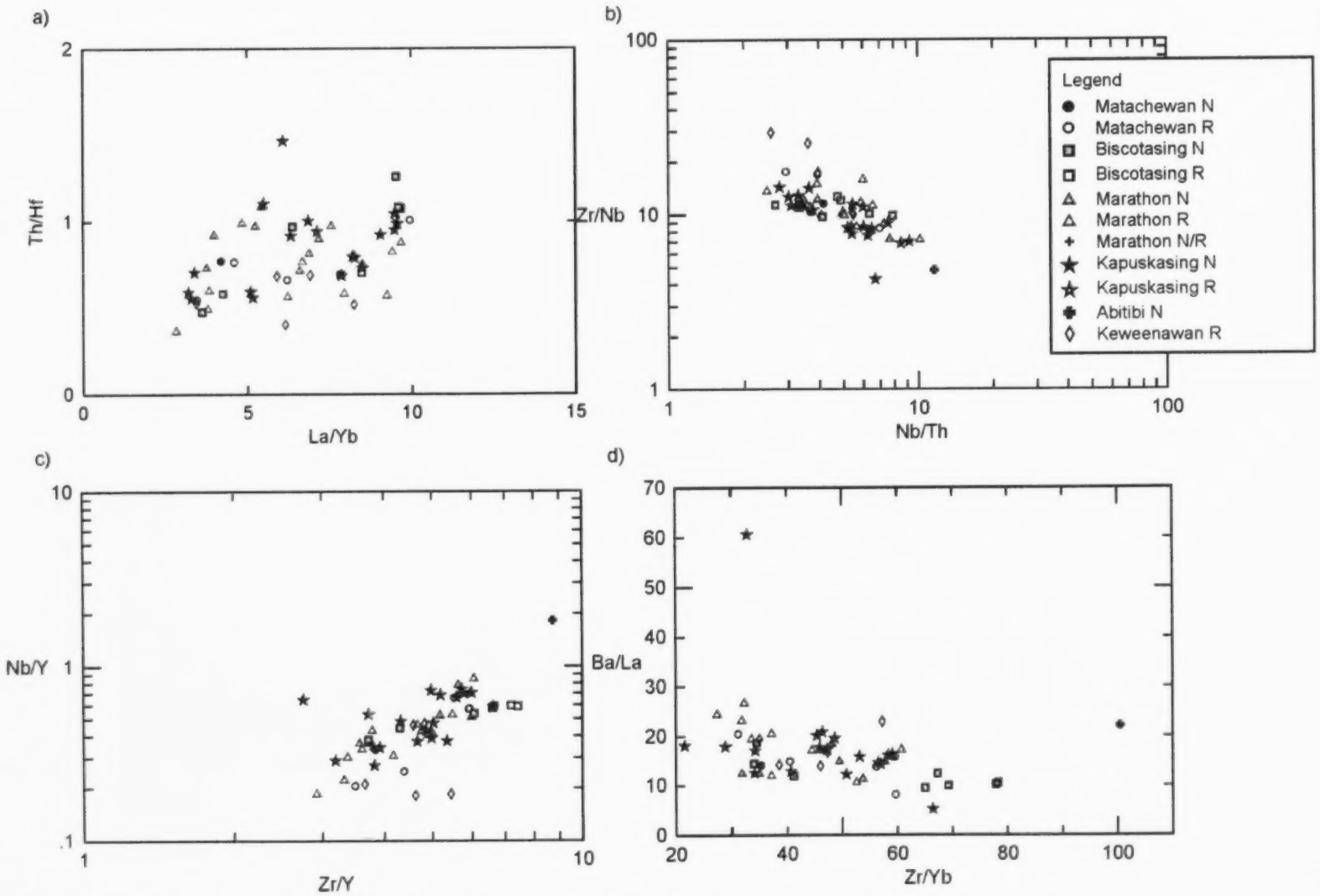

Figure 14. Selected plots of trace elements for the dike swarms, illustrating some limited discrimination among some of the dike swarms.

most of the dike swarms represented here. Figure 15, showing extended Th-Nb-REE plots normalized to primitive mantle after Sun and McDonough (1989), illustrates the wide range in trace and REE concentrations even within individual swarms. There is considerable overlap in the Th-Nb-REE plots amongst all dikes except the Abitibi dike. Variable continental contamination of mafic magma in the dike chill margins is reflected in the enriched light REE relative to HFSE (high field strength elements) Zr, Hf, Nb and Th>Nb<La that dominantly characterise all dike swarms (Figures 15 and 17d).

Matachewan Dikes

Matachewan dikes are dominantly Fe-rich tholeiites with relatively low Zr (104-166 ppm) and with such a spread of trace element and REE values that they cannot easily be discriminated geochemically from the other dike swarms (e.g., Figure 14a and 14b). These dikes contain slightly higher Cr (generally greater than 90 ppm) than most Biscotasing and Kapuskasing dikes but otherwise are comparable with Marathon and Keweenawan dikes. They show a narrower range of Ni values (49-76 ppm) than other dikes. Matachewan R dikes tend to show tighter clusters on trace element ratio plots and lower Nb/Y and Nb/La ratios than most dikes from other swarms apart from Keweenawan R dikes (e.g., Figures 14c and 16a). The single sample of Matachewan N dike generally lies apart from the R dikes geochemically, showing higher Nb and lower Hf, for example, than the R dikes.

Biscotasing Dikes

Biscotasing dikes are generally Fe-rich tholeiites with a broad range of TiO_2 (1.22 to 3.47%) and Zr (63-258 ppm). They are not easily discriminated geochemically from dikes of the other swarms. However, Biscotasing N dikes show lower Zr and Nb/Y ratios than Biscotasing R dikes (Figure 14c). The Biscotasing N dikes tend to show 2 clusters in several trace element ratio plots (e.g., Zr/Yb ratio, Figure 14d) but there is no spatial explanation for this and might be an artifact of the limited sampled set. Figure 15c shows that the spread in concentration of REE and Th-Nb is similar to Marathon dikes and provides no easy geochemical discrimination amongst northeast-striking Marathon and potential Biscotasing dikes east of Lake Nipigon.

Marathon Dikes

Marathon dikes range from Fe-rich tholeiites amongst the N dikes to more Mg-rich tholeiitic amongst the R dikes (Figure 13c). Marathon N dikes tend to have slightly higher V and lower Cr concentrations than Marathon R dikes (Figures 16c and 16d). Marathon R dikes generally have slightly lower, but collectively overlapping, Nb/Y, Nb/La, and Hf/Sm ratios than Marathon N dikes and lower Nb/La ratios than Kapuskasing R dikes (Figures 14c, 16a and 17a). Marathon R dikes generally show lower or comparable Hf/Sm and higher Hf/Th ratios than Marathon N dikes (Figures 17a and 17b). Marathon R dikes have comparable or generally higher Ba/La ratios to most other dikes. Some distinction in trace element ratios, between Marathon N and R dikes, is apparent in plots of La/Sm vs. Gd/Yb and Th/Nb vs. La/Nb (Figures 17c and 17d). Marathon and Kapuskasing dikes both show a broader linear spread and lack of clustering of various trace element ratios compared to other dikes.

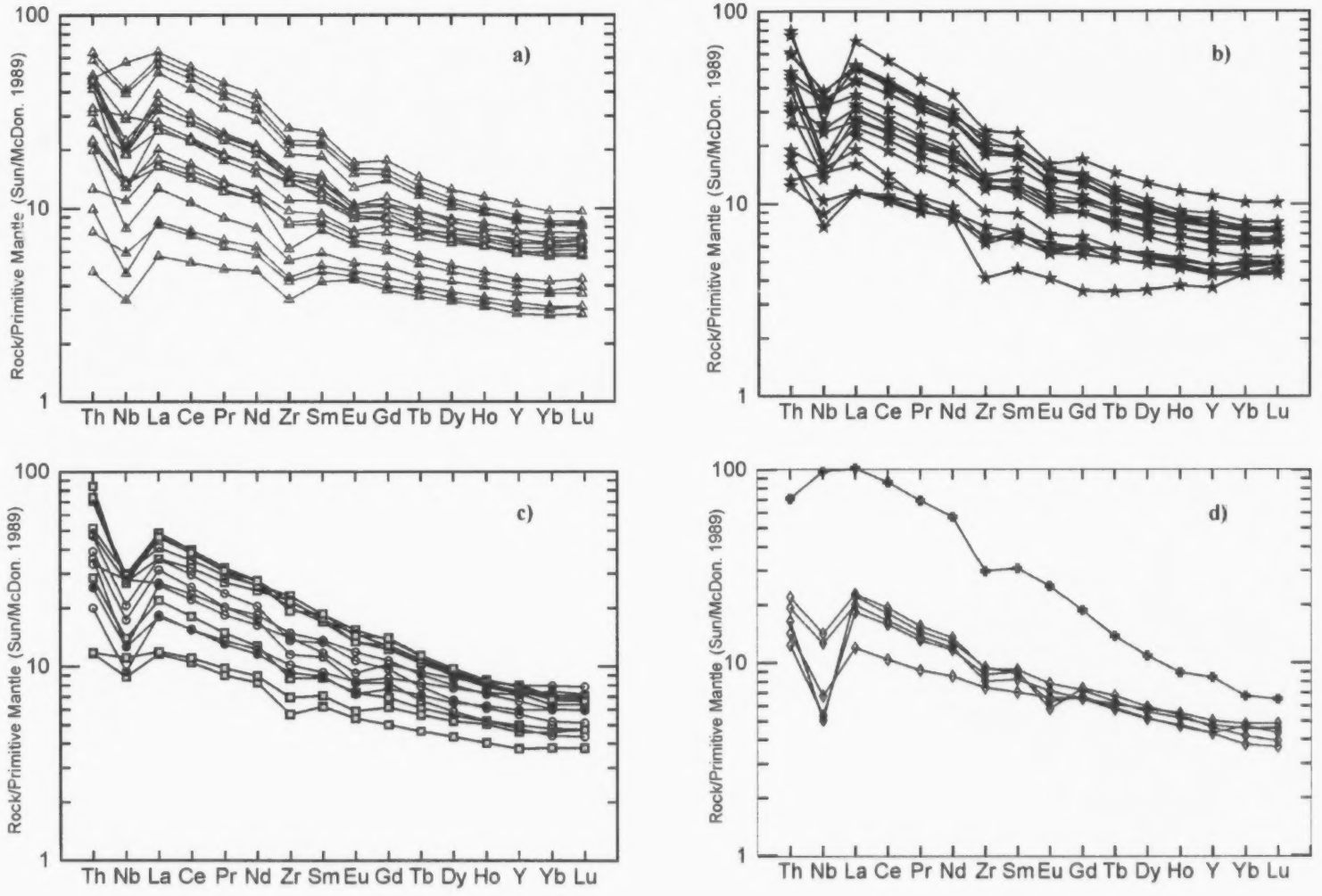

Figure 15. Extended trace element plots normalized to primitive mantle illustrating the overlapping spread amongst the dike swarms. a) Marathon; b) Kapuskasing; c) Biscotasing (squares) and Matachewan (circles); d) Keweenawan (diamonds) and Abitibi (crosses). The diversity is greatest for a) Marathon and b) Kapuskasing dikes. Legend as in Figure 14, with N polarity = filled symbols; R polarity = open symbols.

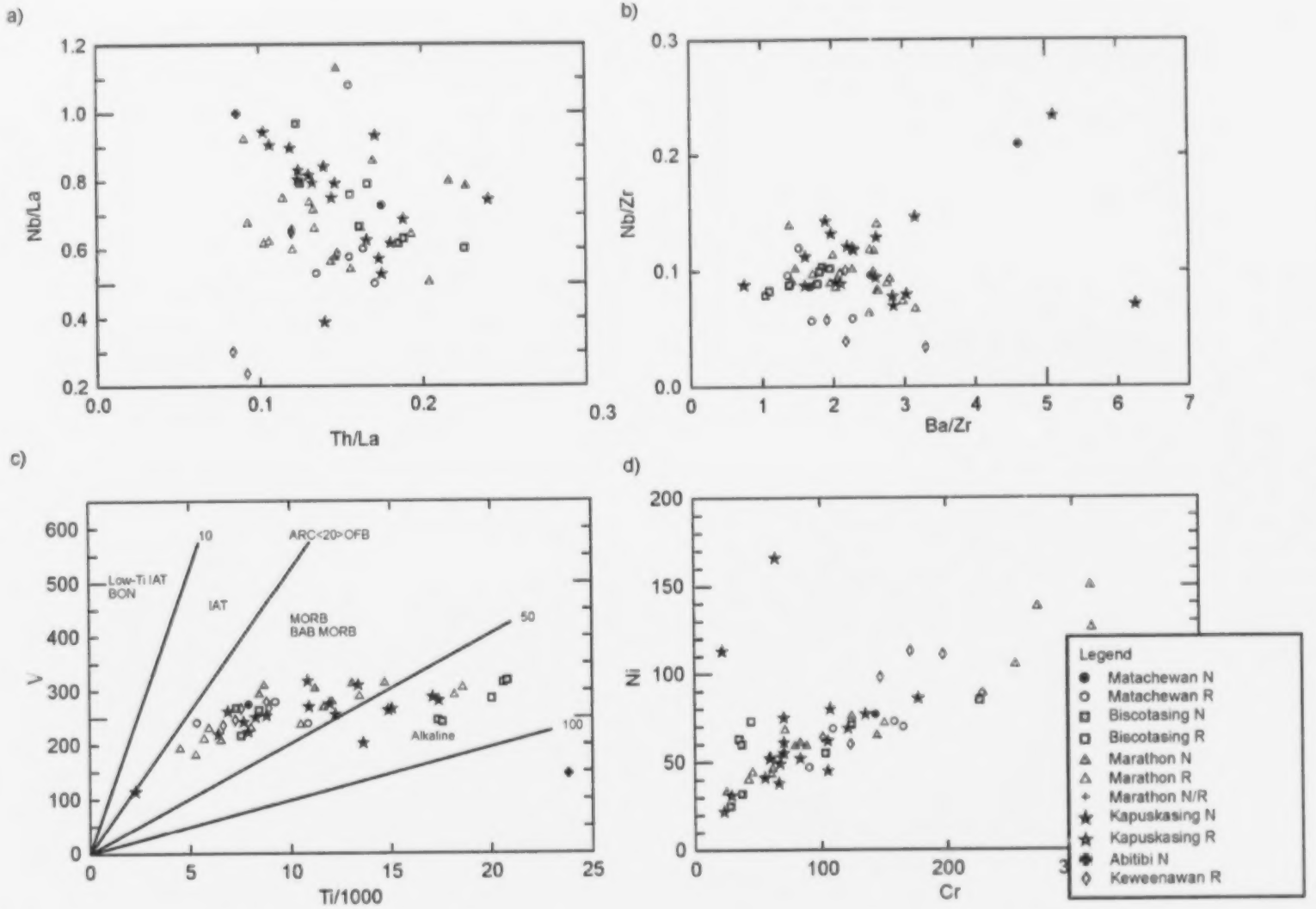

Figure 16. Selected trace element plots illustrating limited discrimination amongst dike swarms. Analytical spread is greatest for Marathon and Kapuskasing dikes.

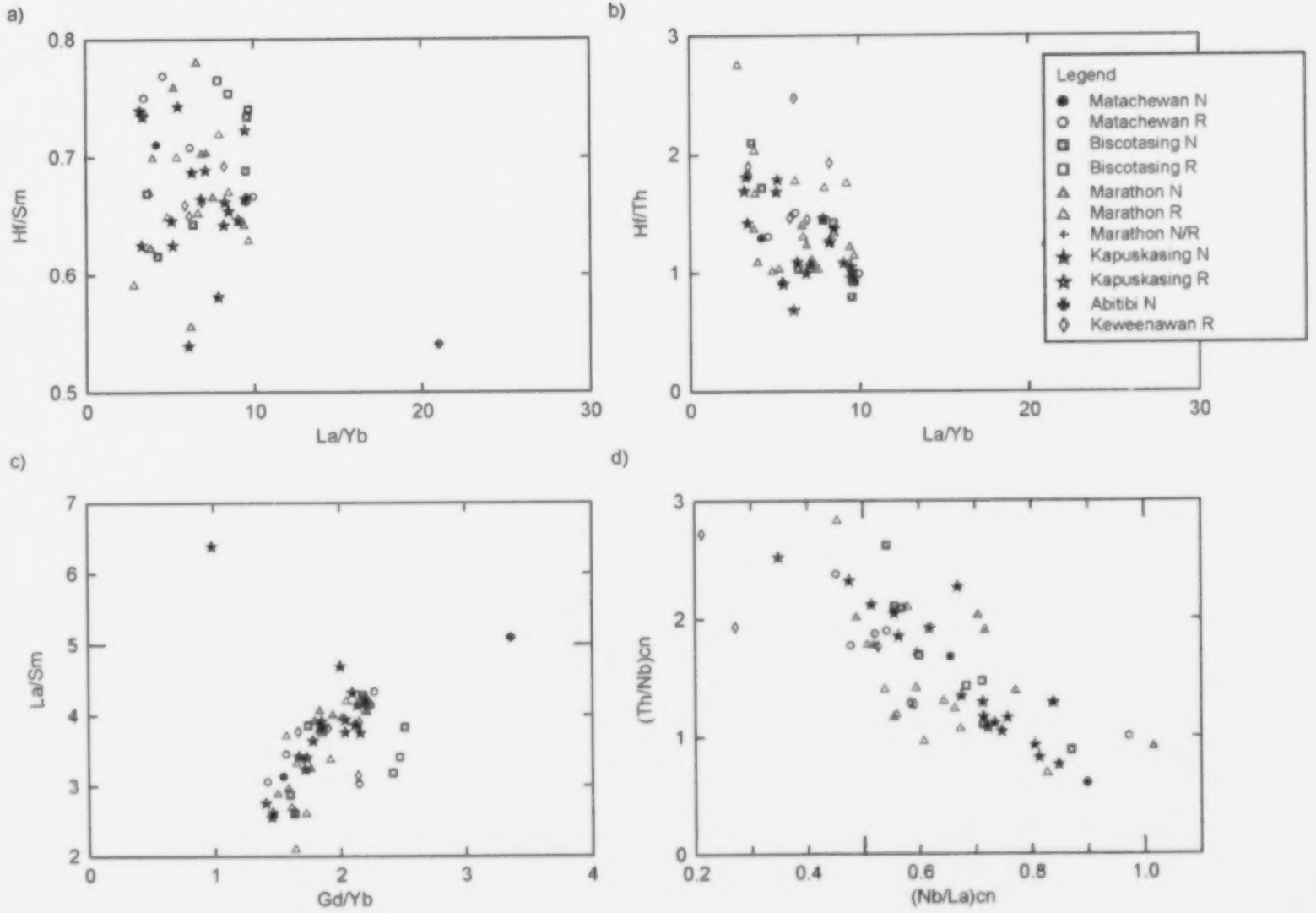

Figure 17. Selected trace element plots for mafic dike swarms with some discrimination as noted in the text.

Kapuskasing Dikes

Kapuskasing (Kap) N dikes show generally lower Nb/La ratios than Kap R and Marathon N dikes (Figure 16a). Kap dikes generally show a broad scatter of trace element ratio values that do not closely correspond to Marathon dikes or any others. These undated dikes remain identified separately until an age determination on these dikes is completed even though they show spreads of values and lack of clustering on trace element plots that are somewhat comparable to but less diverse than the Marathon swarm (e.g., Figure 17d). The Kapuskasing N and R dikes do not closely correspond to the Marathon dikes in trace element compositions. This might reflect spatial differences in source or temporal differences in emplacement yet to be determined.

Keweenawan Dikes

Keweenawan dikes range from Fe-rich to Mg-rich tholeiites but have lower Nb/Y values than other dike swarms and are slightly more calc-alkalic (Figures 14c and 13a). They display a narrower spread in Th/La (Figure 16a), Zr and Yb content, for example, than most other dike swarms. Keweenawan R dikes show higher La/Nb (Figure 17d) and lower S values than most other dikes.

Abitibi Dikes

The Abitibi dike is compositionally distinct from other dikes as is apparent from most trace element plots (e.g., Figures 14c and 14d) This dike sample contains less than 45% SiO_2, low Ni, Cr (Figure 16d) and significantly higher TiO_2 plus Zr/Y and La/Yb (e.g., Figure 17a) ratios compared to other dike swarms.

MICROPROBE MINERAL ANALYSES

The Geoscience Laboratories of the Ontario Geological Survey conducted microprobe analyses of minerals using a CAMECA SX-50 Electron Microprobe equipped with 4 Wavelength Dispersive (WD) Spectrometers. Analyses were done on pyroxenes in thin sections of 4 samples of mafic dikes and on selected samples for amphibole, feldspar, ilmenite and magnetite. The results, provided by D. Crabtree, Geoscience Laboratories, are shown in Table 10 in the Appendix. Each sample number in the table is followed by A, B, C or D (e.g., 03GRS-1C-**A**-pyx1c). These letters refer to analytical regions on the thin sections. The location of the sample (site number in brackets below, or station number in Table 10) is shown in Figure 1. The selection of mineral analyses for each sample is as follows:

Marathon dike 03GRS-1C (DP6) pyx + fsp + amp + oxi (oxi = ilm or mag)
Marathon dike 03GRS-2C (DP7) pyx + fsp + amp + oxi
Marathon dike 03GRS-3C (DP8) pyx
Matachewan dike 03GRS-4C (LL13) pyx + fsp

D. Crabtree reports as follows: most of the minerals in these samples have been altered. There is widely distributed, very fine alteration observed in thin sections and from microprobe analyses of minerals. In the pyroxenes, BSE (back-scattered electron) images show significant atomic contrast on many of the grains so it is difficult to know what is primary. The beam was placed in areas that were thought to be 'fresh'. The feldspars show significant alteration in the sections (some more so than others) and, when zoomed in, it is apparent that this is a 3-phase alteration product. It's difficult to say what these phases are due to extremely fine grain size (beyond the resolution of the electron beam) but the ED (energy dispersive) spectra suggest epidote+albite+musc(?). The slightly depressed totals in some of the

pyroxene and feldspar data may be indicative of alteration. The Fe-Ti oxides display extremely fine intergrowth lamellae (again beyond the resolution of the beam). A few analyses on 03GRS-1C and 2C were done since these samples had some zones of sufficient width for the beam to analyze but it is not certain if the beam was probing 1 phase at a time. A few analyses of amphibole (altered pyroxene) were completed, which showed anomalous F and Cl in them. In general, microprobe analyses of minerals from Marathon dikes show much greater scatter in geochemical compositions than those from Matachewan dikes, which tend to show tighter clustering of analyses. This contrast in the variability of internal alteration between Marathon and Matachewan dikes is similar to the variability in the whole rock geochemistry of these dike swarms. The results of both whole rock and mineral geochemistry illustrate the difficulty in providing geochemical discrimination amongst the dike swarms.

DISCUSSION

The available geochemistry of samples taken from both chilled margins and coarser phases of dikes provide rather limited discrimination amongst the dike swarms. In Table 9, samples from coarser interior phases are identified with sample numbers highlighted in **bold**. All other samples are from chilled margins. Similarities between Kapuskasing and Marathon dikes are apparent by their relative degree of compositional variation compared to other dike swarms. Some dike swarms show tighter clusters in trace element plots, such as the Biscostasing and Matachewan swarms. However, the degree of overlap of these compositional clusters on trace element plots and the limited data set for some of the swarms do not permit clear compositional contrasts amongst these dike swarms.

Conclusions

1. This study has provided new insight on the paleomagnetic characteristics of dikes from several dike swarms in northern Ontario and has added new U/Pb age determinations for 4 of these swarms, thereby raising more questions and the need for further research on the nature of Proterozoic mafic magmatism and crustal block rotations across the Superior Province.

2. The majority of north-striking dikes, east of Lake Nipigon, are related to the Paleoproterozoic Marathon swarm. Amongst them, there are a few parallel dikes, near Beardmore, of R polarity, Keweenawan age in addition to the shallowly west-dipping sills, related to the large, *circa* 1.10 Ga mafic magmatic event represented by the Nipigon embayment (Figure 1). The easternmost, north-striking sill, southeast of Beardmore, has a baddeleyite age of 1103.7 ± 2.3 Ma, the youngest age of magmatism currently known associated with Keweenawan R igneous activity. The results of this study would suggest that the presence of Keweenawan dikes is limited and spatially restricted close to Lake Nipigon.

3. The Marathon swarm, comprising dikes striking north to northeast, has a history of episodic mafic magmatism from 2101 to 2125 Ma. New ages reported here confirm previous work by Buchan et al. (1996) and Hamilton et al. (2002), but also increase the oldest age of Marathon N magmatism to 2125.7 ± 1.2 Ma and demonstrate that the swarm is more extensive than previously thought. Marathon dikes trend both northward and northeastward, with the latter dominated by the older suite of N-polarity dikes. The older N polarity occurred at least prior to 2121 Ma and the younger R polarity occurred at least after about 2107 Ma. The 2125.7 Ma dike at LL20 in the English River Subprovince, strikes northeastward, parallel to Biscotasing dikes farther east. Overlapping north and northeast-striking dikes occur in the northern part of the Onaman–Tashota greenstone belt near

Marshall Lake, suggesting that the older episode of pre-2120 Ma Marathon magmatism was subsequently crosscut by the younger set of north-striking Marathon dikes.

4. The east-northeast-striking Kapuskasing dikes are undated and it remains uncertain whether they are the same age as the Marathon dikes, although they overlap geochemically and show similar progression from N to R polarity. To further unravel the mystery of relative block rotations in and outside of the Kapuskasing Zone will depend on dating these northeast-striking dikes.

5. The period of emplacement of northeast-striking Biscotasing dikes is now shown to straddle a reversal in the Earth's magnetic field. The Hillsport dike, dated here at 2170.7 ± 1.1 Ma, is the first R-polarity Biscotasing dike and is slightly older than previously dated, N-polarity Biscotasing dikes. The paleomagnetic direction of the Hillsport dike is only about 10° from being antipodal to the N-polarity dikes.

6. The Matachewan dike swarm, extending from its focal area near Sudbury, straddles 1 reversal of the Earth's magnetic field from R to N, and spans an emplacement history over 30 million years. The results of this study further demonstrate that the younger N-polarity dikes die out towards the northwest and the R-polarity dikes, which comprise the northwestern part of the swarm near Lake Nipigon, show a counterclockwise rotation of about 23° relative to the dikes south of Wawa. The best estimate of an age for 1 Matachewan dike, northeast of Lake Nipigon, is 2459 ± 5 Ma. This has significantly enhanced the ongoing research into regional-scale crustal rotations across major segments of the Superior Province. This therefore adds further understanding to post-Archean crustal movements that might have some bearing on the localisation of diamondiferous kimberlite pipes.

7. The geochemistry of these dike swarms, based on 61 samples (from chilled margins and coarser interior parts of dikes) taken from east of Lake Nipigon and in the region of the Kapuskasing Zone, provide limited evidence that the swarms can be effectively distinguished by geochemistry alone. Some evidence of differences in the relative size of clustering of trace element ratios and differences in the ratios on some geochemical plots might provide a complementary indication of dike affinity to the N- or R-polarity suites in a given swarm but provide unreliable discrimination between parallel dikes of different swarms.

8. This study has stimulated the continued research, at the University of Toronto Jack Satterly Geochronology Laboratory, into U/Pb dating of complementary minerals such as apatite extracted from those dikes where baddeleyite was absent or of poor quality.

References

Bates, M.P. and Halls, H.C. 1991. Broad-scale Proterozoic deformation of the central Superior Province revealed by paleomagnetism of the 2.45 Ga Matachewan dyke swarm; Canadian Journal of Earth Sciences, v.28, p.1780-1796.

Beck, M. 1980. Paleomagnetic record of plate-margin tectonic processes along the western edge of North America; Journal of Geophysical Research, v.85, p.7115-7131.

Beck, M.E. 1983. Paleomagnetic record of plate margin tectonic processes along the western edge of North America; Journal of Geophysical Research, v.85, p.7115–7131.

Buchan, K.L. and Ernst, R.E. 1994. Onaping fault system: age constraints on deformation of the Kapuskasing structural zone and units underlying the Sudbury Structure; Canadian Journal of Earth Sciences, v.31, p.1197-1205.

Buchan, K.L. and Ernst, R.E. 2004. Diabase dyke swarms and related units in Canada and adjacent regions; Geological Survey of Canada, Map 2022A, scale 1:5 000 000, and accompanying notes.

Buchan, K., Goutier, J., Hamilton, M., Ernst, R. and Matthews, W. 2004. Paleomagnetism of the Lac Esprit dykes and implications for crustal rotation of the Canadian Shield; American Geophysical Union – Canadian Geophysical Union Abstract, May 2004 Montreal.

Buchan, K.L. and Halls, H.C. 1990. Paleomagnetism of Proterozoic mafic dyke swarms of the Canadian Shield; *in* Mafic Dykes and Emplacement Mechanisms, Balkema Press, Rotterdam, p.209-230.

Buchan, K.L., Halls, H.C. and Mortensen, J.K. 1996. Paleomagnetism, U-Pb geochronology and geochemistry of Marathon dykes, Superior Province, and comparison with the Fort Frances swarm; Canadian Journal of Earth Sciences, v.33, p.1583-1595.

Buchan, K.L., Harris, B.A., Ernst, R.E. and Hanes, J.A. 2003. Ar-Ar dating of the Pickle Crow diabase dyke in the western Superior craton of the Canadian Shield of Ontario and implications for a possible plume centre associated with ca. 1880 Ma Molson magmatism of Manitoba; *in Abstracts*, Geological Association of Canada/Mineralogical Association of Canada Annual Meeting, v.28.

Buchan, K.L., Mortensen, J.K. and Card, K.D. 1993. Northeast-trending Early Proterozoic dykes of southern Superior Province: multiple episodes of emplacement recognized from integrated paleomagnetism and U-Pb geochronology; Canadian Journal of Earth Sciences, v.30, p.1286-1296.

Chamberlain, K.R. and Bowring, S.A. 2000. Apatite-feldspar U-Pb thermochronometer: a reliable mid-range (~450°C), diffusion-controlled system; Chemical Geology, v.172, p.173-200.

Cherniak, D.J., Lanford, W.A., Ryerson, F.J. 1991. Lead diffusion in apatite and zircon using ion implantation and Rutherford backscattering techniques; Geochimica et Cosmochimica Acta, v.55, p.1663–1673.

Condie, K.C. 1997. Sources of Proterozoic mafic dyke swarms: constraints from Th/Ta and La/Yb ratios; Precambrian Research, v.81, p.3-14.

Condie, K.C. 2003. Incompatible element ratios in oceanic basalts and komatiites: Tracking deep mantle sources and continental growth rates with time; Geochemistry Geophysics Geosystems, v.4, 1005, doi:10.1029/2002GC000333.

Davis, D.W. 1982. Optimum linear regression and error estimation applied to U-Pb data; Canadian Journal of Earth Sciences, v.19, p.2141-2149.

Davis, D.W. and Green, J.C. 1997. Geochronology of the North American Midcontinent Rift in western Lake Superior and implications for its geodynamic evolution; Canadian Journal of Earth Sciences, v.33, p.476-488.

Davis, D.W. and Stott, G.M. 2003. Geochronology of two Proterozoic mafic dike swarms in northwestern Ontario; *in* Summary of Field Work and Other Activities 2003, Ontario Geological Survey, Open File Report 6120, p.12-1 to 12-7.

Davis, D.W. and Sutcliffe, R.H. 1985. U-Pb ages from the Nipigon plate and northern Lake Superior; Geological Society of America Bulletin, v.96, p.1572-1579.

Dunlop, D.J. 1983. Paleomagnetism of Archean rocks from northwestern Ontario: Wabigoon gabbro, Wabigoon Subprovince; Canadian Journal of Earth Sciences, v.20, p.805-1817.

Ernst, R.E., and Buchan, K.L. 1993. Paleomagnetism of the Abitibi dyke swarm, southern Superior Province and implications for the Logan Loop; Canadian Journal of Earth Sciences, v.30, p.1886-1897.

Ernst, R.E. and Buchan, K.L. 1997. Giant radiating dyke swarms: their use in identifying pre-Mesozoic large igneous provinces and mantle plumes; *in* Large Igneous Provinces: Continental, Oceanic and Planetary Flood Volcanism, American Geophysical Union, Geophysical Monograph 100, p.297-333.

Ernst, R.E. and Buchan, K.L. 2001. The use of mafic dike swarms in identifying and locating mantle plumes; *in* Mantle Plumes: Their Identification Through Time, Geological Society of America, Special Paper 352, p.247-265.

Ernst, R.E., and Halls, H.C. 1984. Paleomagnetism of the Hearst dike swarm and implications for the tectonic history of the Kapuskasing zone, northern Ontario; Canadian Journal of Earth Sciences, v.21, p.1499-1506.

Fahrig, W.F. 1987. The tectonic settings of continental mafic dyke swarms: failed arm and early passive margin; *in* Mafic Dyke Swarms, H.C. Halls and W.F. Fahrig (eds.); Geological Association of Canada, Special Paper 34, p.331-348.

Fahrig, W.F., Gaucher, E.H. and Larochelle, A. 1965. Paleomagnetism of diabase dykes of the Canadian Shield. Canadian Journal of Earth Sciences, v.2, p.278-298.

Halls, H.C. 1986. Paleomagnetism, structure and longitudinal correlation of Middle Precambrian dykes from northwest Ontario and Minnesota; Canadian Journal of Earth Sciences, v.23, p.142-157.

Halls, H.C. 1991. The Matachewan dyke swarm, Canada: an early Proterozoic magnetic field reversal; Earth and Planetary Science Letters, v.105, p.279-292.

Halls, H.C. and Davis, D.W. 2004. Paleomagnetism and U-Pb geochronology of the 2.17 Ga Biscotasing dyke swarm, Ontario, Canada: evidence for vertical-axis crustal rotation across the Kapuskasing Zone; Canadian Journal of Earth Sciences, v.41, p.255-269.

Halls, H.C. and Pesonen, L.J. 1982. Paleomagnetism of Keweenawan Rocks; *in* Tectonic History of the Lake Superior Basin, Geological Society of America Memoir 156, p.173-202.

Halls, H.C., and Palmer, H.C. 1990. The tectonic relationship of two early Proterozoic dyke swarms to the Kapuskasing Structural Zone: a paleomagnetic and petrographic study; Canadian Journal of Earth Sciences, v.27, p.87-103.

Halls, H.C., Palmer, H.C., Bates, M.P., and Phinney, W.C. 1994. Constraints on the nature of the Kapuskasing Structural zone from the study of Proterozoic dyke swarms; Canadian Journal of Earth Sciences, v.31, p.1182-1196.

Halls, H.C. and Shaw, E.G. 1988. Paleomagnetism and orientation of Precambrian dykes, eastern Lake Superior region, and their use in estimates of crustal tilting; Canadian Journal of Earth Sciences, v.25, p.732-743.

Halls, H.C. and Stott, G.M. 2003. Paleomagnetic studies of mafic dikes in the vicinity of Lake Nipigon, northwestern Ontario; *in* Summary of Field Work and Other Activities 2003, Ontario Geological Survey, Open File Report 6120, p.11-1 to 11-7.

Halls, H.C. and Stott, G.M. 2004. Paleomagnetic studies of Proterozoic mafic dikes, eastern Wabigoon and English River subprovinces; *in* Summary of Field Work and Other Activities 2004, Ontario Geological Survey, Open File Report 6145, p.9-1 to 9-4.

Halls, H.C. and Zhang, B. 1995. Magnetic polarity domains in the early Proterozoic Matachewan dyke swarm, Canada: A novel method for mapping major faults; *in* Baer, G., Heimann, A. (eds.), Physics and Chemistry of Dykes, A.A. Balkema, Rotterdam, p.165-170.

Halls, H.C. and Zhang, B. 1998. Uplift structure of the southern Kapuskasing zone from 2.45 Ga dike emplacement; Geology, v.26, p.67-73.

Halls, H.C. and Zhang, B. 2003. Crustal uplift in the southern Superior Province, Canada, revealed by paleomagnetism; Tectonophysics, v.362, p.123-136.

Hamilton, M.A., Davis, D.W., Buchan, K.L., and Halls, H.C. 2002. Precise U-Pb dating of reversely magnetized Marathon diabase dykes and implications for emplacement of giant dyke swarms along the southern margin of the Superior Province, Ontario; Geological Survey of Canada, Current Research 2002-F6, 8p.

Hanes, J.A., Queen, M., and Archibald, D.A.1988. 40Ar/39Ar geochronology of dykes and their contact aureoles in the Kapuskasing uplift; Project Lithoprobe, Kapuskasing Structural Zone Workshop II, University of Toronto, p.165-172.

Heaman, L.M. 1997. Global mafic magmatism at 2.45 Ga: Remnants of an ancient large igneous province?; Geology, v.25, p.299-302.

Heaman, L.M. and Easton, R.M. 2005. Proterozoic history of the Lake Nipigon area, Ontario: Constraints from U-Pb zircon and baddeleyite dating; *in* Institute on Lake Superior Geology, 51st Annual Meeting, Nipigon, Ontario, Part 1 – Proceedings and Abstracts, v.51, part 1, p.15-16.

Jaffey, A.H., Flynn, K.F., Glendenin, L.E., Bentley, W.C. and Essling, A.M. 1971; Precision measurement of half-lives and specific activities of ^{235}U and ^{238}U; Physical Review, v.4, p.1889-1906.

Kirschvink, J.L. 1980. The least squares line and plane and the analysis of paleomagnetic data; Geophysical Journal of the Royal Astronomical Society, v.62, p.699-718.

Krogh, T.E. 1973. A low contamination method for hydrothermal decomposition of zircon and extraction of U and Pb for isotopic age determinations; Geochimica et Cosmochimica Acta, v.37, p.485-494.

Krogh, T.E. 1982. Improved accuracy of U-Pb ages by the creation of more concordant systems using an air abrasion technique; Geochimica et Cosmochimica Acta, v.46, p.637-649.

Ludwig, K.R. 2003. User's manual for Isoplot/Ex rev. 3.00: a geochronological toolkit for Microsoft® Excel; Special Publication, 4, Berkeley Geochronology Center, Berkeley, 70p.

Manson, M.L., and Halls, H.C. 1997. Proterozoic reactivation of the southern Superior Province and its role in the evolution of the Midcontinent Rift; Canadian Journal of Earth Sciences, v.34, p.562-575.

Matthews, W. and Davis, W.J. 1999. A practical image analysis technique for estimating the weight of abraded mineral fractions used in U-Pb dating; *in* Radiogenic Age and Isotopic Studies: Report 12, Geological Survey of Canada, Current Research 1999-F, p.1-7.

McFadden, P.L., and Lowes, F.J. 1981. The discrimination of mean directions drawn from Fisher distributions; Geophysical Journal of the Royal astronomical Society, v.67, p.19-33.

Milne, V.G. 1964. Geology of the Flanders Lake area; Ontario Department of Mines, Report 21, 18p.

Naldrett, A.J. and Lightfoot, P.C. 1993. Ni-Cu-PGE ores of the Noril'sk Region, Siberia: a model for giant magmatic sulfide deposits associated with flood basalts; *in* Giant Ore Deposits, Society of Economic Geologists, Special Publication 2, p.81-124.

Ontario Geological Survey 1992. Tectonic assemblages of Ontario, northern sheet; Ontario Geological Survey, Map 2575, scale 1:1 000 000.

Osmani, I.A. 1991. Proterozoic mafic dike swarms in the Superior Province of Ontario; *in* Geology of Ontario, Ontario Geological Survey, Special Volume 4, Part 1, p.661-681.

Phinney, Wm. C. and Halls, H.C. 2001. Petrogenesis of the Early Proterozoic Matachewan dyke swarm, Canada, and implications for magma emplacement and subsequent deformation; Canadian Journal of Earth Sciences, v.38, p.1541-1563.

Sage, R.P. 1997. Kimberlites of Ontario; *in* Summary of Field Work and Other Activities 1997; Ontario Geological Survey, Miscellaneous Paper 168, p.37-40.

Sage, R.P. 2000. Kimberlites of the Attawapiskat area, James Bay Lowlands, northern Ontario; Ontario Geological Survey, Open File Report 6019, 341p.

Schmitz, M.D., Wirth, K.R. and Craddock, J.P. 1995. Major and trace element geochemistry of Early Proterozoic mafic dykes of northern Minnesota and southwestern Ontario; *in* Physics and Chemistry of Dykes, G. Baer and A. Hiemann (eds.), Balkema Press, Rotterdam, p.219-233.

Söderlund, U. and Johansson, L. 2002. A simple way to extract baddeleyite (ZrO_2); Geochemistry, Geophysics, and Geosystems, 3(2), doi: 10.1029/2001GC000212.

Stacy, J.S. and Kramers, J.D. 1975. Approximation of terrestrial lead isotope evolution by a two-stage model; Earth and Planetary Science Letters, v.26, p.207-221.

Stott, G.M. 2003. Diabase dyke swarms as structural controls for kimberlite pipes under the James Bay and Hudson Bay lowlands, Ontario; 8th International Kimberlite Conference, Victoria, British Columbia, Extended Abstracts, Abstract 317, 3p.

Stott, G.M., Davis, D.W., Parker, J.R., Straub, K.J. and Tomlinson, K.Y. 2002. Geology and tectonostratigraphic assemblages, eastern Wabigoon Subprovince, Ontario; Ontario Geological Survey, Preliminary Map P.3449, or Geological Survey of Canada Open File 4285, scale 1:250 000.

Stott, G.M. and Halls, H.C. 2002. Paleomagnetic, geochemical and U/Pb geochronologic studies of mafic dikes in northern Ontario: relevance to mineralization associated with the Nipigon embayment and kimberlites; *in* Summary of Field Work and Other Activities 2002, Ontario Geological Survey, Open File Report 6100, p.13-1 to 13-10.

Sun, S.S. and McDonough, W.F. 1989. Chemical and isotopic systematics of oceanic basalts: implications for mantle compositions and processes; *in* Magmatism in the Ocean Basins, Geological Society Special Publication No. 42, p.313-345.

Symons , D.T.A., Lewchuk, M.T., Dunlop, D.J., Costanzo-Alvarez, V., Halls, H.C., Bates, M.P., Palmer, H.C., and Vandall, T.A. 1994. Synopsis of paleomagnetic studies in the Kapuskasing Structural Zone; Canadian Journal of Earth Sciences, v.31, p.1206-1217.

Vandall, T. and Symons, D. 1990. Paleomagnetism of Archean granites and Matachewan dykes in the Wawa Subprovince, Ontario: reevaluation of the Archean apparent polar wander path; Canadian Journal of Earth Sciences, v.27, p.1031-1039.

Van Schmus, W.R., Green, J.C. and Halls, H.C. 1982. Geochronology of Keweenawan rocks of the Lake Superior region: A summary; Geological Society of America, Memoir 156, p.165-171.

Wilkinson, L., Kjarsgaard, B.A., LeCheminant, A.N. and Harris, J. 2001. Diabase dyke swarms in the Lac de Gras area, Northwest Territories, and their significance to kimberlite exploration: initial results; Geological Survey of Canada, Current Research 2001-C8, 17p.

Zalnieriunas, R.V. and Sage, R.P. 1995. Known kimberlites of eastern Ontario; Ontario Geological Survey, Preliminary Map P.3321, scale: various.

Appendix

Tables 1 to 10

Table 1. U/Pb isotopic data on baddeleyite from mafic dikes at Sites DP1, DP2 and DP4

No.	Description	Location	Easting	Northing	Wt.	U	Th/U	Pbtot	PbCom	$^{207}Pb/^{204}Pb$	$^{206}Pb/^{238}U$	2 sig	$^{207}Pb/^{235}U$	2 sig	$^{207}Pb/^{206}Pb$ Age (Ma)	2 sig	Disc. %	Corr. Coeff.	Lab No.
		Zone 16 NAD 83			(mg)	(ppm)		(pg)	(pg)										
1.	**02GRS-01A**	**Site DP1**	**462964**	**5574826**	**N-NE trending mafic dike East of Lake Nipigon**														
1	1 badd, brn	NNE trending dike on Deeds Pluton			0.00005	415.0	0.04	7.7	0.73	105.6	0.3770	0.0023	6.817	0.064	2113	11	2.8	0.7466	dwd4422
2	1 badd, brn				0.00003	278	0.06	3.2	0.53	66.31	0.3844	0.0057	6.921	0.138	2106	20	0.5	0.8146	dwd4423
2.	**02GRS-02A**	**Site DP2**	**458602**	**5516981**	**N-NE trending mafic dike East of Lake Nipigon**														
1	1 badd, eq, fresh, dk brn	N trending dike at km24 on Kinghorn Rd			0.0010	215	0.12	83.2	0.8	857.9	0.3859	0.0018	6.960	0.032	2109.0	3.8	0.3	0.8947	dwd4344
2	1 badd, fresh, dk brn				0.0005	448	0.06	84.9	0.6	1226.2	0.3841	0.0021	6.929	0.038	2109.5	2.3	0.8	0.9715	dwd4345
3a	1 badd, flat, fresh, brn				0.0003	721	0.04	81.1	1.2	609.6	0.3820	0.0020	6.874	0.035	2104.9	3.8	1.1	0.9122	dwd4346a
3b	1 badd, flat, fresh, brn				0.0003	721	0.03	81.1	1.5	467.1	0.3829	0.0012	6.901	0.023	2107.6	4.1	1.0	0.7424	dwd4346b
3c	1 badd, flat, fresh, brn				0.0003	721	0.02	80.9	1.8	412.7	0.3822	0.0010	6.885	0.023	2106.8	3.1	1.1	0.8477	dwd4346c
3d	1 badd, flat, fresh, brn				0.0003	721	0.02	81.0	1.9	373.5	0.3832	0.0014	6.901	0.027	2106.0	4.1	0.8	0.8159	dwd4346d
3.	**02GRS-03A**	**Site DP4**	**599810**	**5479539**	**NE trending mafic dike, Hillsport**														
1	1 badd, flat, dull	NE trending dike 5 km W of Hillsport			0.0010	783	0.16	311.5	0.6	4378.4	0.3916	0.0011	7.319	0.022	2171.3	1.8	2.2	0.9429	dwd4347
2	1 badd, flat, dull				0.0005	789	0.06	154.5	0.9	1501.0	0.3952	0.0014	7.381	0.027	2169.8	2.0	1.2	0.9518	dwd4348
3	1 badd, flat, dull				0.0003	1234	0.10	146.7	3.1	420.8	0.3962	0.0009	7.402	0.023	2170.5	3.0	1.0	0.8339	dwd4349

Fractions are ordered from highest to lowest $^{207}Pb/^{206}Pb$ age.
badd = baddeleyite grain; eq = equant.
Pbcom is total measured common Pb assuming the isotopic composition of laboratory blank: 206/204 - 18.221; 207/204 - 15.612; 208/204 - 39.360 (errors of 2%).
Th/U calculated from radiogenic $^{208}Pb/^{206}Pb$ ratio and $^{207}Pb/^{206}Pb$ age assuming concordance.
Disc - per cent discordance for the given $^{207}Pb/^{206}Pb$ age.
Uranium decay constants are from Jaffey et al. (1971).

Table 2. U/Pb isotopic data on baddeleyite for sample site LL16

No.	Fraction	Wt.	U	Th/U	Pbrad	Pbcom	$^{207}Pb/^{204}Pb$	$^{206}Pb/^{238}U$	2 sig	$^{207}Pb/^{235}U$	2 sig	$^{207}Pb/^{206}Pb$	2 sig	Disc.	Error	Analysis No.
		(mg)	(ppm)		(pg)	(pg)						Age (Ma)		%	Correl. Coeff.	
03GRS-29 Site LL16																
1	1 badd, frag, skel, brn	0.0010	104	0.05	18.1	0.52	199.2	0.1849	0.0013	1.967	0.019	1125.4	13.1	3.1	0.7174	dwd4637
2	1 bad, frag, fresh, brn	0.0005	333	0.03	29.1	0.51	315.1	0.1874	0.0005	1.974	0.007	1105.6	5.0	-0.2	0.7157	dwd4642
3	1 badd, flat, brn, fresh	0.0020	210	0.02	73.1	0.61	644.8	0.1872	0.0007	1.971	0.008	1104.4	4.0	-0.2	0.8757	dwd4635
4	1 badd, frag, clr, fresh	0.0005	281	0.03	24.5	0.59	235.0	0.1869	0.0009	1.966	0.011	1102.6	7.9	-0.2	0.7121	dwd4643
5	1 badd, frag, dk, fresh	0.0010	521	0.02	90.4	0.87	559.3	0.1864	0.0006	1.959	0.006	1101.2	4.9	-0.1	0.6803	dwd4636

badd - baddeleyite; frag - fragment; skel - skeletal fragment; brn - brownish; dk - dark brown; clr – colourless.
Pbrad - Radiogenic Pb.
Pbcom - Common Pb, assuming all has blank isotopic composition: 206/204 - 18.221; 207/204 - 15.612; 208/204 - 39.36; 2% errors.
Th/U calculated from radiogenic $^{208}Pb/^{206}Pb$ ratio and $^{207}Pb/^{206}Pb$ age assuming concordance.
Disc - per cent discordance for the given $^{207}Pb/^{206}Pb$ age.

Table 3. Paleomagnetic results for all Matachewan dike sites.

SITE	N	S LAT (°N)	S LON (°W)	STR (°)	W (m)	DEC (°)	INC (°)	PLAT (°S)	PLON (°W)	DEC' (°)	INC' (°)	k	α_{95} (°)
LL1	9	49.80	86.55	285	40	202.5	-14.8	43.7	118.2	207.5	-15.7	72	6.1
LL2	8	49.74	86.78	280	35	195.6	-14.0	45.4	109.1	200.8	-13.9	28	10.6
LL3	9	49.79	86.58	310	20	196.9	-21.6	49.0	112.3	201.6	-21.5	92	5.4
LL4	5	49.68	86.67	327	7+	189.2	-18.0	48.8	100.5	194.2	-16.9	61	9.9
LL5	7	49.80	86.77	315	40+	198.4	-20.1	47.7	114.3	203.3	-20.3	11	19.1
LL8	8	49.71	87.37	285	25	183.1	-14.3	47.5	91.9	188.7	-12.1	174	4.2
LL10	9	50.17	87.66	300	25	187.5	-16.8	48.0	98.8	193.2	-14.7	73	6.0
LL11	7	50.29	87.53	304	10	183.4	-28.4	54.7	93.2	188.4	-25.5	147	5.0
LL13	10	50.33	87.94	320	16	174.2	-16.9	48.0	79.4	180.2	-11.9	47	7.1
LL14	7	50.02	87.46	330	25	192.1	-23.0	50.7	106.3	197.3	-22.1	91	6.4
LL15	11	50.46	86.80	330	25	188.3	-10.3	44.2	98.4	193.8	-7.5	38	7.6
LL19 *	11	50.61	86.71	305	40	185.3	-29.3	54.8	95.6	189.8	-26.1	94	4.7
LL21	8	49.83	86.82	310	25+	196.5	-30.2	53.8	114.4	200.1	-30.1	65	6.9
OL1[1]	7	50.82	87.15	307	34	188.2	-20.4	49.2	99.5	193.4	-17.1	140	5.1
OL2[1]	6	50.80	87.19	311	34	182.7	-29.2	54.8	91.7	187.5	-25.3	38	11.0
OL4[1]	5	50.87	87.18	313	4	181.7	-14.3	46.4	89.6	187.3	-9.6	110	7.1
LL17	5	48.61	85.33	310	40	192.6	-16.5	48.4	75.7	196.7	-17.3	26	14.0

Only those results are given for which α_{95}, the radius of the 95% confidence circle about the mean is ≤15°, and N, the number of sample directions contributing to the mean is ≥ 4. **DEC**, **INC** are the paleomagnetic declination and inclination at the collecting site; **DEC '**, **INC '** are values at Lat 48°N, Long 79°W. **STR**, **W** are dike strike and width. Nearly all dikes in this and other tables dip within 10° of the vertical. **SLON**, **SLAT**, **PLAT**, **PLON** are respectively the site latitude and longitude, virtual pole latitude and longitude; k is the precision parameter. OL sites are from Bates and Halls (1991). The mean direction of sites from the eastern Lake Nipigon region is: DEC ' = 193.5°, INC ' = -18.1°, k = 73, α_{95} = 4.5°, N, the number of sites = 15. Site LL17 lies much farther east than the other sites and therefore is not included in the mean. The asterisk (*) signifies that a U/Pb age exists for the dike. Site LL6, a probable Matachewan dike with NW strike, has highly scattered NRM due to lightning and is therefore not listed. [1] Data from Bates and Halls (1991).

Table 4. Paleomagnetic results for all N-ENE-trending dikes.

SITE	N	SLAT (°N)	SLON (°W)	STR (°)	W (m)	DEC (°)	INC (°)	PLAT (°N)	PLON (°E)	DEC' (°)	INC' (°)	k	α_{95} (°)
BISCOTASING R													
KP20	15	49.14	85.95	060	60	98.0	-54.9	30.8	204.0	103.4	-49.8	50	5.5
DP4 *	4	49.46	85.62	037	100	104.2	-57.2	36.3	202.5	109.3	-52.6	161	7.3
KAPUSKASING R													
KP3	4	47.74	84.12	050	23	171.7	-62.3	82.9	153.4	171.3	-63.5	42	14.3
KP10	5	47.91	84.09	085	13	140.6	-72.3	64.7	222.8	139.6	-73.3	48	11.1
KP13	8	49.13	84.79	045	18	116.3	-67.8	50.3	212.7	116.0	-68.3	119	5.1
TK9	6	47.83	84.43	065	1	158.6	-67.0	75.8	201.0	158.0	-68.1	282	4.0
TK36	17	47.69	83.97	070	1.5	142.4	-75.1	64.6	234.1	141.4	-76.2	362	1.9
186[1]	12	47.95	84.20	060	9	173.0	-54.0	75.6	119.6	172.4	-55.2	-	9.0
214[1]	7	47.86	83.80	085	8	196.0	-83.0	60.9	284.0	201.7	-83.3	-	5.0
180[1]	7	48.13	82.62	060	13	79.0	-85.0	45.4	263.4	67.4	-86.0	-	3.0
228[1]	4	47.93	83.12	075	9+	122.0	-67.0	52.7	211.9	119.9	-68.6	-	5.0
229[1]	6	47.99	82.92	070	4+	167.0	-81.0	64.9	267.9	170.7	-81.7	-	10.0
HP2[1]	4	48.52	82.93	070	34	149.0	-65.0	69.2	194.6	148.2	-66.1	-	9.0
KS3[1]	7	48.38	83.53	040	17	87.0	-71.0	36.6	231.6	84.1	-72.0	-	8.0
KP22	24	47.55	84.80	045	1.6	138.1	-60.6	59.9	189.5	136.8	-62.0	139	2.5

SITE	N	SLAT (°N)	SLON (°W)	STR (°)	W (m)	DEC (°)	INC (°)	PLAT (°N)	PLON (°E)	DEC' (°)	INC' (°)	k	α_{95} (°)
KAPUSKASING N													
KP8	5	48.05	84.10	072	10	306.6	62.2	53.2	199.2	305.1	63.5	84	8.4
KP11	6	47.89	84.01	030	4	315.6	67.0	61.1	206.4	314.3	68.2	508	3.0
KP12	5	47.89	84.01	045	0.5	301.9	63.9	51.1	205.0	300.2	65.2	37	12.8
TK17	5	47.80	84.40	075	14	277.7	76.4	44.9	238.0	274.2	77.1	86	8.3
TK46	4	47.77	84.38	092	13	329.6	76.2	67.0	240.9	329.1	77.1	85	10.0
TK57	4	47.70	84.30	035	1.5	310.4	69.7	58.7	215.2	308.8	70.9	204	6.4
MARATHON R EAST													
TK48*	4	47.77	84.38	048	24	157.0	-38.9	58.3	139.2	156.0	-41.0	45	12.0
TK82	5	47.75	83.91	020	2	138.2	-55.7	57.3	181.0	136.7	-57.4	121	7.0
TK134	4	47.45	83.95	100	3,3	131.2	-39.2	43.7	170.5	129.6	-42.0	65	11.5
MK7 *	6	48.12	84.41	045	50	151.3	-42.1	57.2	149.4	150.4	-43.8	31	12.3
MARATHON N EAST ?													
TK7	5	47.84	84.44	099	1.6	306.0	53.2	47.7	186.5	304.6	54.7	179	5.7
KP21	4	47.95	84.24	055	7	333.1	57.2	68.0	168.3	332.2	58.6	29	15.0
MARATHON R WEST ?													
KP23	7	48.42	85.10	030	5	152.9	-60.7	69.8	175.6	152.4	-61.4	17	15.0
KP27	8	48.34	85.86	035	~50	128.2	-49.1	46.8	178.4	127.8	-49.6	86	6.0
KP32	7	49.46	82.61	080	10	116.0	-60.4	45.7	202.3	114.6	-61.9	398	3.0
DP3	7	49.81	87.65	010	27	120.0	-65.1	51.2	202.2	121.4	-64.0	315	3.4
DP6 *	4	50.15	87.71	032	50	128.2	-57.7	51.9	184.6	129.7	-56.2	284	5.5
MARATHON N WEST ?													
KP24	9	48.72	85.57	015	8	293.2	67.2	47.9	212.4	292.7	67.4	233	3.4
KP30	10	48.71	85.60	015	18	283.6	66.4	41.9	215.2	283.0	66.7	231	3.2
KP28	7	48.72	85.82	025	16	281.1	69.3	42.5	220.8	280.5	69.4	90	6.4
LL20 *	8	50.56	87.15	050	65+	275.2	77.4	46.8	236.5	279.3	76.9	163	4.3
ABITIBI													
SL13	14	48.35	84.67	020	5,8	315.9	62.7	59.6	194.1	315.0	63.6	61	5.1
UNASSIGNED													
LL7	8	49.93	86.82	300	0.25	297.1	65.1	49.5	204.4	298.3	64.4	40	8.8

Only those results are given for which N ≥4 and α_{95} ≤15°. Results that do not meet these criteria are given in Table 8. Measured remanent magnetization declination, DEC, and inclination, INC, have been recomputed to the values they would have (DEC°, INC°) at a common locality. For the 2 Biscotasing sites this locality is 48°N 79°W; for all other sites it is 49°N 86°W, the difference being because the Biscotasing dikes are referred to the original common site given by Buchan et al. 1993. Other symbols as in Table 3. [1] These data are from Halls and Palmer (1990), for which k values were not given. The asterisk (*) denotes dikes for which a U/Pb age exists.

Table 5. Paleomagnetic results for Keweenawan mafic intrusions.

SITE	N	Latitude (N)	Longitude (W)	W (m)	STRIKE	DEC	INC	k	α_{95}
DP5	6	50° 35.511'	89° 22.146	100	320°	114.9°	-70.8°	531	2.9°
DP8	6	49° 36.380'	88° 02.748'	20	005°	90.3°	-71.3°	386	3.4°
DP10	2	50° 34.818	89° 24.979	3.5	320°	76.5°	-61.4°	146	21.0°
DP11	5	49° 36.434'	87° 57.104'	30+	350°	119.8°	-74.3°	120	7.0°
LL12	6	50° 34.906'	89°25.006'	1	297°	95.9°	-70.4°	685	2.6°
LL16	4	49° 27.002'	87° 44.743'	?	325°	105.9°	-73.7°	132	8.0°
LL18	8	48° 41.469'	86° 00.398'	26	280°	286.8°	25.2°	47	8.2°
LL22	3	49° 38.894'	87° 56.492'	40	010°	120.9°	-80.4°	25	25.0°

W and **Strike** are respectively the thickness and azimuthal orientation of the dike; **DEC** and **INC** define the direction of the remanent magnetization; **n** is the number of samples in a site used to determine the paleomagnetic direction; **k** is precision parameter; and α_{95} is the radius of the 95% confidence circle about the mean direction. Note that site LL18 has a direction similar to that for N-polarity Keweenawan igneous rocks.

Table 6. Summary of paleomagnetic results from the Lake Gamitagama and Ranger Lake areas.

SITE	N, *N*	DEC (°)	INC (°)	PLAT (°S)	PLON (°W)	DEC' (°)	INC' (°)	α_{95} (°)
RANGER LAKE								
HS21	4	209.7	-22.1	46.5	129.0	212.9	-26.6	15.1
HS32	4	227.8	-26.7	38.4	150.8	231.2	-32.0	8.6
HS41	4	210.4	-24.5	47.4	130.8	213.4	-29.0	4.0
HS43	4	205.5	-6.4	41.0	118.6	208.9	-11.2	2.5
HS45	5	200.6	-4.2	41.7	112.1	204.1	-8.5	12.8
MEAN	*5*					213.6	-21.7	13.7
GAMITAGAMA								
GD2	5	202.9	-16.1	46.1	118.4	206.6	-19.8	14.0
GD6	5	219.0	-9.7	35.8	135.3	222.9	-15.1	3.2
GD7	5	218.3	-16.7	39.3	137.0	222.1	-21.8	11.6
GD8	5	221.2	-20.1	39.2	141.6	225.1	-25.4	5.1
KP22	5	207.9	-26.4	49.2	128.6	211.2	-30.2	12.6
HS2	6	214.3	-14.8	40.6	132.1	218.1	-20.0	4.4
MEAN	**6**					217.7	-22.1	7.1

Only those results are given for which **N**, the number of samples, ≥ 4 and $\alpha_{95} \leq 15°$. **PLAT**, **PLON** are virtual pole latitude, longitude; **DEC '**, **INC '** are paleomagnetic declination, inclination, recomputed for the location 48°N, 79°W. GD sites are from Vandall and Symons (1990); HS sites from Halls and Shaw (1988). Site KP22 is from a Matachewan dike (trend 340°, dip 70° NE, and width 12 m) which is cut by a NE-trending dike (*see* Table 4). Vandall and Symons (1990) describe GD dikes as "vertical with NNW trends". The mean direction for the Ranger Lake and Gamitagama data combined is DEC ' = 216.3°, INC ' = -21.1°, k = 50, α_{95} = 6.6°, *N*, number of dikes, = 11.

Table 7. Summary of mean paleomagnetic directions and pole positions for different dike swarms and combinations of data.

DIKE SWARM	MDEC' (°)	MINC' (°)	N	k	α_{95} (°)	PLAT	PLON	dp (°)	dm (°)	λ
MATACHEWAN										
Nipigon	193.5°	-18.1°	15	73	4.5	49.6°S	99.8°W	2.4	4.7	9°S
Gamitagama + Ranger Lk	215.9	-22.0	11	54	6.3	42.7°S	130.5°W	3.5	6.7	11°S
MARATHON										
Marathon R WEST	133.3	-55.0	14	46	5.9	53.6°S	360.0°W	5.9	8.4	36°S
Marathon R EAST	143.7	-46.5	4	50	13.2	55.0°S	19.9°W	10.9	16.9	28°S
Marathon N WEST	295.5	59.7	18	40	5.6	44.9°N	161.3°W	6.4	8.4	41°N
Marathon N EAST	317.7	57.4	2	54	34.5	57.9°N	180.2°W	36.8	50.4	38°N
KAPUSKASING										
Kapuskasing R	144.2	-73.2	13	41	6.6	67.1°S	317°W	10.5	11.8	59°S
Kapuskasing N	305.7	70.9	6	111	6.4	57.0°N	144°W	8.4	9.8	55°N
Kap+Mar R East	143.9	-67.0	17	24	7.5	66.7°S	340.5°W	10.2	12.4	49.6°S
Kap+Mar N East	310.6	67.2	9	71	6.2	58.5°N	155°W	8.5	10.2	49.9°N

For example, Kap + Mar R East indicates that the Kap R data have been combined with the Marathon R East data. **MDEC'**, **MINC'** are the mean declination and inclination at the common site Lat 48°N, Long. 79°W for Matachewan dikes and Lat. 49°N, Long. 86°W for all other dikes; **PLAT**, **PLON** are pole latitude, longitude; *N* is the number of sites; k is the precision parameter; α_{95} is the radius of the 95% circle of confidence about the mean direction; dp,dm are the semi minor and major axes of the 95% confidence ellipse about the pole; λ is the paleolatitude.

Table 8. All paleomagnetic sites in N- to ENE-striking dikes that did not attain the acceptance criteria of N ≥ 4 and/or α_{95} ≤15°.

SITE	SLAT (°N)	SLON (°W)	W (m)	STRIKE (°)	N	DEC (°)	INC (°)	k	α_{95} (°)
KAPUSKASING R ?									
KP2	47° 57.6'	84° 19.0'	5	045	7	10.1	-81.2	14	16.5
TK8	47° 50.1'	84°26.3'	9	075	3	14.6	-73.8	20	28.5
KP7	48° 00.8'	84° 07.2'	11	050	3	29.3	-70.8	451	5.8
SL17	48° 18.0'	85° 58.0'	25	060	1 [4]	104.0	-62.0	21	28.0
KAPUSKASING N ?									
KP5	47° 57.8'	84° 06.6'	17	075	7	293.8	77.6	13	17.6
KP6	47° 58.5'	84° 06.5'	10	058	3	288.5	65.4	81	13.8
TK23	47° 47.0'	84° 23.5'	30	050	3	300.8	81.8	19	28.9
OL1+2	50° 48.2'	87° 10.0'	34	055	7	187.2	82.8	9	20.8
MARATHON R EAST ?									
TK5	47° 52.0'	84° 27.5'	1	100	2	354.1	-61.5	373	13.0
TK6	47° 50.6'	84° 26.5'	0.2	075	3	148.5	-65.9	92	12.9
TK20	47° 47.8'	84° 24.0'	22	060	1	145.2	-46.2	-	-
MARATHON R WEST									
DP9	50° 19.0'	87° 50.4'	26	040	3	126.2	-51.0	23	12.0

Sites from which no coherent remanence could be obtained are KP1, KP4, KP9, KP25, DP1, and DP2. N is number of samples yielding directional estimates; in brackets is the number of additional samples yielding remagnetization circles.

Table 9. [1]Geochemistry of selected Proterozoic mafic dikes east of Lake Nipigon and in the region of the Kapuskasing Zone.

Sample No.	03GRS-0037A	03GRS-0001A	03GRS-0042A	03GRS-0047A	03GRS-0049A	03GRS-0054A	04GRS-0059A
Site No.	DP3	DP6	DP9	KP23	KP27	KP32	MK 7-3-1
Swarm N or R	Marathon R	Marathon R	Marathon R	Marathon R	Marathon R	Marathon R	Marathon R
SiO2 (%)	51.58	49.05	49.68	47.86	54.3	50.84	49.4
TiO2	0.99	1.26	1.09	2.24	1.75	1.48	1.34
Al2O3	14.63	14.6	15.5	13.3	14.16	14.48	14.4
Fe2O3	11.89	13.32	11.54	16.49	13.46	15.97	14.2
MnO	0.2	0.3	0.19	0.21	0.18	0.23	0.19
MgO	7.49	6.77	8.02	4.67	4.15	4.55	6.02
CaO	11.59	9.79	11.98	8.21	8.03	8.65	9.64
Na2O	1.99	2.87	1.86	3.31	3.68	2.5	2.33
K2O	0.55	1.21	0.3	0.92	0.94	0.87	1.02
P2O5	0.07	0.13	0.13	0.31	0.31	0.15	0.15
CO2	0.41	0.13	0.63	0.22	0.21	1.06	0.46
S	0.12	0.12	0.1	0.18	0.11	0.16	0.12
LOI	0.66	1.78	0.31	1.73	0.7	0.88	0.95
TOTAL	101.64	101.08	100.59	99.26	101.66	100.62	99.7
La (ppm)	8.71	14.19	11.56	34.49	22.06	18.04	13.8
Ce	19.02	30.89	26.28	73.3	48.54	38.87	29.96
Pr	2.45	4.04	3.44	9.04	6.14	4.84	3.81
Nd	10.65	18.08	15.14	38.44	25.66	20.39	15.97
Sm	2.62	4.05	3.42	8.21	5.56	4.86	3.68
Eu	0.88	1.36	1.09	2.15	1.59	1.48	1.15
Gd	2.97	4.51	3.57	8.32	5.6	5.23	3.84
Tb	0.48	0.71	0.56	1.26	0.84	0.84	0.61
Dy	3.09	4.27	3.47	7.48	5.1	5.45	3.75
Ho	0.65	0.88	0.71	1.55	1.06	1.15	0.77
Er	1.93	2.54	2.04	4.44	3	3.46	2.23
Tm	0.28	0.36	0.3	0.63	0.43	0.5	0.32
Yb	1.8	2.27	1.86	4.06	2.78	3.33	2.07
Lu	0.27	0.35	0.29	0.62	0.42	0.51	0.32
Th	1.68	1.57	1.07	4.13	2.33	3.68	1.84
U	0.29	0.26	0.21	0.69	0.44	0.83	0.32
Ba	169	283	138	365	326	369	236
Rb	13.87	61.53	13.34	23.22	20.67	28.74	11.78
Sr	159.4	225.1	163.3	186	285.5	204.2	185.3
Cs	0.6	1.23	2.07	2.44	1.1	1.71	0.66
Be	0.31	0.57	0.32	0.81	0.54	0.54	0.48
Sc	33.8	40.9	29.1	29.9	24.8	35.4	28.1
V	230.3	319.2	208.2	289	237.2	>320.0	231.2
Y	16.75	23.51	18.28	38.95	26.76	29.71	19.75
Zr	60.4	84.7	69.1	213.5	160.4	123.8	92.1
Nb	5.6	10.2	7.8	20.6	13.7	9.1	9.1
Hf	1.7	2.5	1.9	5.5	4	3.4	2.4
Ta	0.34	0.68	0.47	1.19	0.79	0.54	0.53
Cr	161.92	116.84	177.84	41.72	47.4	19.54	104.29
Co	45	74	45	42	35	49	45
Ni	81	89	92	49	64	42	69
Cu	266	94	163	84	90	81	63
Zn	97	190	87	131	111	133	115
Ga	16	19	18	19	21	21	19
Pb	14	29	7	8	8	ND	5
Pd	ND	ND	ND	ND	ND	ND	
Pt	ND	ND	ND	ND	ND	ND	
Au	ND	6.63	ND	ND	ND	ND	

Sample No.	04GRS-0075A	04GRS-0066A	04GRS-0070A	04GRS-0071A	04GRS-0073A	03GRS-0041A	02GRS-02B
Site No.	TK13-4-1	TK20-1-2	TK48-13-1	TK48-17&18	TK82-5	DP8	DP2
Swarm N or R	Marathon R	Marathon R	Marathon R	Marathon R	Marathon R	Mar athon R	Marathon N
SiO2 (%)	50.48	50.3	48.1	49.14	48.8	44.86	49.78
TiO2	0.88	0.95	3.03	3.1	0.75	3.46	1.68
Al2O3	13.79	14.3	12.6	12.97	15.5	12.91	13.2
Fe2O3	12.66	12.2	16.9	16.74	11.5	16.93	16.12
MnO	0.18	0.2	0.23	0.25	0.18	0.26	0.24
MgO	7.41	8.19	4.86	4.75	8.44	5.26	6.08
CaO	15.04	11.9	8.76	8.22	12.1	9.01	9.52
Na2O	1.29	1.88	2.46	2.79	1.62	1.78	2.29
K2O	0.15	0.28	1.19	1.52	0.32	1.35	0.79
P2O5	0.09	0.08	0.55	0.56	0.07	0.55	0.16
CO2	0.45	0.37	1.31	0.48	0.37	0.35	0.24
S	0.08	0.1	0.16	0.17	0.05	0.56	0.12
LOI	0.43	0.05	0.05	0.43	0.85	2.94	1.08
TOTAL	102.39	100.2	98.7	100.47	100.1	99.3	100.94
La (ppm)	5.86	5.62	37.9	40.9	3.9	44.06	18.71
Ce	13.47	12.84	82.84	88.72	9.35	95.39	40.24
Pr	1.88	1.74	10.41	11.12	1.34	12.24	5.09
Nd	8.55	7.79	43.56	46.7	6.45	52.26	21.24
Sm	2.25	2.09	9.35	9.86	1.86	10.85	5.18
Eu	0.8	0.75	2.54	2.7	0.72	2.88	1.54
Gd	2.64	2.38	8.91	9.46	2.26	10.51	5.09
Tb	0.43	0.41	1.32	1.41	0.38	1.56	0.86
Dy	2.74	2.55	7.89	8.3	2.44	9.21	5.05
Ho	0.57	0.54	1.57	1.66	0.51	1.88	1.11
Er	1.68	1.56	4.48	4.73	1.51	5.24	3.04
Tm	0.24	0.23	0.63	0.67	0.21	0.74	0.44
Yb	1.53	1.48	4.03	4.23	1.38	4.77	2.96
Lu	0.23	0.23	0.6	0.63	0.21	0.71	0.46
Th	0.84	0.64	4.94	5.43	0.4	3.99	3.51
U	0.2	0.14	0.89	0.96	0.08	0.89	0.62
Ba	156	130	597	645	95	758	
Rb	34.52	2.38	19.93	32.68	25.14	52.57	29.21
Sr	169.7	137	206	222.1	150.1	241.7	199.37
Cs	1.36	0.33	0.46	0.58	1.97	5.98	1.76
Be	0.24	0.27	0.94	0.98	0.19	1.7	ND
Sc	28	25.8	24.5	26.7	30.2	32.6	38
V	181.4	210.9	290.7	304.6	192.6	>320.0	323
Y	14.88	13.96	39.84	42.06	12.96	47.83	31.45
Zr	49.4	47.1	237.3	250.4	37.9	289.7	132.36
Nb	3.3	4.2	27.9	29.2	2.4	40.5	14.4
Hf	1.4	1.3	6	6.2	1.1	7	3.29
Ta	0.19	0.25	1.59	1.69	ND	2.27	0.72
Cr	195.09	215.55	48.69	54.98	231.04	45.94	69.58
Co	49	42	34	38	52	38	63
Ni	133	112	44	48	140	42	67
Cu	1855	139	100	113	149	40	61
Zn	210	76	141	148	83	91	137
Ga	19	19	24	24	16	24	
Pb	101	ND	10	16	ND	5	7
Pd						ND	ND
Pt						2.85	ND
Au						ND	ND

Sample No.	03GRS-0046A	04GRS-0096A	03GRS-0048A	03GRS-0050A	03GRS-0052A	04GRS-0007D	04GRS-0062A
Site No.	KP21	KP21-5-2	KP24	KP28	KP30	LL20	TK7-4-1
Swarm N or R	Marathon N	Marathon N	Marathon N	Marathon N	Marathon N	Marathon N	Marathon N
SiO2 (%)	50.81	50.18	50.95	49.43	51.24	49.54	51.3
TiO2	2.01	1.94	1.41	2.18	1.45	1.87	2.45
Al2O3	14.57	14.1	14.07	14.21	13.83	14.72	12.5
Fe2O3	15.94	14.5	13.85	13.48	14.12	15.03	16.6
MnO	0.21	0.23	0.22	0.28	0.23	0.22	0.23
MgO	4.52	5.11	6.01	6.26	6.15	5.86	4.29
CaO	8.73	9.29	9.42	8.3	10.39	9.64	8.68
Na2O	2.1	2.17	3.02	3.66	2.62	2.29	2.32
K2O	1.31	0.89	0.46	0.78	0.4	0.73	1.1
P2O5	0.26	0.25	0.12	0.26	0.16	0.16	0.27
CO2	0.17	0.24	0.33	0.46	0.28	0.16	0.61
S	0.13	0.14	0.14	0.18	0.15	0.08	0.14
LOI	0.43	0.14	1.7	2.03	0.7	0.93	0.3
TOTAL	100.89	98.79	101.24	100.86	101.29	101	100.1
La (ppm)	26.6	23.98	12.3	24.07	11.21	18.96	17.12
Ce	54.68	51.12	27.83	51.08	25.16	40.91	39.61
Pr	6.73	6.51	3.68	6.37	3.35	5.26	5.13
Nd	28.5	27.89	16.68	27.62	15.09	22.17	22.16
Sm	6.54	6.12	4.15	6.01	3.88	5	5.27
Eu	1.75	1.76	1.28	1.68	1.24	1.54	1.59
Gd	6.81	6.27	4.89	6.19	4.47	5.28	5.77
Tb	1.06	1.05	0.81	0.97	0.76	0.82	0.92
Dy	6.51	6.3	5.18	5.84	4.87	5.07	5.77
Ho	1.37	1.28	1.12	1.21	1.04	1.04	1.2
Er	3.99	3.87	3.26	3.44	3.11	2.98	3.49
Tm	0.57	0.55	0.48	0.5	0.45	0.44	0.51
Yb	3.71	3.49	3.09	3.19	2.98	2.88	3.27
Lu	0.55	0.52	0.47	0.48	0.45	0.43	0.5
Th	4.14	3.5	2.66	3.89	1.9	2.79	3.88
U	0.64	0.61	0.6	0.47	0.44	1.03	1.16
Ba	454	442	153	358	139	214	294
Rb	24.61	17.83	20.71	31.37	18.67	41.04	3.47
Sr	184.7	171.3	193.4	327.3	170	168.3	94.4
Cs	0.49	0.41	4.53	1.12	4.1	2.16	0.69
Be	0.59	0.58	0.46	1.64	0.54	0.56	0.61
Sc	30.3	28.8	36.7	31.1	39.9	32.4	22.4
V	279.3	268.8	293.2	313.1	308.9	303.8	313.5
Y	34.79	34.32	28.38	30.49	26.56	27.46	31.66
Zr	173.7	167.8	108	157.8	94.8	154.7	150.4
Nb	14.4	13.8	9.8	15.9	9.6	21.4	13.4
Hf	4.6	4.3	2.9	4	2.6	3.9	4
Ta	0.84	0.79	0.57	0.9	0.56	1.24	0.79
Cr	49.91	47.28	52.24	103.24	49.86	84.04	12.19
Co	43	45	43	36	48	40	32
Ni	53	54	54	59	59	72	34
Cu	85	97	132	52	514	109	453
Zn	132	131	102	191	137	116	139
Ga	22	23	18	21	19	20	25
Pb	6	9	ND	20	26	ND	29
Pd	ND		ND	ND	ND	ND	
Pt	ND		ND	ND	ND	2.23	
Au	ND		ND	ND	6.52	ND	

Sample No.	02GRS-01B	03GRS-0038A	04GRS-0095A	04GRS-0090A	04GRS-0091A	04GRS-0092A	04GRS-0093A
Site No.	DP1	DP4	KP20-1-5	KP15-7-2	KP17-1-3	KP18-7-1	KP19-7-1
Swarm N or R	Marathon N/R	Biscotasing R	Biscotasing R	Biscotasing N	Biscotasing N	Biscotasing N	Biscotasing N
SiO2 (%)	49.48	46.02	45.7	50	50.4	50.2	49.6
TiO2	1.09	3.44	3.34	2.89	1.41	2.93	1.26
Al2O3	14.62	14.17	12.8	13.1	14.2	12.9	13.4
Fe2O3	12.35	18.38	18.4	14.5	14.1	14.8	14.2
MnO	0.21	0.25	0.31	0.18	0.22	0.18	0.22
MgO	7	5.01	5.3	4.43	6.78	4	6.73
CaO	9.79	8.32	7.34	7.09	10.3	8.05	9.95
Na2O	2.63	2.78	2.94	3.05	2.29	2.38	2.23
K2O	1.5	0.96	1.14	1.58	0.32	1.65	0.8
P2O5	0.1	0.42	0.45	0.38	0.17	0.38	0.13
CO2	0.18	0.28	0.46	0.36	0.58	0.41	0.44
S	0.1	0.22	0.23	0.2	0.1	0.15	0.15
LOI	2.11	1.17	1.15	1.85	0.05	1.3	1.5
TOTAL	100.88	100.93	99	99.2	100.4	99	100.1
La (ppm)	10.41	28.05	24.55	32.43	15.02	33.3	7.95
Ce	23.04	62.43	56.73	67.76	32.17	70.68	18.62
Pr	3.03	8.08	7.46	8.45	4.11	8.83	2.48
Nd	12.88	35.48	33.24	35.12	17.3	37.45	11.19
Sm	3.01	8.22	7.71	7.56	3.89	7.9	2.76
Eu	1.11	2.59	2.49	2.25	1.23	2.25	0.91
Gd	3.11	8.19	7.57	7.3	4.12	7.63	2.99
Tb	0.54	1.22	1.15	1.12	0.66	1.17	0.5
Dy	3.16	6.98	6.56	6.69	4.13	6.9	3.19
Ho	0.7	1.4	1.29	1.33	0.86	1.36	0.66
Er	1.87	3.78	3.63	3.72	2.51	3.89	1.98
Tm	0.27	0.52	0.5	0.53	0.36	0.55	0.29
Yb	1.67	3.31	3.13	3.35	2.36	3.47	1.87
Lu	0.27	0.49	0.47	0.5	0.35	0.52	0.28
Th	1.17	4.36	4.08	6.01	2.42	6.27	0.99
U	0.21	1.27	1.31	1.39	0.46	1.55	0.22
Ba		284	257	400	179	331	115
Rb	88.27	37.43	23.26	35.08	11.92	83.61	1.28
Sr	419.98	245	234.5	202.8	171.7	253.5	122.2
Cs	1.57	1.88	1.76	2.13	1.21	5.62	0.91
Be	ND	0.96	0.92	1.26	0.46	1.23	0.35
Sc	36	23.7	22	21.6	30	21.1	24.2
V	243	315	284.7	245.3	263.5	242.1	217.4
Y	19.21	35.83	33.03	33.92	22.66	36.47	17.1
Zr	69.71	257.8	245.1	225.5	97.3	240.4	63.6
Nb	8.64	21.3	19.4	20	10	21	6.3
Hf	1.8	6.2	5.9	5.6	2.5	5.8	1.7
Ta	0.45	1.3	1.24	1.2	0.58	1.24	0.38
Cr	117.37	36.4	33.06	32.94	86.16	27.48	61.14
Co	55	42	42	30	46	29	41
Ni	75	63	58	34	73	31	52
Cu	65	436	215	46	396	47	176
Zn	85	196	172	89	130	103	100
Ga		26	27	26	20	26	23
Pb	7	29	19	10	22	10	14
Pd	ND	ND					
Pt	ND	ND					
Au	11.54	ND					

Sample No.	03GRS-0051A	03GRS-0053A	04GRS-0109A	03GRS-0045A	04GRS-0009B	04GRS-0104A	04GRS-0107A
Site No.	KP29	KP31	DP11-2-1	LL16	LL22	LS3-2	LS4-9
Swarm N or R	Biscotasing N	Biscotasing N	Keweenawan R	Keweenawan R	Keweenawan R	Keweenawan R	Keweenawan R
SiO2 (%)	48.98	47.25	51.16	52.25	48.19	45.69	52.79
TiO2	1.22	3.47	1.49	1.26	1.21	1.47	1.11
Al2O3	14.76	13.96	12.64	12.63	14.71	14.35	12.49
Fe2O3	12.45	17.13	14.37	14.2	13.24	12.15	8.02
MnO	0.2	0.21	0.26	0.25	0.2	0.18	0.1
MgO	7.88	4.31	6.39	7.25	6.25	11.18	7.48
CaO	10.51	7.92	10.2	10.42	10.94	5.17	9.01
Na2O	2.28	3.42	2	2.27	2.35	1.81	4.35
K2O	0.43	0.93	0.68	0.49	0.54	0.66	0.71
P2O5	0.12	0.41	0.17	0.13	0.13	0.12	0.15
CO2	0.36	0.17	0.31	0.12	0.24	0.16	1.38
S	0.1	0.19	0.13	0.04	0.08	0.02	0.02
LOI	2.21	1.38	0.4	ND	1.43	7.07	0.99
TOTAL	101.04	100.38	99.77	101.15	99.18	101.29	97.2
La (ppm)	8.17	31.71	15.6	8.21	13.73	12.6	15.23
Ce	19.56	68.31	34.22	18.44	29.44	28.11	32.06
Pr	2.7	8.54	4.29	2.52	3.79	3.62	4.02
Nd	12.08	37.19	18.29	11.52	16.23	15.78	17.33
Sm	3.14	8.28	4.08	3.12	3.64	4	3.9
Eu	0.99	2.43	1.31	1.11	1.2	0.97	1.06
Gd	3.67	8.37	4.3	3.88	3.88	4.39	3.98
Tb	0.61	1.23	0.68	0.66	0.62	0.73	0.63
Dy	3.86	7.17	4.11	4.24	3.78	4.36	3.81
Ho	0.83	1.39	0.85	0.9	0.78	0.88	0.77
Er	2.4	3.77	2.47	2.59	2.26	2.41	2.21
Tm	0.35	0.53	0.35	0.38	0.32	0.34	0.3
Yb	2.25	3.33	2.26	2.38	2.33	2.05	1.85
Lu	0.35	0.49	0.34	0.36	0.32	0.29	0.27
Th	1	7.16	1.86	1.21	1.64	1.05	1.4
U	0.24	2.1	0.32	0.34	0.28	0.3	0.34
Ba	152	301	218	159	195	211	349
Rb	20.17	30.08	13.25	11.38	14.17	16.51	18.85
Sr	195.6	141	179.7	153.7	193.8	169.3	367.9
Cs	2.67	2.18	1.57	0.55	1.8	2.43	1.96
Be	0.53	1.18	0.43	0.3	0.42	1.95	0.84
Sc	35.7	25.1	29.5	28.3	30.3	29.1	23.7
V	267.7	318.2	267.8	266.7	246	279.2	236.2
Y	20.86	35.66	21.57	22.8	19.62	21	19.46
Zr	77.6	216.6	104	83.3	89.8	97	105.9
Nb	7.9	19.1	10.1	4.8	9	3.8	3.6
Hf	2.1	5.7	2.7	2.3	2.4	2.6	2.7
Ta	0.47	1.22	0.58	0.29	0.54	0.23	0.22
Cr	158.99	38.1	57.4	109.81	89.57	91.51	136.02
Co	44	40	46	46	45	48	39
Ni	78	55	62	99	67	95	105
Cu	90	159	168	149	51	164	137
Zn	105	132	123	103	113	104	107
Ga	16	27	20	21	I8	23	21
Pb	6	13	9	ND	ND	232	19
Pd	4.39	ND		16.42	ND		
Pt	5.65	ND		5.39	ND		
Au	ND	ND		ND	ND		

Sample No.	03GRS-0004A	04GRS-0003C	04GRS-0008C	03GRS-0044A	03GRS-0055A	03GRS-0057A	04GRS-0112A
Site No.	LL13	LL19	LL21	LL7	OL1	OL2-12	214-16
Swarm N or R	Matachewan R	Matachewan R	Matachewan R	Matachewan R	Matachewan R	Matachewan R	Matachewan N
SiO2 (%)	49.78	48.5	48.35	48.17	50.37	51.18	51.83
TiO2	1.46	1.54	1.32	2.82	1.81	0.89	1.32
Al2O3	14.89	14.31	13.48	13.69	12.5	13.86	12.28
Fe2O3	15.98	16.2	15.83	16.17	11.56	7.18	12.33
MnO	0.24	0.23	0.24	0.23	0.2	0.15	0.22
MgO	4.71	4.94	5.27	4.91	6.4	9.54	6.56
CaO	8.85	9.74	9.8	9.08	8.69	13.66	11.04
Na2O	2.58	2.47	2.54	2.27	5.91	2.5	3.68
K2O	1.29	0.72	0.67	0.81	0.37	0.44	0.32
P2O5	0.14	0.18	0.14	0.3	0.24	0.11	0.13
CO2	0.29	0.13	0.13	0.46	0.41	0.37	0.15
S	0.11	0.09	0.12	0.12	0.11	0.11	0.09
LOI	1.28	0.2	0.88	2.32	0.51	0.08	0.13
TOTAL	101.22	99.03	98.53	100.76	98.57	99.59	99.82
La (ppm)	12.65	17.96	14.28	18.42	21.47	24.44	12.37
Ce	27.51	39.15	31.2	41.9	45.38	52.52	27.64
Pr	3.75	5.09	4.1	5.55	5.58	6.55	3.59
Nd	16.6	22.15	17.56	24.99	23.5	27.61	15.66
Sm	4.13	5.2	4.34	6.07	4.95	5.89	3.94
Eu	1.41	1.55	1.36	1.99	1.38	1.8	1.21
Gd	5.19	6.13	5.14	6.38	4.91	5.76	4.56
Tb	0.89	1.01	0.86	0.98	0.72	0.85	0.77
Dy	5.71	6.4	5.6	5.9	4.33	4.95	4.79
Ho	1.2	1.36	1.17	1.18	0.86	1	1.03
Er	3.68	4.09	3.54	3.39	2.44	2.83	3.07
Tm	0.55	0.59	0.52	0.48	0.34	0.4	0.45
Yb	3.66	3.91	3.43	2.97	2.16	2.57	2.95
Lu	0.53	0.58	0.51	0.44	0.32	0.38	0.44
Th	1.7	3.06	2.57	2.85	3.32	3.99	2.16
U	0.46	0.78	0.64	0.88	0.5	0.6	0.58
Ba	259	268	208	253	175	387	175
Rb	99.68	22.39	26.05	63.76	10.75	14.51	13.26
Sr	165.9	153.2	152.5	179.5	211.8	259.8	145.8
Cs	3	1.18	2.81	2.82	1.04	1.77	0.61
Be	0.59	0.49	0.41	0.75	0.64	0.81	0.41
Sc	41	26.4	30.1	30.6	24.1	24	33.8
V	>320.0	279.4	295.5	>320.0	239.5	241.3	274.7
Y	32.59	36.14	32.38	30.16	21.79	25.77	27.12
Zr	113.9	158.2	132.2	166.7	128.9	153	104
Nb	6.7	9	6.5	19.9	12.4	14.7	9
Hf	3.1	4	3.3	4.3	3.3	3.9	2.8
Ta	0.51	0.55	0.4	1.2	0.71	0.84	0.53
Cr	71.31	74.7	88.49	45.07	118.01	116.97	92.6
Co	74	36	41	34	42	43	44
Ni	63	69	62	49	68	65	76
Cu	226	128	148	70	289	183	258
Zn	195	150	144	110	119	105	103
Ga	21	19	19	21	20	21	19
Pb	9	6	7	7	17	17	8
Pd	ND	2.42	ND	ND	ND	ND	
Pt	1.31	4.26	3.3	ND	ND	ND	
Au	6.71	ND	ND	ND	ND	ND	

Sample No.	04GRS-0100A	04GRS-0101A	04GRS-0102A	04GRS-0086A	04GRS-0089A	04GRS-0077A	04GRS-0079A
Site No.	186-5-1	229-5-1	HP2-1-2	KP10-1&4	KP13-1-1	KP2-1-3	KP3-2-4
Swarm N or R	Kapuskasing R	Kapuskasing R	Kapuskasing R	Kapuskasing R	Kapuskasing R	Kapuskasing R	Kapuskasing R
SiO2 (%)	48.1	50.6	48.1	47.1	51.5	51.2	47.1
TiO2	1.81	1.15	2.23	2.04	1.07	1.32	2.85
Al2O3	13.6	14.2	12.9	12.7	13.7	13.7	12.9
Fe2O3	14.9	14	16.7	18.6	13.4	14	17
MnO	0.21	0.22	0.24	0.27	0.21	0.21	0.23
MgO	6.7	6.14	5.48	5.45	5.97	6.01	5.11
CaO	9.91	10.8	9.47	9.59	10.4	9.81	9.13
Na2O	2.07	1.88	2.19	1.92	2.19	2.19	2.38
K2O	0.89	0.36	0.85	0.6	0.51	0.69	0.97
P2O5	0.28	0.11	0.34	0.24	0.12	0.17	0.43
CO2	0.18	0.82	0.19	0.19	0.28	0.39	0.36
S	0.19	0.12	0.19	0.21	0.06	0.11	0.2
LOI	0.4	0.7	0.1	0.75	0.75	0.4	<0.01
TOTAL	98.9	100.1	98.7	99.3	99.8	99.9	98.3
La (ppm)	35.91	7.94	25.23	18.55	7.87	15.36	30.16
Ce	77.62	18.27	55.13	41.27	18.98	33.22	65.83
Pr	9.73	2.49	7.14	5.53	2.55	4.22	8.55
Nd	40.98	11.57	30.42	24.39	11.32	17.48	36.13
Sm	8.66	3.04	6.71	5.73	2.86	3.92	7.8
Eu	2.53	1.04	2.08	1.86	0.93	1.16	2.24
Gd	8.48	3.52	6.54	6.25	3.26	4	7.52
Tb	1.3	0.63	1.01	1.02	0.56	0.63	1.14
Dy	7.7	3.96	6.1	6.35	3.62	3.89	6.83
Ho	1.51	0.83	1.21	1.31	0.78	0.8	1.36
Er	4.44	2.51	3.5	3.92	2.39	2.35	3.86
Tm	0.62	0.36	0.49	0.56	0.35	0.34	0.55
Yb	3.97	2.41	3.21	3.64	2.32	2.16	3.55
Lu	0.59	0.36	0.47	0.55	0.36	0.33	0.53
Th	5.17	1.05	2.68	2.2	1.48	2.54	3.72
U	0.93	0.28	0.61	0.49	0.5	0.49	0.72
Ba	514	142	493	238	477	265	441
Rb	29.42	7.47	24.34	30.77	38.04	5.12	9.08
Sr	228.3	150.1	232.3	150.8	179.7	150.2	181.1
Cs	1.08	0.24	0.66	4.1	1.17	0.56	1.75
Be	0.93	0.32	0.76	0.64	0.57	0.44	0.85
Sc	28.8	33.6	31.6	36	28.3	25.2	22.7
V	317.7	261.5	310.1	>320.0	219.5	223.7	287.5
Y	40.48	21.82	31.44	34.33	19.96	20.31	34.64
Zr	226.3	69.7	156.1	148.2	76.3	102	200.6
Nb	26.9	6.3	22.8	16.6	5.4	9.6	24.2
Hf	5.6	1.9	3.9	3.7	2.1	2.7	5.1
Ta	1.55	0.37	1.28	0.96	0.33	0.56	1.4
Cr	45.52	34.62	45.9	45.62	68.01	52.13	76.66
Co	43	48	43	54	44	43	35
Ni	50	61	47	74	78	53	56
Cu	519	141	341	263	431	65	545
Zn	193	100	164	161	111	104	174
Ga	23	17	22	22	18	20	24
Pb	32	ND	23	12	20	ND	36
Pd							
Pt							
Au							

Sample No.	04GRS-0081A	04GRS-0097A	04GRS-0068A	04GRS-0063A	04GRS-0065A	04GRS-0087A	04GRS-0088A
Site No.	KP7-1-1	KS13-4	TK36-20-1	TK8-6	TK9-3-2	KP11-3-1	KP12-3-1
Swarm N or R	Kapuskasing R	Kapuskasing R	Kapuskasing R	Kapuskasing R	Kapuskasing R	Kapuskasing N	Kapuskasing N
SiO2 (%)	50.1	50.5	47.1	51.3	48	49.5	49.77
TiO2	1.47	1.28	0.38	2.51	2.9	1.99	2.04
Al2O3	13.7	13.3	17.8	12.6	12.5	13.4	13.36
Fe2O3	15	14.4	11.4	16.4	17.6	14.9	15.41
MnO	0.22	0.21	0.17	0.22	0.23	0.2	0.17
MgO	6.25	6.3	7.83	4.03	4.85	5.09	5.14
CaO	10.3	9.97	10.5	8.34	8.84	8.65	8.01
Na2O	2.22	2.87	2.39	2.5	2.48	2.6	2.32
K2O	0.51	0.54	0.44	1.12	1	1.26	2.61
P2O5	0.17	0.13	0.11	0.29	0.46	0.28	0.3
CO2	0.38	0.28	1.67	0.93	0.27	0.34	0.41
S	0.17	0.12	0.03	0.13	0.16	0.16	0.11
LOI	0.1	0.8	1.8	0.15	0.3	1	1.61
TOTAL	100.1	100.3	100	99.5	98.7	99	100.74
La (ppm)	35.36	7.95	13.02	16.96	29.5	22.38	19.08
Ce	74.86	19.45	25.08	37.81	66.44	48.91	42.02
Pr	9.45	2.74	2.89	4.85	8.48	6.17	5.38
Nd	38.94	12.19	11.13	20.75	35.76	26.15	23.29
Sm	8.44	3.11	2.04	4.98	7.86	5.87	5.24
Eu	2.47	0.98	0.69	1.5	2.18	1.72	1.59
Gd	8.23	3.6	2.11	5.35	7.71	6.06	5.38
Tb	1.23	0.62	0.38	0.86	1.16	0.97	0.87
Dy	7.27	4.07	2.64	5.3	6.96	5.91	5.35
Ho	1.43	0.86	0.62	1.11	1.41	1.22	1.11
Er	4.1	2.57	2	3.21	3.96	3.55	3.23
Tm	0.58	0.38	0.31	0.47	0.57	0.51	0.47
Yb	3.73	2.48	2.14	3.09	3.57	3.27	3.02
Lu	0.55	0.37	0.35	0.46	0.55	0.49	0.46
Th	6.37	1.36	1.61	4.08	4.11	3.91	3.3
U	1.64	0.45	0.29	1.13	0.84	0.61	0.53
Ba	185	136	236	299	483	450	397
Rb	43.59	1.83	9.55	12.99	3.83	3.7	1.36
Sr	261.4	110.4	208.6	96.4	167.6	166.4	105.1
Cs	2.81	0.43	0.25	0.65	1.91	2.25	2.25
Be	1.1	0.38	0.24	0.58	0.88	0.57	0.53
Sc	22.3	24	24.3	19.8	23	24	20.1
V	253.7	242.3	114.4	265.8	281.1	275.6	255.7
Y	37.43	21.68	16.77	29.22	35.2	31.85	28.14
Zr	247.8	84.9	46.2	141.8	210.9	148.4	140
Nb	21.8	7.4	10.8	12.6	24.8	11.8	10.9
Hf	6.1	2.3	1.1	3.7	5.2	3.9	3.6
Ta	1.3	0.47	0.49	0.78	1.42	0.65	0.61
Cr	28.33	75.25	40.44	11.97	45.26	46.13	42.56
Co	30	40	52	29	37	40	34
Ni	32	63	161	28	41	53	38
Cu	105	319	76	215	40	1471	91
Zn	143	85	83	112	147	208	137
Ga	27	22	15	29	25	23	24
Pb	14	15	ND	17	ND	92	10
Pd							
Pt							
Au							

Sample No.	04GRS-0080A	04GRS-0083A	04GRS-0069A	04GRS-0072A	04GRS-0098A
Site No.	KP5-7	KP8-11-1	TK46-4-1	TK57-3-1,2	SL13-11-1
Swarm N or R	Kapuskasing N	Kapuskasing N	Kapuskasing N	Kapuskasing N	Abitibi N
SiO2 (%)	50.3	53.1	48.4	48.2	44.1
TiO2	1.82	2.27	1.38	2.48	3.97
Al2O3	13.8	12.6	13.7	13.6	14.2
Fe2O3	13.2	15.2	14.5	15.9	16.8
MnO	0.22	0.2	0.22	0.22	0.22
MgO	6.01	3.53	7.06	5.35	4.84
CaO	9.9	7.37	10.8	8.99	7.55
Na2O	2.41	2.56	1.88	2.31	3.34
K2O	0.69	1.6	0.4	1.03	1.94
P2O5	0.21	0.46	0.12	0.36	1.45
CO2	0.4	0.52	0.47	0.75	0.37
S	0.18	0.14	0.19	0.31	0.1
LOI	1.1	0.2	0.25	1.35	0.25
TOTAL	99.7	99.3	98.8	99.9	98.5
La (ppm)	21.47	48	10.94	34.49	69.77
Ce	45.56	98.28	22.3	73.12	152.31
Pr	5.86	12.14	3	8.92	19.05
Nd	24.64	49.48	13.03	37	77.06
Sm	5.45	10.23	3.2	7.98	13.69
Eu	1.69	2.69	0.94	2.21	4.19
Gd	5.34	10.04	3.54	7.63	11.16
Tb	0.82	1.56	0.56	1.17	1.49
Dy	4.97	9.45	3.61	7.06	8
Ho	0.99	1.91	0.76	1.4	1.46
Er	2.84	5.56	2.24	4.08	3.93
Tm	0.42	0.79	0.33	0.57	0.53
Yb	2.62	5.02	2.12	3.64	3.32
Lu	0.39	0.75	0.32	0.55	0.48
Th	2.79	6.7	1.12	5.04	6.01
U	0.53	0.93	0.31	0.83	1.43
Ba	262	760	137	554	1539
Rb	34.45	52.26	10.74	45.41	23.94
Sr	233.5	232	150.6	193.4	573.6
Cs	1.82	3.38	0.68	2.99	1.39
Be	0.66	0.76	0.43	0.89	1.24
Sc	29.5	26.4	31.8	26.9	14.2
V	270.1	202.8	250.6	263	145.5
Y	25.61	49.89	19.45	37.05	38.22
Zr	132.9	266.7	72.3	212.4	333.6
Nb	17.5	18.6	10.3	27.3	69.6
Hf	3.5	6.8	2	5.3	7.4
Ta	1.01	1.04	0.61	1.56	3.94
Cr	75.74	20.32	125.43	115.35	6
Co	40	34	55	44	38
Ni	47	114	83	74	39
Cu	205	>6000	78	553	185
Zn	111	914	79	168	177
Ga	20	24	23	22	27
Pb	15	632	ND	34	18
Pd					
Pt					
Au					

[1]Sample numbers shown in **bold** are coarser-grained samples. All other samples are fine-grained from chilled margins. **ND** = not determined.

Table 10a. Microprobe analyses of pyroxenes from Marathon and Matachewan dikes.

Sample	Dike Swarm	Station number	SiO2	TiO2	Al2O3	Cr2O3	MgO	CaO	MnO	FeO*	Na2O	K2O	Total
03GRS-1C-A-pyx1c	Marathon	DP6	51.427	0.498	2.761	0.163	15.252	20.552	0.209	7.792	0.262	0.002	98.918
03GRS-1C-A-pyx1i	Marathon	DP6	52.135	0.364	2.024	0.096	14.993	19.794	0.400	9.439	0.259	0.000	99.503
03GRS-1C-A-pyx1r	Marathon	DP6	50.458	0.600	1.618	0.004	10.462	19.758	0.545	15.951	0.250	0.002	99.648
03GRS-1C-A-pyx2c	Marathon	DP6	51.939	0.360	2.328	0.166	15.569	20.454	0.256	7.692	0.244	0.005	99.012
03GRS-1C-A-pyx2i	Marathon	DP6	51.950	0.416	2.064	0.047	15.240	18.898	0.347	10.207	0.240	0.000	99.410
03GRS-1C-A-pyx2r	Marathon	DP6	50.506	0.628	1.735	0.007	12.012	17.970	0.413	15.356	0.211	0.002	98.839
03GRS-1C-B-pyx3c	Marathon	DP6	52.218	0.436	2.180	0.072	16.560	18.429	0.254	9.311	0.218	0.000	99.678
03GRS-1C-B-pyx3i	Marathon	DP6	50.363	0.719	1.796	0.005	12.924	16.636	0.394	16.213	0.224	0.000	99.273
03GRS-1C-B-pyx3r	Marathon	DP6	50.594	0.705	1.672	0.014	11.965	17.204	0.431	16.751	0.224	0.000	99.560
03GRS-1C-C-pyx4c	Marathon	DP6	52.313	0.393	2.558	0.203	17.300	18.459	0.237	7.946	0.199	0.000	99.608
03GRS-1C-C-pyx4i	Marathon	DP6	52.308	0.375	2.124	0.118	17.148	18.033	0.216	8.629	0.208	0.000	99.157
03GRS-1C-C-pyx4r	Marathon	DP6	52.076	0.367	2.133	0.089	15.966	19.187	0.268	8.673	0.228	0.000	98.986
03GRS-1C-D-pyx5c	Marathon	DP6	51.210	0.557	2.110	0.012	15.246	16.851	0.313	12.669	0.228	0.000	99.196
03GRS-2C-A-pyx1c	Marathon	DP7	50.945	0.633	1.722	0.009	13.260	15.218	0.432	17.419	0.224	0.000	99.860
03GRS-2C-A-pyx1i	Marathon	DP7	49.974	0.680	1.672	0.006	10.699	16.080	0.507	20.238	0.183	0.001	100.040
03GRS-2C-A-pyx1r	Marathon	DP7	49.539	0.610	1.613	0.003	10.086	15.449	0.517	21.682	0.207	0.000	99.706
03GRS-2C-B-pyx2c	Marathon	DP7	52.848	0.344	1.915	0.104	17.562	18.093	0.223	8.208	0.202	0.000	99.498
03GRS-2C-B-pyx2i	Marathon	DP7	52.221	0.366	2.234	0.094	16.251	19.010	0.272	8.770	0.227	0.000	99.444
03GRS-2C-B-pyx2r	Marathon	DP7	50.208	0.583	1.429	0.008	12.777	13.261	0.494	20.422	0.179	0.003	99.364
03GRS-2C-C-pyx3c	Marathon	DP7	52.362	0.343	2.197	0.151	17.249	18.789	0.194	7.443	0.213	0.000	98.941
03GRS-2C-C-pyx3i	Marathon	DP7	52.531	0.357	2.221	0.160	17.779	17.756	0.251	8.284	0.203	0.002	99.544
03GRS-2C-C-pyx3r	Marathon	DP7	50.189	0.443	2.843	0.012	14.436	17.049	0.368	12.875	0.247	0.008	98.470
03GRS-4C-A-pyx1c	Matachewan	LL13	50.582	0.600	2.452	0.081	14.380	17.264	0.311	13.600	0.209	0.000	99.478
03GRS-4C-A-pyx1r	Matachewan	LL13	50.762	0.521	2.393	0.115	14.477	16.228	0.328	14.179	0.185	0.001	99.188
03GRS-4C-C-pyx3c	Matachewan	LL13	50.602	0.486	2.389	0.044	13.980	17.335	0.379	13.975	0.234	0.000	99.424
03GRS-4C-C-pyx3r	Matachewan	LL13	49.766	0.632	2.467	0.000	12.659	16.883	0.328	16.074	0.277	0.000	99.086
03GRS-4C-B-pyx2c	Matachewan	LL13	51.163	0.466	2.788	0.275	15.675	17.529	0.277	11.294	0.207	0.000	99.674
03GRS-4C-B-pyx2r	Matachewan	LL13	50.617	0.430	2.201	0.118	15.549	15.127	0.317	14.259	0.217	0.007	98.841
03GRS-3C-A-pyx1c	Marathon	DP8	49.825	1.476	2.654	0.000	12.904	17.921	0.368	14.164	0.251	0.000	99.563
03GRS-3C-A-pyx1r	Marathon	DP8	49.831	1.010	2.085	0.010	12.454	17.222	0.410	15.763	0.235	0.000	99.020
03GRS-3C-B-pyx2c	Marathon	DP8	49.589	1.176	2.409	0.009	12.673	17.057	0.413	15.667	0.233	0.001	99.227
03GRS-3C-B-pyx2r	Marathon	DP8	48.950	0.751	1.938	0.000	11.689	16.312	0.459	17.853	0.190	0.003	98.143

Table 10b. Microprobe analyses of amphiboles from Marathon dikes.

Sample	Dike Swarm	Station Number	SiO2	TiO2	Al2O3	C⁻2O3	MgO	CaO	MnO	FeO	NiO	Na2O	K2O	F	Cl	Total
03GRS-1C-C-pyx4r(alt)	Marathon	DP6	50.813	0.166	1.541	0.025	9.967	16.977	0.447	17.575	0.001	0.659	0.015	0.001	0.092	98.275
03GRS-1C-D-amp5r?	Marathon	DP6	44.380	1.575	6.327	0.000	6.958	9.665	0.362	25.592	0.010	1.926	0.786	0.757	0.402	98.739
03GRS-2C-D-amp1	Marathon	DP7	43.582	1.760	6.576	0.000	5.988	10.332	0.343	26.443	0.011	1.682	0.905	0.437	0.559	98.618

Table 10c. Microprobe analyses of plagioclase feldspar from Marathon and Matachewan dikes.

Sample	Dike Swarm	Station Number	SiO2	TiO2	Al2O3	CaO	FeO	SrO	BaO	Na2O	K2O	Total
03GRS-1C-A-fsp1c	Marathon	DP6	53.816	0.058	27.660	11.597	0.818	0.083	0.034	4.746	0.229	99.039
03GRS-1C-A-fsp1r	Marathon	DP6	55.591	0.081	26.765	10.050	0.876	0.099	0.027	5.617	0.314	99.419
03GRS-1C-B-fsp2c	Marathon	DP6	55.206	0.070	25.936	10.165	0.624	0.070	0.051	5.782	0.250	98.153
03GRS-1C-B-fsp2r	Marathon	DP6	54.834	0.071	26.933	10.373	0.761	0.120	0.037	5.491	0.278	98.898
03GRS-1C-C-fsp3c	Marathon	DP6	54.014	0.073	27.805	11.672	0.868	0.100	0.000	4.800	0.238	99.571
03GRS-1C-C-fsp3r	Marathon	DP6	53.789	0.103	27.730	11.529	1.210	0.067	0.016	4.976	0.274	99.693
03GRS-1C-C-fsp4c	Marathon	DP6	52.424	0.053	28.333	12.771	0.815	0.104	0.049	4.292	0.163	99.005
03GRS-1C-C-fsp5c	Marathon	DP6	53.811	0.076	27.379	11.502	0.763	0.071	0.021	4.861	0.223	98.706
03GRS-2C-B-fsp1c	Marathon	DP7	56.424	0.050	26.247	9.730	0.632	0.062	0.051	5.855	0.304	99.355
03GRS-2C-D-fsp2c	Marathon	DP7	55.953	0.061	26.397	9.950	0.620	0.126	0.024	5.791	0.313	99.234
03GRS-2C-D-fsp2r	Marathon	DP7	54.566	0.065	26.894	11.065	0.892	0.131	0.000	5.228	0.237	99.079
03GRS-2C-E-fsp3c	Marathon	DP7	54.123	0.054	27.440	11.265	0.792	0.073	0.000	5.017	0.254	99.018
03GRS-4C-A-fsp1c	Matachewan	LL13	54.210	0.055	27.412	11.344	0.708	0.090	0.016	4.949	0.171	98.955
03GRS-4C-A-fsp1r	Matachewan	LL13	55.012	0.049	27.683	11.087	0.846	0.022	0.008	5.208	0.181	100.096
03GRS-4C-B-fsp2c	Matachewan	LL13	54.352	0.049	27.600	11.560	0.687	0.083	0.009	4.920	0.178	99.438
03GRS-4C-B-fsp2r	Matachewan	LL13	58.025	0.018	25.321	8.055	0.470	0.102	0.031	6.825	0.292	99.140
03GRS-4C-C-fsp3c	Matachewan	LL13	53.102	0.043	27.989	12.130	0.737	0.061	0.028	4.486	0.168	98.744
03GRS-4C-C-fsp3r	Matachewan	LL13	53.513	0.042	27.870	11.943	0.958	0.072	0.035	4.736	0.152	99.320

Table 10d. Microprobe analyses of ilmenite and magnetite from Marathon dikes.

Sample	Dike Swarm	Station Number	SiO2	TiO2	Nb2O5	Al2O3	Cr2O3	V2O5	MgO	MnO	FeO*	NiO	ZnO	Total	Fe2O3	FeO	Total
03GRS-1C-A-ilm1	Marathon	DP6	0.000	50.211	0.016	0.008	0.024	0.000	0.009	3.289	45.104	0.005	0.019	98.684	3.670	41.801	99.052
03GRS-1C-A-mag1	Marathon	DP6	0.075	17.552	0.004	1.912	0.087	1.196	0.026	1.231	72.696	0.004	0.002	94.783	27.817	47.665	97.570
03GRS-2C-B-ilm1	Marathon	DP7	0.000	50.205	0.095	0.019	0.013	0.000	0.041	2.595	46.336	0.004	0.021	99.330	4.233	42.527	99.754
03GRS-2C-B-mag1	Marathon	DP7	0.097	18.643	0.045	4.874	0.098	0.870	0.039	1.127	70.134	0.011	0.019	95.956	23.439	49.043	98.305
03GRS-2C-B-ilm2	Marathon	DP7	0.025	50.433	0.033	0.016	0.021	0.000	0.037	2.652	46.037	0.000	0.016	99.269	3.763	42.651	99.646
03GRS-2C-B-mag2	Marathon	DP7	0.069	18.395	0.000	0.764	0.044	0.548	0.006	1.104	74.154	0.009	0.028	95.121	29.630	47.493	98.089

Metric Conversion Table

Conversion from SI to Imperial			Conversion from Imperial to SI		
SI Unit	*Multiplied by*	*Gives*	*Imperial Unit*	*Multiplied by*	*Gives*
		LENGTH			
1 mm	0.039 37	inches	1 inch	**25.4**	mm
1 cm	0.393 70	inches	1 inch	**2.54**	cm
1 m	3.280 84	feet	1 foot	**0.304 8**	m
1 m	0.049 709	chains	1 chain	20.116 8	m
1 km	0.621 371	miles (statute)	1 mile (statute)	**1.609 344**	km
		AREA			
1 cm^2	0.155 0	square inches	1 square inch	**6.451 6**	cm^2
1 m^2	10.763 9	square feet	1 square foot	**0.092 903 04**	m^2
1 km^2	0.386 10	square miles	1 square mile	2.589 988	km^2
1 ha	2.471 054	acres	1 acre	0.404 685 6	ha
		VOLUME			
1 cm^3	0.061 023	cubic inches	1 cubic inch	**16.387 064**	cm^3
1 m^3	35.314 7	cubic feet	1 cubic foot	0.028 316 85	m^3
1 m^3	1.307 951	cubic yards	1 cubic yard	0.764 554 86	m^3
		CAPACITY			
1 L	1.759 755	pints	1 pint	0.568 261	L
1 L	0.879 877	quarts	1 quart	1.136 522	L
1 L	0.219 969	gallons	1 gallon	**4.546 090**	L
		MASS			
1 g	0.035 273 962	ounces (avdp)	1 ounce (avdp)	28.349 523	g
1 g	0.032 150 747	ounces (troy)	1 ounce (troy)	**31.103 476 8**	g
1 kg	2.204 622 6	pounds (avdp)	1 pound (avdp)	**0.453 592 37**	kg
1 kg	0.001 102 3	tons (short)	1 ton (short)	**907.184 74**	kg
1 t	1.102 311 3	tons (short)	1 ton (short)	**0.907 184 74**	t
1 kg	0.000 984 21	tons (long)	1 ton (long)	**1016.046 908 8**	kg
1 t	0.984 206 5	tons (long)	1 ton (long)	**1.016 046 90**	t
		CONCENTRATION			
1 g/t	0.029 166 6	ounce (troy)/ ton (short)	1 ounce (troy)/ ton (short)	34.285 714 2	g/t
1 g/t	0.583 333 33	pennyweights/ ton (short)	1 pennyweight/ ton (short)	1.714 285 7	g/t

OTHER USEFUL CONVERSION FACTORS

	Multiplied by	
1 ounce (troy) per ton (short)	31.103 477	grams per ton (short)
1 gram per ton (short)	0.032 151	ounces (troy) per ton (short)
1 ounce (troy) per ton (short)	20.0	pennyweights per ton (short)
1 pennyweight per ton (short)	0.05	ounces (troy) per ton (short)

Note: Conversion factors which are in bold type are exact. The conversion factors have been taken from or have been derived from factors given in the Metric Practice Guide for the Canadian Mining and Metallurgical Industries, published by the Mining Association of Canada in co-operation with the Coal Association of Canada.

ISSN 0826-9580
ISBN 0-7794-8963-2